Regulation of redox signaling by ceramide during pulmonary *Pseudomonas aeruginosa* infections

Ph.D. thesis

Inaugural-Dissertation

Zur

Erlangung des Doktorgrades

Dr. rer. nat.

der Fakultät
Biologie und Geografie

an der

Universität Duisburg-Essen

vorgelegt von

Xiang Li, M.S.

Hubei, P.R.China

September 2010

Die der vorliegenden Arbeit zugrundeliegenden Experimente wurden am Institut für Molekularbiologie (Tumorforschung) der Universität-Gesamthochschule Essen durchgeführt.

1. Gutachter: Ruth Grümmer

2. Gutachter: Erich Gulbins

3. Gutachter: Hemmo Meyer

Vorsitzender des Prüfungsausschusses: Shirley Knauer

Tag der mündlichen Prüfung: 23.11.2010

Parts of this thesis are published or submitted for publication in the following articles:

1. Zhang Y, **Li X** (co-first author), Carpinteiro A, Gulbins E. Acid sphingomyelinase amplifies redox signaling in *Pseudomonas aeruginosa*–induced macrophage apoptosis. *J Immunol.* 2008 181:4247-4254.

2. Zhang Y, **Li X**, Grassmé H, Döring G, Gulbins E. Alterations in ceramide concentration and pH determine the release of reactive oxygen species by *Cftr*-deficient macrophages upon infection. *J. Immunol.* 2010 184: 5104-5111.

3. **Li X**, Katrin Anne Becker, Zhang Y. Ceramide in redox signaling and cardiovascular diseases. *Cell. Physiol. Biochem*. 2010 256: 41-48.

4. Zhang Y, **Li X**, Carpinteiro A, Soddman M, Gulbins E. A novel role of kinase suppressor of ras-1 in pulmonary *Pseudomonas aeruginosa* infections. *Nat. Med.* (in revision).

INDEX

LIST OF FIGURES

ABBREVIATIONS

ASM	Acid Sphingomyelinase
ATP	Adenosine Tri-Phosphate
BAL	bronchoalveolar lavage
CAPK	ceramide-activated protein kinase
CAPP	ceramide-activated protein phosphatase
CFTR	Cystic Fibrosis Transmembrane Conductance Regulator
DAG	diacylglycerol
DCF	dichlorofluorescin
DETAPAC	Diethylenetriaminepentaacetic Acid
DISC	death-inducing signaling complex
DPI	diphenyleneiodonium
DTT	Dithiothreitol
EDTA	Ethylenediamine Tetraacetic Acid
ELISA	Enzyme-linked immunosorbent assay
FACS	Fluorescence Activated Cell Sorting
FCS	Fetal Calf Serum
FITC	fluorescein isothiocyanate
GPI	glycophosphatidylinositol
IL	Interleukin
KO	knockout
LAMP1	lysosomal-associated membrane protein 1
LPS	lipopolysaccharide
LUV	large unilamellar vesicles
MOI	multiplicity of infection
NAC	N-acetylcysteine

NADPH	nicotinamide adenine dinucleotide phosphate
PA	*P. aeruginosa*
PAF	platelet-activating factor
PBS	Phosphate Buffered Saline
PCR	Polymerase Chain Reaction
PFA	Paraformaldehide
PLC	phospholipase C
PMA	phorbol 12-myristate l3-acetate
RFU	Relative fluorescence unit
rhASM	recombinant human acid sphingomyelinase
ROS	Reactive oxygen species
SDS	Sodium dodecyl sulphate
SOD	superoxide dismutase
TLB	Tissue Lysis Buffer
TMR	tetramethylrhodamine
TSB	tryptic soy broth
WT	wild type
UV	ultraviolet
v-ATPase	V-type adenosine triphosphatase

1. INTRODUCTION

1.1 Ceramide generation and ceramide-enriched membrane domains

1.1.1 Lipid interactions and domain formation

The plasma membrane of mammalian cells consists primarily of (glycero) phospholipids, sphingolipids and cholesterol (Hakomori, 1983). The classic fluid mosaic model, introduced by Singer and Nicolson in 1972, predicts free movement of proteins in the lipid bilayer; this model was based on biophysical experiments that determined the melting temperatures of lipids (Singer and Nicolson, 1972). However, in the past 10 to 15 years, this concept has been revised; it currently indicates that lipids in cell membranes do not form a homogenous liquid phase, but are ordered into distinct membrane domains that are enriched by sphingolipids and cholesterol (Simons and Ikonen, 1997).

Sphingolipids consist of a hydrophobic ceramide moiety and a hydrophilic headgroup. The ceramide moiety is composed of D-erythro-sphingosine and a fatty acid whose acyl chain contains 2 to 28 carbon atoms and is connected via an amide ester bond. Ceramides are further modified by attachments of headgroups to form, for instance, sphingomyelin, gangliosides, sulfatides, globosides or cerebrosides. Sphingomyelin is the most prevalent cellular sphingolipid, which is synthesized on the luminal side of the Golgi apparatus or the plasma membrane, and, thus, localizes predominantly to anti-cytoplasmic leaflets of the cell membrane and intracellular vesicles (Jeckel et al., 1990; Futerman et al., 1990). This distribution pattern of sphingomyelin results in lipid bilayer asymmetry, which is critical for the genesis of distinct membrane domains and, as discussed below, signal transduction. Sphingomyelin is comprised of a highly hydrophobic ceramide moiety and a hydrophilic phosphorylcholine headgroup (Barenholz and Thompson, 1980; Kolesnick et al., 2000). The hydrophilic phosphorylcholine groups tightly interact with each other, other hydrophilic headgroups of glycosphingolipids and the hydrophilic parts of cholesterol. The ceramide moiety of sphingomyelin binds to cholesterol via hydrophobic van der Waal interactions (Simons and Ikonen, 1997; Harder and Simons, 1997; Brown and London, 1998). The tight hydrophilic and hydrophobic interactions and the high local concentration of sphingolipids and cholesterol mediate a lateral association of these lipids in the cell membrane, separation from other phospholipids within the bilayer and the spontaneous formation of distinct domains (Simons et al., 1997; Harder and Simons, 1997; Brown and

London, 1998). These very small, tightly packed sphingolipid- and cholesterol-enriched membrane domains are named **rafts** that seem to exist in a more ordered liquid phase than other parts of the cell membrane (Simons and Ikonen, 1997; Harder and Simons, 1997; Brown and London, 1998) (**Figure 1.1**). Recent microscopy studies demonstrated that the size of these rafts is approximately 20 nm (Eggeling et al., 2009). Cholesterol and some cholesterol precursors do not only interact with sphingolipids in these rafts, but also stabilize the structure of rafts by filling void spaces between the bulky sphingolipids (Harder and Simons, 1997; Xu et al., 2001). This notion is consistent with the finding that extraction of cholesterol from membranes using drugs as beta-cyclodextrin, nystatin or filipin that binds cholesterol, destroys membrane rafts (Keller and Simons, 1998). Many studies characterized rafts by their resistance to detergents, which are caused by the high biophysical order in this phase, although the use of detergents might be problematic to investigate the physiology of lipids and detergent-resistant membrane domains are not the same as membrane rafts (Munro, 2003; Lichtenberg et al., 2005).

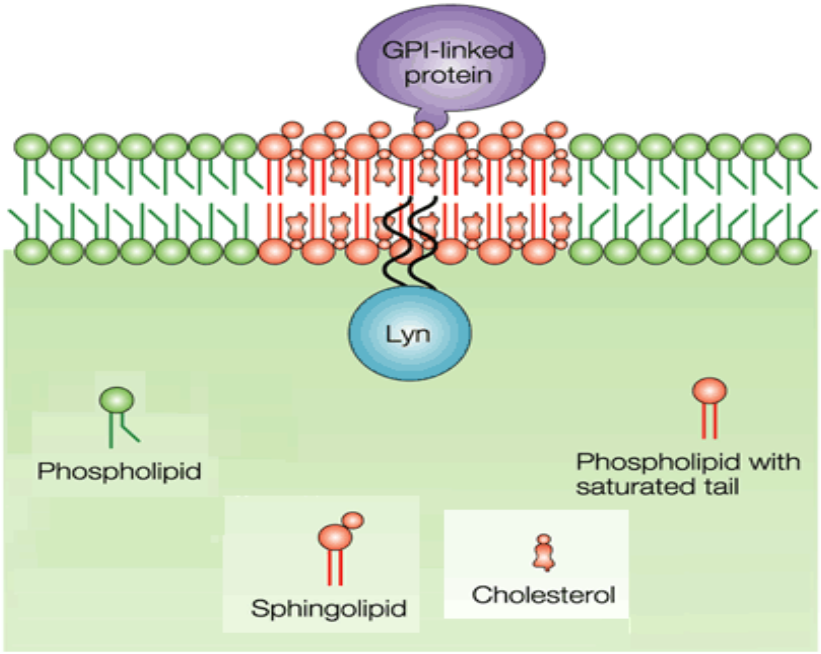

Figure 1.1 Membrane lipid raft structure and componets.

Membrane lipid rafts consist of dynamic assemblies of cholesterol and lipids with saturated fatty acid chains, sphingolipids and glycosphingolipids in the outside membrane of lipid bilayer and phospholipid with saturated chains in the inner membrane. These sphingolipids and phospholipids interact with cholesterol and form a tightly packed lipid microdomain. These lipid microdomains are relatively stable as they are resistant to several non-ionic detergents. This unique biophysical property differentiates lipid rats from other membrane parts. Since the other phospholipids are relative fluid, these lipid microdomains seem to float in the ocean of phospholipids and thereby they were termed lipid rafts. Due to this unique biophysical property, lipid rafts show high affinity for certain proteins such as glycophosphatidylinositol (GPI)-anchored proteins, cholesterol-linked

proteins and some transmembrane proteins or receptors. (Nature Reviews *Immunology* 2; 96-105, 2002)

1.1.2 Synthesis, metabolism and signaling of ceramide

Ceramide is generated by several enzymatic pathways in mammalian cells. Two major pathways are the sphingomyelinase pathway that ceramide generates from sphingomyelin by the activities of sphingomyelinases and the *de novo* synthesis pathway that synthesizes ceramide from serine and palmitoyl-CoA by the activity of ceramide synthase. Sphingomyelinases belong to the family of sphingomyelin-specific phospholipase C (PLC), which hydrolyzes sphingomyelin to ceramide and phosphorylcholine. Sphingomyelin can be regenerated from ceramide by sphingomyelin synthase. Ceramide can also be converted into other sphingolipids, such as ceramide-1-phosphate, sphingosine, and sphingosine-1-phosphate (**Figure 1.2**). Recent studies further revealed three additional pathways for the formation of ceramide, i.e. by the reverse activity of the acid ceramidase catalyzing synthesis of ceramide from sphingosine (Okino et al., 2003), by hydrolysis of complex-glycosylated lipids (Ishibashi et al., 2007) and by hydrolysis of ceramide-1-phosphate (Mitra et al., 2007).

At least five types of sphingomyelinase have been described. These enzymes are (1) the lysosomal acid sphingomyelinase, (2) the Zn^{2+}-dependent acid sphingomyelinase, (3) the membrane-bound magnesium-dependent neutral sphingomyelinase, (4) the magnesium-independent neutral sphingomyelinase, and (5) the alkaline sphingomyelinase. With respect to cell signaling, acid sphingomyelinase and neutral sphingomyelinase are considered the two major sphingomyelinases. They can be activated by growth factors, cytokines, chemotherapeutic agents, irradiation, nutrient removal, and stress to produce ceramide and other downstream sphingolipids and therefore they are involved in the regulation of cell growth, differentiation, cell cycle arrest, and apoptosis.

The *de novo* synthesis of ceramide begins with the condensation of serine and palmitoyl-CoA by serine palmitoyl-transferase, which forms 3-ketosphingosine, which then undergoes reduction to dihydrosphingosine. By addition of a C_{16} to C_{24} fatty acid to the amino group of dihydrosphingosine via ceramide synthase, dihydroceramide is produced, which is immediatedly converted to ceramide by the introduction of a *trans* double bond between carbons 4 and 5 of the sphingoid base. Originally, this *de novo* synthesis was not considered as an important signaling pathway since the synthesis reaction is relatively slow

compared to the sphingomyelin pathway. However, recent studies have demonstrated that the *de novo* synthesis occurs also rapidly when cells are exposed to many stimuli (Chalfant et al., 2002; Wang et al., 2002; Seumois et al., 2007). Therefore, the *de novo* synthesis is currently classified as a signaling enzymatic pathway.

Ceramide-mediated transmembrane and intracellular signaling has been demonstrated in a variety of mammalian cells. There is general agreement that sphingomyelin and its metabolites constitute a novel ubiquitous and evolutionarily conserved signaling pathway similar to the phosphoinositide and diacylglycerol (DAG) systems, where ceramide serves as an important mediator to regulate a number of cellular functions or activities. It has been suggested that ceramide, once generated, may directly or indirectly regulate the activity of various signaling components including ceramide-activated protein kinase (CAPK), ceramide-activated protein phosphatase (CAPP), sphingolipid-sensitive Ca^{2+} channels, and protein kinase C. However, the mechanisms responsible for the action of ceramide on these downstream targets are not fully understood.

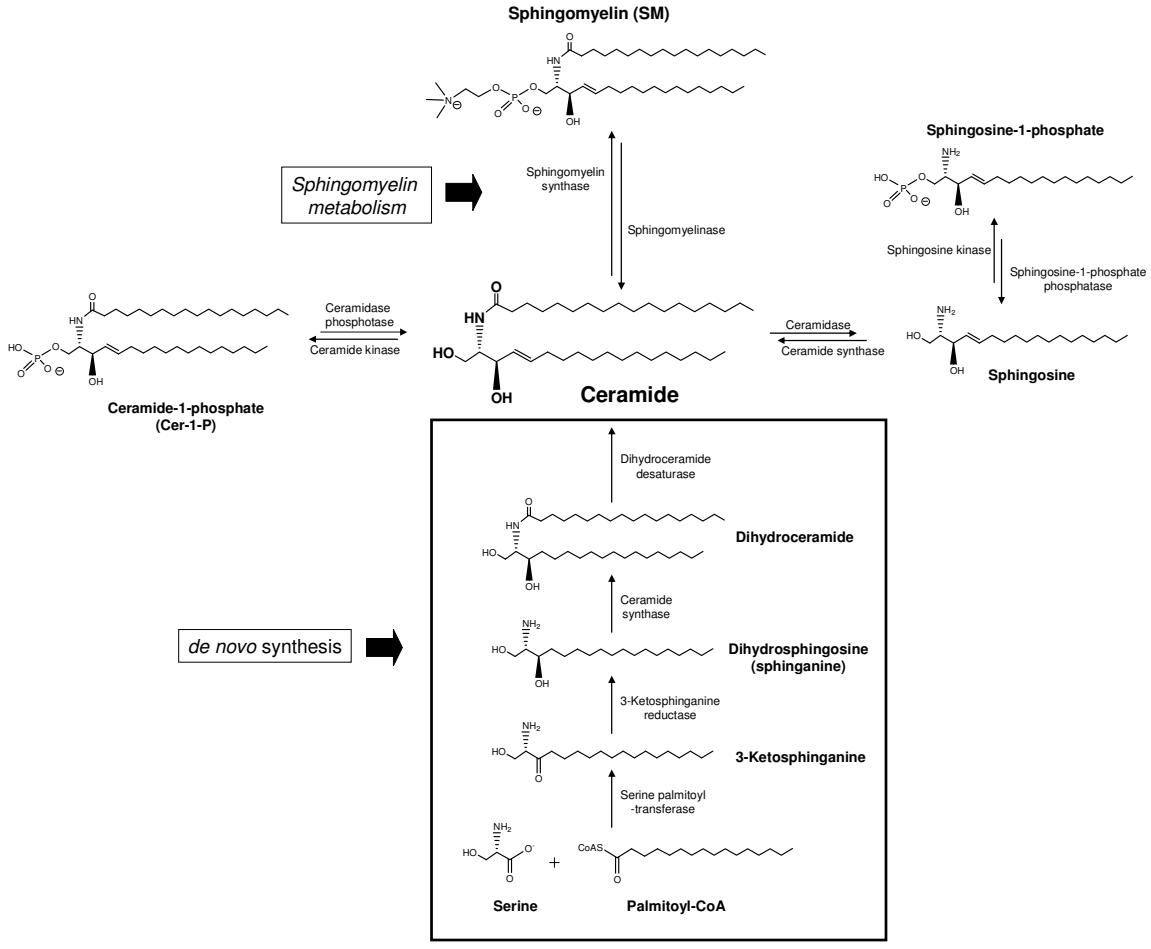

Figure 1.2 Ceramide synthesis and metabolism.

Ceramide can be generated from the sphingomyelin via sphingomyelinase pathway (sphingomyelin metabolism) or via the *de novo* synthesis pathway where cells synthesize ceramide from serine and

palmitoyl-CoA (*de novo* synthesis). Ceramide can be further converted into other sphingolipids such as ceramide-1-phosphate, sphingosine and sphingosine-1-phosphate.

1.1.3 Acid sphingomyelinase and ceramide-enriched membrane domains

Acid sphingomyelinase is the first and best-characterized sphingomyelinase and the enzyme was shown to be critically involved in many forms of cell activation (Samet and Barenholz, 1999; Gulbins and Kolesnick, 2003). Acid sphingomyelinase hydrolyzes sphingomyelin to ceramide, preferentially at an acidic pH. However, because other lipids crucially influence the Michaelis-Menten constant (K_m) of the enzyme to its substrate, the enzyme seems to be able to hydrolyze sphingomyelin also under almost neutral conditions (Schissel et al., 1996 and 1998).

The acid sphingomyelinase exists in two forms, a lysosomal acid sphingomyelinase and a secretory acid sphingomyelinase that are both derived from the same gene, but differ in their glycosylation pattern and are also differentially processed at the NH_2-terminus (Schissel et al., 1998). Most of acid sphingomyelinase seems to reside in classic lysosomes, where it mediates the catabolism of sphingomyelin. A genetic defect in acid sphingomyelinase leads to the accumulation of sphingomyelin and a lysosomal storage disorder named Niemann-Pick disease type A and B. The pool of acid sphingomyelinase insecretory lysosomes seems to participate in signal transduction events (Schissel et al., 1996 and 1998; Grassmé et al., 2001a; Herz et al., 2009; Bao et al., 2010). Mobilization of these vesicles triggers the fusion of secretory lysosomes and the cell membrane, and this fusion results in the exposure of acid sphingomyelinase on the outer leaflet of the cell membrane (Herz et al., 2009; Bao et al., 2010).

Activation of several receptors, such as CD95, DR5, CD40, and the platelet-activating factor (PAF) receptor, but also some bacterial and viral infections or stress stimuli, trigger the surface exposure of acid sphingomyelinase (Grassmé et al., 2001a; Cremesti et al., 2001). Further, changes in the glycosylation pattern of acid sphingomyelinase result in the expression of a secretory form of acid sphingomyelinase that is released upon stimulation, for instance by activation of interleukin-1 receptors (Schissel et al., 1996 and 1998).

Acid sphingomyelinase and secretory acid sphingomyelinase hydrolyze sphingomyelin from membrane and generate ceramide within cell membranes. The release of ceramide within the cell membrane alters the biophysical characteristics of membranes, because they

spontaneously self-associate to small, highly dydrophobic, and ordered ceramide-enriched membrane microdomains, which tend to fuse spontaneously to larger **ceramide-enriched membrane platforms**. Ceramide-enriched membrane domains seem to be tightly packed and, thus, rather stabile membrane domains, consistent with the observation that ceramide promotes the formation of membrane domains into a liquid ordered state (Megha and London, 2004; Veiga et al., 1999).

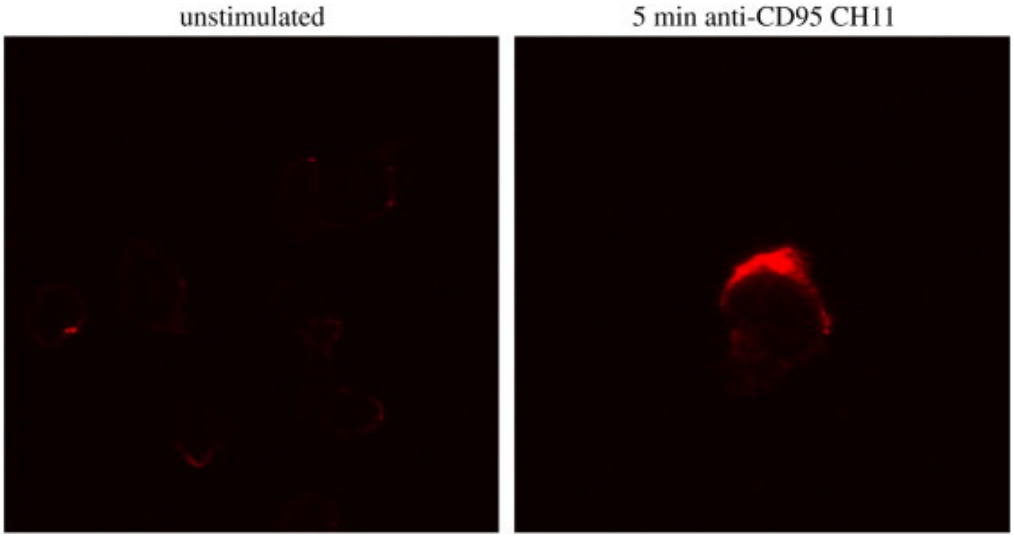

Figure 1.3 CD95 stimulation induces ceramide-enriched membrane platforms.

Stimulation of Jurkat T-lymphocytes via CD95 results in the formation of ceramide-enriched membrane platforms on the cell surface. Cells were stimulated, fixed, stained with Cy3-coupled anti-ceramide antibodies and analyzed by confocal microscopy. (Grassmé et al., J. Biol. Chem, 2001a)

Ceramide-enriched membrane domains were demonstrated in living cells by fluorescence microscopy (**Figure 1.3**) (Grassmé et al., 2001a). Studies on phosphatidylcholine /sphingomyelin-composed unilamellar vesicle that were treated with sphingomyelinase immobilized onto a microbead confirmed the formation of ceramide-enriched membrane macrodomains (Nurminen et al., 2002). The formation of distinct membrane domains by ceramide is also indicated by magnetic resonance spectroscopy and atomic force microscopy studies that revealed laminar phase separation of long chain ceramides in glycerophospholipid/cholesterol bilayers and formation of stable, distinct domains that correspond with a transition of fluid phospholipid bilayers into a gel-like phase (Veiga et al., 1999; Huang et al., 1999). Finally, biophysical studies demonstrated that small amounts of ceramide significantly increased the gel-to-fluid transition temperature of sphingomyelin suggesting the formation and stabilization of a liquid ordered state (Huang et al., 1999).

1.1.4 Function of ceramide-enriched membrane platforms and receptor clustering

Many diverse receptors and stimuli trigger the release of ceramide and the formation of ceramide-enriched membrane domains, including CD95 (Grassme et al., 2001a and 2003; Cremesti et al., 2001), CD40 (Grassme et al., 2002), DR5 (Dumitru et al., 2006), FcγRII (Abdel Shakor et al., 2004), the PAF-receptor (Goggel et al., 2004), CD14 (Pfeiffer et al., 2001), infection with *P. aeruginosa* (Grassme et al., 2003), *S. aureus* (Esen et al., 2001), *N. gonorrhoeae* (Grassme et al., 1997; Hauck et al., 2000), Rhinovirus (Grassme et al., 2005), application of stress stimuli such as γ-irradiation (Santana et al., 1996), UV-light (Charruyer et al., 2005) and in some conditions of developmental death.

Ceramide-enriched membrane domains are perfect structures to sort proteins in cells and to provide a mean for the spatial re-organization of receptors and intracellular signalling molecules upon cellular stimulation. Ceramide-enriched membrane platforms were shown to trap and, thus, cluster receptor molecules (Grassmé et al., 2001a and 2003; Nurminen et al., 2002; Cremesti et al., 2001). Clustering of receptor molecules results in a very high receptor density within a small area of the cell membrane, a phenomenon that is required for the transmission of signals via many receptor molecules. Receptor aggregation and trapping in ceramide-enriched membrane domains may limit lateral diffusion and, thus, stabilize the interaction of a ligand with its receptor, in particular if the ligand is also trapped in distinct membrane domains. The interaction of ligand-bound receptors with the very hydrophobic ceramide-enriched membrane platform and/or individual ceramide molecules may in addition stabilize conformational changes that may occur upon activation of a receptor by its ligand. Clustering of receptors also results in clustering of receptor-associated signalling molecules within or at ceramide-enriched domains. Furthermore, ceramide-enriched membrane domains, although present in the outer leaflet of the cell membrane, may sort intracellular signalling molecules, for instance via farnesyl- or geranyl-moieties. This sorting function may result in the spatial association of activated receptors with signalling molecules that transmit the signal from the receptor into the cell, while at the same time inhibitory molecules are excluded from this area of the cells. In addition, a high concentration and close vicinity of enzymes may permit enhanced transactivation of enzymes associating with the activated receptor, for instance of caspases associating with death receptor.

Thus, these considerations suggest that ceramide-enriched membrane platforms have a general function in signal transduction, i.e. they may primarily function to spatially

organize receptors and the intracellular signalosome in and at the cell membrane to facilitate and amplify signaling processes. The amplification function of ceramide-enriched membrane platforms has been demonstrated for CD95 signaling on B-lymphocytes lacking functional acid sphingomyelinase expression (Grassmé et al., 2001a and 2003). These cells fail to release ceramide upon CD95 stimulation. Binding of CD95 ligands to CD95 only resulted in a very weak activation in these cells as indicated by levels of recruitment of FADD and stimulation of caspase 8 that only reached approximately 1% of the levels achieved after maximal activation of CD95 in wild type, acid sphingomyelinase-positive cells. These studies demonstrate that ceramide-enriched membrane platforms serve to cluster activated receptor molecules and provide a feed-forward mechanism resulting in recruitment of signaling molecules and marked amplification of a primary weak signal.

1.2 Redox signaling

1.2.1 Reactive oxygen species (ROS)

Redox signaling is a fundamental signaling mechanism in cell biology. Various ROS, including $O_2^{\cdot -}$, H_2O_2, $^{\cdot}OH$, and $ONOO^{\cdot -}$, participate in cell signaling under certain physiological or pathological conditions. The most important of these ROS is $O_2^{\cdot -}$, which is unstable and short-lived because it has an unpaired electron, and it is highly reactive with a variety of cellular molecules, including proteins and DNA. $O_2^{\cdot -}$ is reduced to H_2O_2 by superoxide dismutase (SOD), and both $O_2^{\cdot -}$ and H_2O_2 can diffuse from their sites of generation to other cellular locations. H_2O_2 is further reduced to generate the highly reactive $^{\cdot}OH$ through the Haber-Weiss or Fenton reaction under pathological conditions. In contrast to $O_2^{\cdot -}$ and H_2O_2, $^{\cdot}OH$ is highly reactive and, therefore, causes primarily local damage. In addition, $O_2^{\cdot -}$ can also interact with NO to form another reactive oxygen free radical, $ONOO^{\cdot -}$. Under physiological conditions, O_2^{-} preferably produces H_2O_2 via the dismutation reaction. However, when excess $O_2^{\cdot -}$ is produced, a substantial amount of $O_2^{\cdot -}$ reacts with NO to produce $ONOO^{\cdot -}$. Taken together, these ROS constitute a redox regulatory network that controls cellular activity and function. Unbalanced or enhanced production of ROS impaired function of the antioxidant system, or both result in oxidative stress.

$O_2^{\cdot -}$ has been considered the progenitor of other ROS. In mammalian cells, many pathways are involved in the production of $O_2^{\cdot -}$, including nicotinamide adenine dinucleotide phosphate (NADPH) oxidase, xanthine oxidase, mitochondrial respiration chain, and NO synthase-uncoupling. NADPH oxidase has been detected in nearly every tissue, and in many cells, such as those in the phagocytes and vascular cells, it is the primary source of ROS. Recent studies suggest that NADPH oxidase localizes to specific subcellular compartments, including lamellipodial focal complexes and focal adhesions, membrane ruffles, caveolae and lipid rafts, endosomes, sarcoplasmic reticulum, and the nucleus. NO synthases normally localize in caveolae and function as homodimers to synthesize NO. When exposed to oxidative or nitrosative stress, NOS becomes structurally unstable ("uncoupling state") and exhibits NADPH oxidase activity resulting in $O_2^{\cdot -}$ formation. Given that ROS are short-lived and diffusible, the localization of ROS signals in specific subcellular compartments suggests that mammalian cells contain temporally and spatially organized redox signaling pathways that regulate various cellular functions.

1.2.2 NADPH oxidase

NADPH oxidase, identified and characterized first in neutrophils, catalyzes the 1-electron reduction of oxygen producing $O_2^{\cdot-}$ using NADPH as the electron donor. This neutrophil oxidase consists of at least five subunits: two membrane-bound subunits gp91^{phox} and p22^{phox} and three cytosolic subunits p47^{phox}, p40^{phox} and p67^{phox}. gp91^{phox} and p22^{phox} form an integral membrane complex termed cytochrome b_{558}, and the other three subunits, p47^{phox}, p67^{phox}, and p40^{phox} localize in the cytosol in resting cells. Upon stimulation, these cytosolic subunits translocate to the cell membrane and bind to cytochrome b558 to function as an oxidase. In addition, a cytosolic GTPase, Rac importantly participates in the activation of NADPH oxidase by assembling the NADPH oxidase complexes in the membrane. (**Figure 1.4**)

To date, several homolog proteins of gp91^{phox} were discovered in nonphagocytic cells and termed Nox (for NADPH oxidase) proteins. There are five Nox isoforms identified, namely Nox1-5, among which Nox2 is gp91^{phox}. Noxs are encoded by separate individual genes. gp91^{phox} or Nox2 is highly abundant in phagocytes and is the major enzyme responsible for respiratory burst of ROS upon bacterial infection, a key event in the defense against pathogenic bacteria.

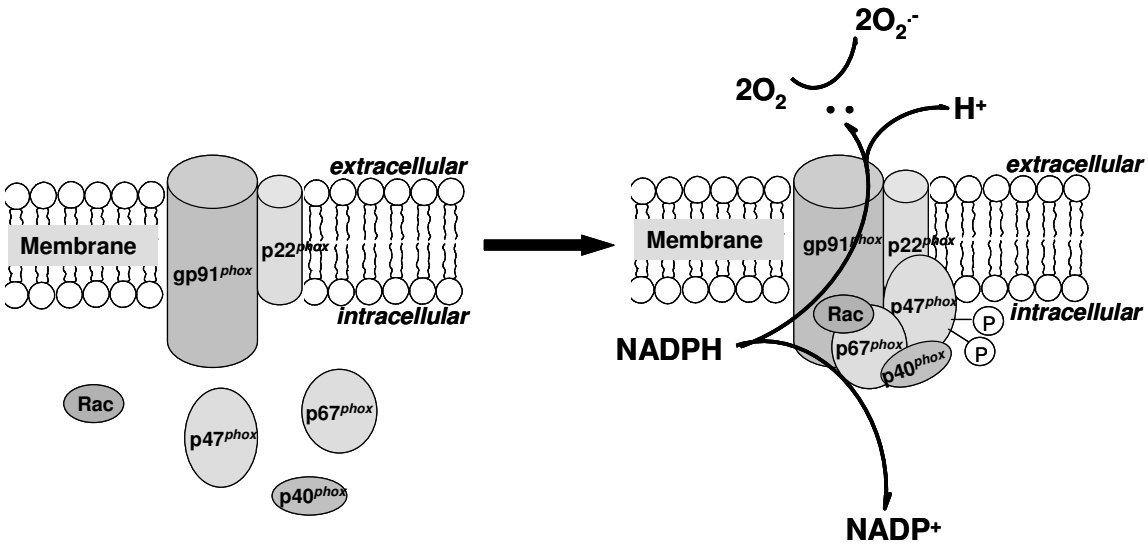

Figure 1.4 Phagocytic NADPH oxidase mediated electron transfer and O2$^{\cdot-}$ production.

Upon stimulation, p47^{phox} is phosphorylated and translocates to the membrane. NADPH oxidase subunits aggregate in the membrane to form a functional enzyme. gp91^{phox} uses NADPH as substrate to transfer two electrons to molecular oxygen on the opposite side of the membrane to produce $O_2^{\cdot-}$.

1.3 Cystic fibrosis and pulmonary *Pseudomonas aeruginosa* (*P. aeruginosa*) infections

1.3.1 Cystic fibrosis

Cystic fibrosis is caused by mutations of the Cystic Fibrosis Transmembrane Conductance Regulator (CFTR) and constitutes with 1 case per 2500 births the most common autosomal recessive disorder in the EU and the USA (Kerem et al., 1989; Rommens et al., 1989; Riordan et al., 1989). Approximately 40 000 children and young adults are affected in the EU.

Many mutations in the CFTR gene have been found to induce cystic fibrosis, however, the mutations that cause most clinical cases are those of amino acids 508 and 551 (Kerem et al., 1989; Rommens et al., 1989; Riordan et al., 1989). Genetic defects in the CFTR molecule result in several clinical symptoms, the most common of which are pulmonary and gastrointestinal problems. Gastrointestinal symptoms include malabsorption, intestinal obstruction, defects in the secretion of pancreatic enzymes, pancreatitis, and alterations in the liver. Pulmonary symptoms are mucus plugging and chronic bacterial infection, accompanied by a pronounced inflammatory response; damage the airways, ultimately leading to bronchiectasis and respiratory insufficiency. In particular cystic fibrosis patients suffer recurrent and chronic infections with *P. aeruginosa* and *Burkholderia cepacia*, but also *Staphylococcus aureus* and *Haemophilus influenzae*. At present, the pulmonary problems are most important for the disease course and for patients' life expectancy. However, the cause for the high sensitivity of cystic fibrosis patients to develop these pulmonary infections is unknown.

1.3.2 Pulmonary *P. aeruginosa* infections

P. aeruginosa is a Gram-negative, aerobic, rod-shaped bacterium with unipolar motility. It is an environmental pathogen found in moist areas such as sinks and drains. *P. aeruginosa* infections are most important in patients with cystic fibrosis, immunosuppression, ventilation, lung wounds. Once past early childhood a very high percentage of patients with cystic fibrosis suffer from recurrent and finally chronic *P. aeruginosa* pneumonia. More than 80% of adult cystic fibrosis patients are infected with the pathogen and chronic *P. aeruginosa* lung infections are the leading cause of morbidity and mortality in cystic

fibrosis. Smaller numbers of cystic fibrosis patients will become infected with other organisms such as *S. maltophilia*, *B. cepacia* and non-tuberculous mycobacteria, some of which appear to be increasing in prevalence.

In the healthy host bacteria entering the lungs are cleared rapidly, without the initiation of an inflammatory response, by a variety of innate host defense strategies, both mechanical (mucocilary clearance) and immunological (resident macrophages and anti-microbial peptides). In certain clinical situations, this first line of defense fails and these normally harmless bacteria survive, multiply and lead to organ damage. Such situations include mechanically ventilated patients in intensive care, those with defective immunity or severe burns and patients with cystic fibrosis.

1.3.3 Mechanisms involved in development of cystic fibrosis

The hallmarks of cystic fibrosis lung disease are early and persistent infection with a relatively narrow range of bacteria and severe and sustained neutrophil-mediated inflammation. The exact role of CFTR dysfunction in the sequence of events leading to chronic airway infection and irreversible damage is controversial and incompletely understood. However, it is presumed that bacterial adherence (either to airway secretions or directly to the cell surface) and resistance to innate defenses are key factors. Many studies have demonstrated that the development of this disease is very complex. Several explanations have been postulated, including (1) impairments in the mucociliary system and impaired function of anti-microbial peptides, (2) alterations in the mucus that lines the respiratory tract, (3) defective ingestion of bacteria by epithelial cells lacking CFTR, (4) alterations in the frequency of cell death induced in mammalian cells by pathogens, (5) alterations in the function of neutrophils and macrophages, (6) and low levels of defence molecules such as nitric oxide and glutathione and (7) changes in lipid metabolism. The relative importance of certain of these mechanisms *in vivo* has not yet been determined.

Because CFTR exhibits chloride channel activity, researchers speculated that the changes in water absorption by the mucus found on epithelial cells of the respiratory tract, which finally may result in a reduced mucociliary clearance and a reduced ability to eliminate *P. aeruginosa* (Matsui et al., 2005; Boucher, 2007). The increased viscosity of the mucus may also affect the ability of neutrophils to migrate to and kill bacteria in the respiratory tract. However, although *in vitro* experiments suggested the concept of reduced mucociliary clearance in cystic fibrosis (Matsui et al., 2005), *in vivo* studies on cystic fibrosis patients

failed to demonstrate a significant and uniform reduction of the mucociliary clearance in these individuals (Boucher, 2007).

A defect in the chloride channel function of CFTR may also result in changes of the ion concentration in the mucus. The altered concentration of ions may then impair the function of defensins and other anti-microbial peptides and, thus, reduce the elimination of *P. aeruginosa* in the lung (Goldman et al., 1997). However, at present it is unknown whether the defect of CFTR really results in hypertonic salt concentrations on the respiratory epithelium *in vivo* and, thus, dysfunction of antimicrobial peptides.

Pier et al. demonstrated a defect of the innate immune function of epithelial cells in the respiratory tract of cystic fibrosis mice. They showed that the lipopolysaccharide (LPS)-molecule of *P. aeruginosa* binds to a short amino acid sequence in CFTR (AA 103-117) (Pier et al., 1996). This interaction mediates internalisation of *P. aeruginosa* into lung epithelial cells. Deficiency of Cftr or blockade of the binding sequence prevents *P. aeruginosa* internalisation (Pier et al., 1996). Bacterial internalisation correlates with the defence against *P. aeruginosa* in lungs of infected mice, although the causative role of the internalisation defect for the high sensitivity of these mice to develop *P. aeruginosa* infections remains to be demonstrated. Further studies suggested that internalisation of *P. aeruginosa* is also mediated by other mechanisms. The uptake mechanisms also seem to depend on the bacterial strain, since rough, mucoid strains of *P. aeruginosa* are able to enter epithelial cells independent of CFTR expression (Schroeder et al., 2001).

Studies by several groups demonstrate that *P. aeruginosa* triggers cell death of Cftr-positive epithelial cells *in vitro* as well as in a focal pattern in bronchial epithelial cells in the lung. Apoptosis is mediated by an activation of the endogenous CD95 receptor/CD95 ligand-system within distinct membrane domains in epithelial cells upon infection with *P. aeruginosa* (Grassme et al., 2000; Jendrossek et al., 2001 and 2003; Kowalski et al., 2004; Grassme et al., 2003). *In vivo* studies indicate that stimulation of CD95 and, thus, presumably induction of apoptosis in epithelial cells is central for a coordinated defense against pulmonary *P. aeruginosa* infections. It might be possible that the induction of apoptosis in epithelial cells modulates the local immune response to the pathogen and prevents an over-shooting release of cytokines (Grassmé et al., 2003). In contrast, induction of apoptosis of epithelial cells by *P. aeruginosa* is abrogated in *Cftr*-deficient cells, which might contribute to inflammation and infection susceptibility (Grassmé et al.,

2003). Studies from Kumar et al. on two independent cystic fibrosis patient cohorts demonstrate that allelic variants within intron 2 of the CD95 gene modulate the manifestation of cystic fibrosis disease further suggesting a role of CD95-mediated signalling/apoptosis in cystic fibrosis (Kumar et al., 2008).

Several studies in the recent years suggest an imbalance between pro-inflammatory and anti-inflammatory cytokines in the airways of cystic fibrosis patients as one of the leading causes to result in destruction of the lung and the high susceptibility of these patients to infections with *P. aeruginosa*. It was demonstrated that cells lacking functional CFTR secrete increased amounts of Interleukin (IL)-1, IL-8/KC, TNF-alpha and Mip-2 upon infection with *P. aeruginosa* compared to control cells (Tirouvanziam et al., 2000; Inoue et al., 1994; Oceandy et al., 2002; Bonfield et al., 1995). IL-8 is already increased in the trachea of non-infected *Cftr*-deficient mice (Inoue et al., 1994), while the synthesis of anti-inflammatory cytokines, in particular IL-10 (Bonfield et al., 1995), has been shown to be reduced in Cftr-deficient mice under basal conditions as well as after infection with *P. aeruginosa*. The increased release of pro-inflammatory cytokines from CFTR-deficient epithelial cells correlates with a constitutive activation of NFκB in these cells (Venkatakrishman et al., 2000). However, at present, the mechanisms how a defect in CFTR results in an increased NFκB-activity, an enhanced release of pro-inflammatory cytokines and a decreased formation of anti-inflammatory cytokines are unknown.

1.3.4 Ceramide in cystic fibrosis

Recent studies highlight a critical role of ceramide in the development of cystic fibrosis and the high sensitivity of *Cftr*-deficient mice to *P. aeruginosa* infections (Teichgräber et al., 2008; Brodlie et al., 2010). Teichgräber and co-workers showed an accumulation of ceramide in lungs of different *Cftr*-deficient mouse strains (Teichgräber et al., 2008). This increase of ceramide was also observed in the lower airway epithelium of people with advanced cystic fibrosis (Brodlie et al., 2010). Teichgräber found ceramide particularly accumulates in epithelial cells of large and small bronchi in different *Cftr*-deficient mouse strains. Of note, ceramide accumulates in these cells prior to any infection. Further, ceramide accumulates in the lungs of *Cftr*-deficient mice in an age-dependent manner, which seems to mimic the delayed onset of symptoms in humans. The accumulation of ceramide in *Cftr*-deficient cells has been attributed to an alteration of the pH particular in secretory lysosomes, prelysosomes and/or lysosomes. Since the signaling pool of the acid

sphingomyelinase seems to be predominantly localized to secretory lysosomes, a primary accumulation of ceramide may occur within these vesicles. Since the enzymes that control ceramide metabolism in acidic vesicles are pH-dependent, an alkalinization of these vesicles has a dramatic effect on ceramide concentrations; sphingomyelin is constitutively metabolized to ceramide by the acid sphingomyelinase and consumed to sphingosine by the activity of the acid ceramidase. An increase of the pH from values around 4.5 to pH 6.0 reduces the activity of the acid sphingomyelinase by only ~30%, while the acid ceramidase is almost inactived at pH 6.0. The imbalance of the two enzymes activities with a relative over-activity of the acid sphingomyelinase may then result in an accumulation of ceramide. Increased ceramide concentrations in bronchial epithelial cells and lung macrophages of *Cftr*-deficient mice trigger several hallmarks of cystic fibrosis, i.e. death of respiratory epithelial cells and deposition of DNA in bronchi, chronic pulmonary inflammation and high susceptibility of *Cftr*-deficient mice to develop pulmonary *P. aeruginosa* infections (Teichgräber et al., 2008). In this respect, inhalation of inhibitors of the acid sphingomyelinase reduces DNA-deposits in lungs of cystic fibrosis mice and prevents infection with *P. aeruginosa* (Becker et al., 2009).

Recent study also demonstrated a defective activation of acid sphingomyelinase pathway upon *P. aeruginosa* infection in both a cystic fibrosis bronchial epithelial cell line and in the lungs of Cftr-deficient mice as compared with control epithelial cells and wild-type mice (Yu et al., 2009). Acid sphingomyelinase activity and total ceramide levels significantly increased in control epithelial cells and wild-type mice upon *P. aeruginosa* infection, but not in Cftr-deficient cells and mice. This defective acid sphingomyelinase pathway in cystic fibrosis may be attributing to alkalinization of the vesicles containing signaling acid sphingomyelinase.

1.4 Aims of the study

As described above, recent studies using human subjects and animal studies using Cftr-deficient mice highlight a role of ceramide in the development of this inherited disease (Teichgräber et al., 2008; Becker et al., 2009; Yu et al., 2009; Brodlie et al., 2010). Particularly, our group has demonstrated that alteration in ceramide metabolism contributes to the pathological development of cystic fibrosis. Age-dependent accumulation of ceramide was detected in the epithelium of the lungs of Cftr-deficient mice. However, it is unknown whether ceramide is also altered in other lung cells. Alveolar macrophages serve as the first line of host defense to clear extracellular bacteria from the lung. These lung resident macrophages are critically involved in coordinating the innate immune response during the bacterial infection. At present, the role of alveolar macrophage in cystic fibrosis is not well understood.

The present thesis first defines the role of ceramide-mediated signaling in regulating functions of lung alveolar macrophages during pulmonary *P. aeruginosa* infections. Because ceramide is an important signaling molecule that regulates redox signaling (Zhang et al., 2007), the present study will investigate whether *P. aeruginosa* infections result in activation of acid sphingomyelinase, formation of ceramide-enriched membrane platforms and clustering of NADPH oxidase in the plasma membrane. The importance of acid sphingomyelinase and ceramide platforms for NADPH oxidase-derived ROS production will be tested by using Acid sphingomyelinase-deficient cells.

The second part of the study addresses whether *Cftr*-deficiency results in alterations of ceramide metabolism and ceramide-mediated redox signaling in lung alveolar macrophages. Because CFTR increases pH in at least some intracellular vesicles such as lysosomes by its action to mediate the influx of counterions into intracellular vesicles (Barasch et al., 1991; Poschet et al., 2002; Di et al., 2006; Teichgräber et al., 2008; Deriy et al., 2009). It will be tested whether *Cftr*-deficiency causes defects in lysosomal acidification, acid sphingomyelinase/ceramide-mediated amplification of redox signaling and killing invaded *P. aeruginosa* by these lung macrophages.

Our results will increase the understanding of the signaling mechanisms that cause defects in innate responses of cystic fibrosis lungs and the high susceptibility to *P. aeruginosa* infections.

2. MATERIALS

Chemicals

Aqua ad Injectabilia	DeltaSelect GmbH, Dreieich
Acetic acid ($C_2H_4O_2$)	Merck, Darmstadt
Adenosine Tri-Phosphate (ATP)	Sigma-Aldrich Chemie GmbH, Steinheim
Apocynin	Sigma-Aldrich Chemie GmbH, Steinheim
Bafilomycin	Sigma, Deisenhofen, Germany
β-mercaptoethanol	Sigma-Aldrich Chemie GmbH, Steinheim
Bromphenol blue	Sigma-Aldrich Chemie GmbH, Steinheim
C_{16}-Ceramide	Biomol, PA, USA
Calcium chloride ($CaCl_2$)	Sigma-Aldrich Chemie GmbH, Steinheim
Cardiolipin	Sigma-Aldrich Chemie GmbH, Steinheim
Chloroform ($CHCl_3$)	Ridel-de Haen, Seelze
Diethylenetriaminepentaacetic Acid (DETAPAC)	Sigma-Aldrich Chemie GmbH, Steinheim
Dithiothreitol (DTT)	Carl-Roth GmbH & Co, Karlsruhe
Ethidium bromide	Sigma-Aldrich Chemie GmbH, Steinheim
Ethylenediamine Tetraacetic Acid (EDTA)	Serva Electrophoresis GmbH, Heidelberg
FACS buffer	BD Biosciences, Heidelberg, Germany
Glucose	Sigma-Aldrich Chemie GmbH, Steinheim
Glycerol	Fluka Chemie GmbH, Buchs
H_2DCFDA	Molecular Probes, Eugene, OR
Hepes	Carl-Roth GmbH & Co, Karlsruhe
Hydrochloric acid (HCl)	Sigma-Aldrich Chemie GmbH, Steinheim
Imidazole ($C_3H_4N_2$)	Sigma-Aldrich Chemie GmbH, Steinheim

Ionophore nigericin	Invitrogen, Karlsruhe, Germany
Isopropanol	Sigma-Aldrich Chemie GmbH, Steinheim
Ketamine	Ceva Tiergesundheit GmbH, Duesseldorf
Magnesium chloride ($MgCl_2$)	Sigma-Aldrich Chemie GmbH, Steinheim
Magnesium sulphate ($MgSO_4$)	Sigma-Aldrich Chemie GmbH, Steinheim
Methanol (CH_3OH)	Fluka Chemie GmbH, Buchs
Mowiol	Kuraray Specialities Europe GmbH, Frankfurt
MTT	Sigma-Aldrich Chemie GmbH, Steinheim
N-octylglucopyranoside	Sigma-Aldrich Chemie GmbH, Steinheim
Paraformaldehide (PFA)	Sigma-Aldrich Chemie GmbH, Steinheim
Phosphatase inhibitor	Sigma-Aldrich Chemie GmbH, Steinheim
Potassium chloride (KCl)	Sigma-Aldrich Chemie GmbH, Steinheim
Potassium dihydrogenphosphate (KH_2PO_4)	Sigma-Aldrich Chemie GmbH, Steinheim
Protease inhibitor	Carl-Roth GmbH & Co, Karlsruhe
RPMI-1640	Gibco/Invitrogen, Karlsruhe, Germany
Saponin	Serva Electrophoresis GmbH, Heidelberg
Sodium acetate (CH_3COONa)	Sigma-Aldrich Chemie GmbH, Steinheim
Sodium chloride (NaCl)	Carl-Roth GmbH & Co, Karlsruhe
Sodium dodecyl sulphate (SDS)	Serva Electrophoresis GmbH, Heidelberg
Sodium hydroxide (NaOH)	Sigma-Aldrich Chemie GmbH, Steinheim
Sodium phosphate (Na_2HPO_4)	Merck, Darmstadt
Taq Polymerase	Invitrogen, Karlsruhe, Germany
Tryptic soy broth (TSB)	BD Biosciences, Heidelberg, Germany
Tris	Carl-Roth GmbH & Co, Karlsruhe
Triton X-100	Sigma-Aldrich Chemie GmbH, Steinheim
Xylazin	Ceva Tiergesundheit GmbH, Duesseldorf

Antibodies, dye and ELISA kit

Alkaline phosphatase-coupled secondary antibodies	Santa Cruz Biotechnology, CA, USA
Anti-ceramide (clone 15B4) Mouse IgM	Glyobiotech, Kükels, Germany
Anti-gp91^{phox} Mouse IgG	BD Biosciences, Heidelberg, Germany
Anti-JNK1 Rabbit IgG	Santa Cruz Biotechnology, CA, USA
Anti-phospho-c-Jun Rabbit IgG	Cell signaling, Danvers, MA, USA
Anti-phospho-JNK Rabbit IgG	Cell signaling, Danvers, MA, USA
Cy3-anti-rabbit IgG	Jackson Immunoresearch, West Grove, PA, USA
Cy3-goat anti-mouse IgM	Jackson ImmunoResearch Laboratories
Cy5-anti-mouse IgM F(ab')$_2$	Jackson Immunoresearch, West Grove, PA, USA
FITC-goat anti-mouse IgG	Jackson Immunoresearch, West Grove, PA, USA
KC ELISA kit	R&D Systems, Wiesbaden-Nordenstadt, Germany
LysoSensor Green DND-189	Molecular Probes, Invitrogen, Karlsruhe, Germany
LysoSensor Green DND-153	Molecular Probes, Invitrogen, Karlsruhe, Germany
MIP-2 ELISA kit	R&D Systems, Wiesbaden-Nordenstadt, Germany
TMR-dextran	Molecular Probes, Invitrogen, Karlsruhe, Germany

PCR primers

ASM-PA 1-2	Hermann GbR, Freiburg

5´-CGA GAC TGT TGC CAG ACA TC-3´

ASM-PA 2-2 Hermann GbR, Freiburg
5´-GGC TAC CCG TGA TAT TGC TG-3´

ASM-PS-2 Hermann GbR, Freiburg
5´-AGC CGT GTC CTC TTC CTT AC-3´

Myco P1 Hermann GbR, Freiburg
5´-GTG CCA GCA GCC GCG GTA ATA C-3´

Myco P4 Hermann GbR, Freiburg
5´-TAC CTT GTT ACG ACT TCA CCC CA-3´

IMR1125 Hermann GbR, Freiburg
5'-GAG AAC TGG AAG CTT CAG AGG-3'

IMR1126 Hermann GbR, Freiburg
5'-TCC ATC TTG TTC AAT GGC C-3'

IMR1127 Hermann GbR, Freiburg
5'-TCC ATG TAG TGG TGT GAA CG-3'

3473f Hermann GbR, Freiburg
5'-CTC GTG CTT TAC GGT ATC GCC-3'

3473r Hermann GbR, Freiburg
5'-TGC TGT AGT TGG CAA GCT TTG A-3'

5012f Hermann GbR, Freiburg
5'-CCT TCC ATG TAC CCC TCC TCA CTT-3'

5012r Hermann GbR, Freiburg
5'-CCC GGC ATA ATC CAA GAA AAT TG-3'

Animals

Acid sphingomyelinase-deficient (sphingomyelin phosphodiesterase 1 (*Smpd1*$^{-/-}$) knockout) mice (on a C57Bl/6 background) were kindly provided by Dr. R. Kolesnick (Memorial Sloan-Kettering Cancer Center, NY, USA). Syngenic wild-type mice from the same heterozygous breeding were used as control. The mice used in the present study show the earliest clinical manifestation of Niemann-Pick disease type A between 12-16 weeks of age; therefore, all the experiments involving cells from acid sphingomyelinase-deficient mice were carried out with animals younger than 12 weeks of age, before any biochemical, histological or clinical manifestations of Niemann-Pick disease type A were apparent. This excluded that the effects observed in the acid sphingomyelinase-deficient cells were due to

altered cellular processes but instead, were completely dependent on the lack of acid sphingomyelinase.

Two mouse strains of Cftr-deficient mice were used, one is B6.129P2(CF/3)-Cftr$^{TgH(neoim)Hgu}$ (abbreviated *Cftr^{MHH}*, syngenic to C57BL/6; kindly provided by Dr. B. Tümmler, Medizinische Hochschule Hannover) and the other is strain Cftr^{tm1Unc}-Tg$^{(FABPCFTR)}$ (abbreviated *Cftr^{KO}*; obtained from Jackson Laboratory, Bar Harbor, ME). Neither of these Cftr-deficient mouse strains requires a special diet. This characteristic is important because some diets have been shown to alter membrane lipid composition (Borowitz et al., 2005; Cottart et al., 2007; Teichgraber et al., 2008; Becker et al., 2009). Changes in lipid composition, in particular an alteration in cholesterol and sphingolipids concentrations, may regulate the activity of ion channels and pumps (Schreur and Liu, 1997; Gulbins et al., 1997; Lepple-Wienhues et al., 1999). Littermates of the C57BL/6 mice were used as control animals.

Wild-type and *Asm*-deficient or *Cftr*-deficient mice were propagated in the Animal Facility of the Uniklinikum Essen. Homozygocity of wild-type and *Asm*- or *Cftr*-deficient mice were propagated in the Animal Facility of the Uniklinikum Essen. Homozygocity of WT and *Asm*- or *Cftr*-deficient mice was verified by PCR analysis. Mice were housed in pathogen-free conditions under diurnal lighting alternated with a dark phase between 18.00 – 6.00, allowed daily food "Zuchthaltungsfutter Maus-Ratte 10 H 10" (Eggersmann) and water *ad libitum*. All mice were repeatedly tested for the presence of pathogens and were free of any pathogens according to the criteria of the Federation of Laboratory Animal Science Associations.

Radioactive substances

[^{32}P] gamma-ATP	Hartmann Analytic, Braunschweig
[^{14}C] Sphingomyelin	Perkin Elmer, Boston, MA, USA

Other materials

ADEFO X-Ray Developer Concentrate	Adefo Chemie GmbH, Dietzenbach

ADEFO X-Ray Fixer Concentrate	Adefo Chemie GmbH, Dietzenbach
CDP-Star Chemiluminescence Reagent	PerkinElmer, Waltham, MA, USA
Coverslips 12 mm diameter	Carl-Roth GmbH & Co, Karlsruhe
Cuvettes 10 x 4 x 45 mm	Sarstedt, Numbrecht
FACS Polystyrene Round-Bottom Tubes	Beckton Dickinson Labware, Le Point de Claix, France
LeicaConfocal software (Leica)	Leica Microsystems, Germany
Microscopy glass slides 76 x 26 mm	Engelbrecht, Edermunde
Minisart syringe filters	Vivascience AG, Hannover
Parafilm	Peckiney, Chicago, IL, USA
Steritop Vacuum-driven disposable top filters	Millipore, Billerica, MA, USA
tryptic soy agar plates	BD Biosciences, Heidelberg, Germany
Whatman filter paper	Whatman, Maidstone, UK
X-Ray films	Amersham Biosciences, Buckinghamshire, UK

Special laboratory equipment

Portable Datalogging Spectrophotometer	Bachofer, Reutlingen, Germany
fluorescence-activated cell sorter	FACScalibur, BD Biosciences, San Jose, CA, USA
Fluorescence Microplate Reader	BMG Labtech, Offenburg, Germany
Leica TCS SP confocal microscope equipped with a 100× oil objective	Leica Microsystems, Wetzlar, Germany
Sonorex bath sonicator	Bandelin electronic, Berlin, Germany
TriCarb Liquid scintillation Analyzer	Perkin Elmer, USA
Tropix system	Bedford, MA

Buffer and Solutions

Anesthesia cocktail	10% Ketamin 2ml 2% Xylazin 0.5ml dH_2O 10ml
ASM lysis buffer	0.2% Trition X-100 50 mM sodium acetate pH 5.0
DAG-assay Buffered Saline Solution	135 mM NaCl 1.5 mM $CaCl_2$ 0.5 mM $MgCl_2$ 5.6 mM Glucose 10 mM Hepes pH 7.2
DAG-assay detergent solution	7.5% N-octylglucopyranoside 5 mM cardiolipin 1 mM DETAPAC
DAG-kinase diluents	1 mM DETAPAC (pH 6.6) 0.01 M imidazole/HCl
DAG-kinase reaction buffer	100 mM imidazole/HCl pH 6.6 100 mM NaCl 25 mM $MgCl_2$ 2 mM EDTA 2.8 mM DTT 5 uM ATP 10 uCi [^{32}P] gamma-ATP
HEPES buffer	132 mM NaCl 20 mM Hepes pH 7.4 5 mM KCl 1 mM $CaCl_2$ 0.7 mM $MgCl_2$ 0.8 mM $MgSO_4$
Lysosomal calibration buffer	120 mM KCl 20 mM NaCl 1 mM $CaCl_2$ 1 mM $MgCl_2$ 10 mM HEPES adjusted the pH to either 4.5, 5.0, 5.5, 6.0, or 6.5, respectively
Mowiol	6 g Glycerol 2.4 g Mowiol 6 ml H_2O 12 ml 0.2 M Tris pH 8.5 0.1% DABCO
PA medium	500 ml RPMI-1640 1 mM Hepes pH 7.4

PFA 2%	2.5 ml PFA stock solution 7.5 ml PBS
PFA stock solution	8g PFA 100 ml PBS
Phosphate Buffered Saline (PBS)	137 mM NaCl 2.7 mM KCl 7 mM $CaCl_2$ 0.8 mM $MgSO_4$ 1.4 mM KH_2PO_4 6.5 mM Na_2HPO_4
SDS-sample buffer	62.5 mM Tris pH 6.8, 10% glycerol, 2% SDS, 0.04% bromphenol blue 5% β-mercaptoethanol
10 x TBE	890 mM Tris Base 890 mM Boric Acid 20 mM EDTA
Tissue Lysis Buffer (TLB)	10% 10 x PCR buffer 0.5 mM $MgCl_2$ 0.045% Tween-20 0.045% NP-40 300 µg/ml Proteinase K
10 x Tris-buffered Saline-supplemented with 0.1% Tween-20 (TBS-T)	200 mM Tris pH 7.4 1500 mM NaCl 1% Tween-20

3. METHODS

Isolation of alveolar macrophages from mice

Lung macrophages were freshly isolated by bronchoalveolar lavage (BAL) from 6-8 week old mice. To this end, the mice were anesthetized with i.p. injection of 250 µL anesthesia cocktail and then the trachea was opened and cannulated with a polyethylene tube. Then, the lung was lavaged with a total of 15 ml ice-cold PBS (see Materials) in 20 aliquots (0.75 ml/aliquot). Approximately 0.5 to 1×10^6 cells per mouse were consistently obtained. Cells were pelleted by centrifugation at 300×g for 15 min, resuspended, and cultured for 1h in PA medium (see Materials) in 24-well plates at a density of 10^5 cells per well. Because alveolar macrophages are extremely adhesive cells, after other blood cells were washed off, we were left with a pure cell culture in which more than 99% of cells were macrophages, as confirmed by flow cytometry after staining with FITC-coupled anti-CD11b antibodies.

Infection experiments

The laboratory strains of *P. aeruginosa* ATCC 27853 were plated overnight on tryptic soy agar plates at 37°C, resuspended in 20 mL tryptic soy broth (TSB) at an optical density of 0.25 at 550 nm, and incubated at 37°C for 1 h with shaking at 120 rpm. Bacteria were harvested in the early logarithmic growth phase and washed twice in PA medium. Macrophages were infected with *P. aeruginosa* at a multiplicity of infection (MOI) of 100 or 1 (1 macrophage was infected with 100 or 1 bacteria). For *P. aeruginosa* ATCC 27853 infection, synchronous infection conditions and an enhanced bacterium-host cell interaction were achieved by a 2-min centrifugation (300×g) of the bacteria onto the cells. The end of the centrifugation step was defined as the starting point of all infections. For *P. aeruginosa* PAO1 infection, bacteria were cultured and harvested similar to strain ATCC 27853, but were added without centrifugation. Bacterial CFUs were counted by serial dilution and plating on TSB agar plates.

Acid sphingomyelinase activity assay

Activity of the acid sphingomyelinase was measured by the consumption of radioactive [^{14}C]-sphingomyelin to ceramide and [^{14}C]-phosphorycholine. To this end, 10^5 cells in a 12-well plate were infected, washed and lysed in 200 µl ice-cold ASM lysis buffer (see Materials) with a cocktail of protease and phosphatase inhibitors (see Materials). The cells

were removed from the plate, transferred into eppendorf tubes and immediately sonicated three times (3×10 s). The substrate ([^{14}C]-sphingomyelin) was dried prior to use and resuspended in ASM lysis buffer followed by 10 min bath sonication to promote the formation of micelles. The lysates were incubated with 0.02 µCi [^{14}C]-sphingomyelin for 30 min at 37 °C. The reaction was stopped by addition of 1 ml of $CHCl_3$:CH_3OH (v/v). Phases were separated by 5 min centrifugation at 14,000 rpm and an aliquot of aqueous phase was applied for liquid scintillation counting. Hydrolysis of [^{14}C]-sphingomyelin by sphingomyelinase results in release of [^{14}C]-choline chloride into the aqueous phase, whereas ceramide and unreacted [^{14}C]-sphingomyelin remain in the organic phase. Therefore, the release of [^{14}C]-choline chloride (pmol/10^5 cells/h) serves to determine the activity of the acid sphingomyelinase.

Ceramide measurement by DAG kinase assay

Cellular ceramide was measured by DAG kinase assay, in which ceramide is converted to a quantifiable product (ceramide-1-phosphate) by transfer of [^{32}P]-phosphate to [^{32}P]-gamma ATP to ceramide. To this purpose, cells were infected as above, extracted in $CHCl_3$:CH_3OH:1 N HCl (100:100:1, v/v/v). The resulting biphasic mixture is composed of a lower liquid-containing organic phase, and an upper aqueous phase. The upper phase and any resulting precipitate at the interface were removed and the lipids in the lower organic phase were collected, dried by evaporation of the chloroform in a SpeedVac. The dried lipids were subjected to alkaline hydrolysis of diacylglycerol in 0.1 N methanolic KOH at 37 °C for 60 min. Samples were re-extracted, the lower phase dried, and 20 µl of a detergent solution consisting of DAG-assay detergent solution (see Materials) were added to the samples. Samples were sonicated for 10 min in a bath sonicator, and 50 µl of DAG-kinase reaction buffer (see Materials), and 10 µl of DAG kinase diluted with DAG-kinase diluents (see Materials) were added. The kinase reaction was performed for 30 min at room temperature, and the samples were extracted in 1 ml of $CHCl_3$:CH_3OH:1 N HCl (100:100:1, v/v/v), 170 µl of DAG-assay buffered saline solution (see Materials) and 30 µl of a 100 mM EDTA solution. Samples were vortexed and centrifuged, the lower phase was collected, dried, and dissolved in 20 µl of $CHCl_3$:CH_3OH (1:1, v/v). Lipids were separated on a Silica G-60 TLC plate. A solvent system of $CHCl_3$:CH_3COCH_3:CH_3OH:CH_3COOH:H_2O (10:4:3:2:1, v/v/v), was added to the TLC chamber, and was allowed to saturate the atmosphere for 1 h by using a sheet of Whatman filter paper. The silica plates were loaded with the solubilized lipids, placed into the TLC chamber and the solvent front was allowed to migrate to the top of the plate. The plate was then removed, air dried and exposed to X-

ray films for 24 hrs. Ceramide spots were identified by comigration with a C_{16}-ceramide standard, removed from the plate, and incorporation of ^{32}P into ceramide was quantified by liquid scintillation counting. Comparison with a standard curve using C_{16}-ceramide permitted the determination of ceramide amounts.

Flow cytometry analysis of surface ceramide

Fluorescence Activated Cell Sorting (FACS) allows the analysis and sorting of cell populations based on their morphology and fluorescence after staining with different fluorochrome-conjugated antibodies. To detect surface ceramide in the plasma membrane, cells were left uninfected or infected with *P. aeruginosa* and fixed in 2% PFA for 10 min. The cells were incubated in PBS/5% fetal calf serum (FCS) for 30 min at room temperature to block unspecific binding sites and stained with a ceramide antibody (1:200 dilution) for 1 hour. Cells were then washed in PBS containing 1% FCS and stained for 45 min with Cy3-goat anti-mouse IgM. After a final PBS wash, cells were resuspended in 300 µL FACS buffer, transferred into FACS polystyrene tubes and analyzed on a fluorescence-activated cell sorter (see material).

Determination of ROS burst

ROS production can be determined by using a ROS probe, H_2DCFDA (see materials), which is only fluorescent when it is oxidized by ROS. To measure ROS burst, cells were cultured in 96-well plates (10^5cells/well) and incubated with 10 µM H_2DCFDA for 30 min at 37^{o}C. Cells were infected with *P. aeruginosa* for 30 min and the fluorescence was determined by fluorescence micro-plate reader at excitation/emission: 485/520 nm. Relative fluorescence unit (RFU) over time (ΔRFU/min) was used to represent total ROS release.

Flow cytometry analysis of intracellular ROS accumulation

To determine intracellular ROS production, cells were loaded with 10 µM cell membrane permeable H_2DCFDA for 30 min at 37 ^{o}C. After incubation, cells were extensively washed with PBS to remove extracellular H_2DCFDA and further incubated at 37 ^{o}C for 10 min to allow cleavage of H_2DCFDA to cell membrane impermeable H_2DCF by intracellular esterase. After infection, the cell fluorescence was determined by flow cytometry analysis.

Fluorescence microscopy

Cells were left uninfected or infected with *P. aerugionsa* as above and fixed in 2% PFA/PBS for 10 min. For intracellular staining, cells were permeablized with 0.1% Triton X-100/PBS for 15 min at room temperature. Cells were washed again with PBS and incubated for 30 min in PBS supplemented with 5% FCS to block nonspecific binding sites. Cells were washed and incubated for 45 min with either anti-ceramide IgM (see Materials) and anti-gp91^{phox} IgG, or a anti-phospho-c-Jun IgG. Cells were then washed in PBS with 0.05% Tween-20 and incubated for an additional 45 min with FITC-labeled goat anti-mouse IgG, Cy3-anti-rabbit IgG or Cy5-anti-mouse IgM F(ab')$_2$ fragments antibodies. After a final PBS wash, cells were mounted on glass coverslips with moviol. Control experiments were performed with irrelevant mouse or rabbit antibodies and secondary antibodies. Control antibodies did not significantly bind to the cells. Cells were examined on a Leica TCS SP confocal microscope equipped with a 100× oil objective and images were analyzed using LeicaConfocal software (Leica).

Immunoblot analyses

Cells were infected and lysed in SDS-sample buffer (see material), boiled, and sonicated (3×10 s) on ice to break chromosomal DNA and decrease sample viscosity. Then proteins were separated by 10% SDS–PAGE and transferred to nitrocellulose membranes. The blots were blocked in 4% BSA in TBS-T and incubated overnight at 4 ^{o}C with anti-phospho-JNK (1:1000 dilution in 4% BSA) or anti-JNK1 (1:1000 dilution) antibodies. Blots were labeled with alkaline phosphatase-coupled secondary antibodies (see material) and developed using the Tropix system.

Analysis of lysosomal pH

To observe lysosomal alkalinization, we incubated lung macrophages in PBS buffer with or without 100 nM bafilomycin, an H^+-ATPase pump inhibitor (see material), for 30 min. The cells were then loaded with LysoSensor Green DND-189 (1 μM) in PBS buffer for 15 min at 37^{o}C. Cells were washed twice with PBS and immediately visualized with a Leica SP2 confocal microscope. We measured the relative mean fluorescence intensity of at least 200 cells per sample. To obtain a pH standard curve, we loaded cells with LysoSensor Green DND-189 for 15 min at 37^{o}C; the lysosomal pH was equalized by incubating cells for 15 min at 37°C either in PBS containing the ionophore nigericin (10 μM) or in a

lysosomal calibration buffer (see material). We observed no differences in fluorescence between the cells incubated in PBS and those incubated in the HEPES buffers.

To determine whether LysoSensor Green DND-189 and TMR-dextran (10 kDa) target the same vesicle population, we incubated lung macrophages with TMR-dextran of various concentrations (1 mg/mL, 200 μg/mL, 50 μg/mL, 20 μg/mL and 10 μg/mL) in PA medium for 1 h at 37°C and then washed them with PBS. Cells were reincubated in fresh medium at 37°C for 1 h to allow TMR-dextran to accumulate in lysosomes. The cells were then loaded with LysoSensor Green DND-189 for 15 min at 37°C, washed twice, and analyzed as described above. When indicated, cells were stained with LysoSensor Green DND-153 (1 μM) according to a protocol similar to that used for LysoSensor Green DND-189. For flow cytometry, the macrophages were labeled as above, carefully removed from the culture plates, and immediately analyzed with a fluorescence-activated cell sorter.

Bactericidal capability assay

To determine bactericidal capability, we cultured macrophages in 96-well plates (10^5 cells per well) and infected them with *P. aeruginosa* strain ATCC 27853 or PAO1 opsonized in 5% mouse serum (MOI, 1). Phagocytosis of ATCC 27853 was synchronized by centrifugation at 300×g for 5 min, and macrophages were infected for 20 min at 37°C. Infection with PAO1 bacteria was performed without centrifugation. Macrophages were then gently washed three times with sterile PBS for removal of extracellular or attached bacteria. Macrophages were further infected for 0 or 60 min at 37°C in the absence or presence of the NADPH oxidase inhibitor apocynin (100 μM). After infection, macrophages were incubated with 20 μL saponin (5 mg/mL) for 5 min for release of intracellular bacteria. Then 100 μL tryptose phosphate broth and 15 μL MTT in PBS (5 mg/mL) were added to each well, and the cells were incubated at 37°C for 4 h. Reactions were stopped by adding 100 μL isopropanol with 0.04 M HCl, and absorbance (A_{570nm}) was measured at 570 nm with a microplate reader (see material). To obtain the A_{570nm}-CFU relationship, we incubated 10^4 to 10^5 *P. aeruginosa* ATCC 27853 or PAO1 bacteria with 100 μL tryptose phosphate broth and 20 μL MTT in PBS (5 mg/mL) without macrophages for 4 h (see **Figure 3.1** below).

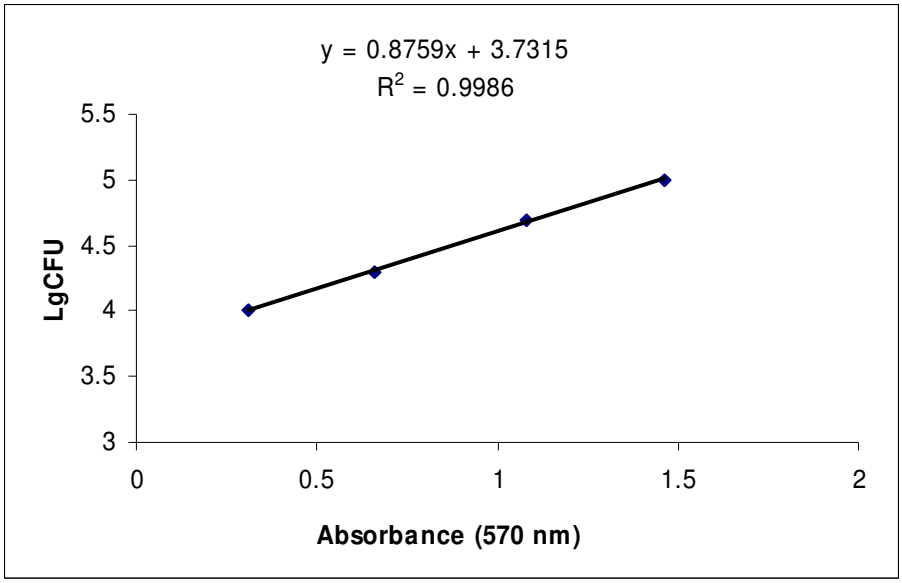

Figure 3.1 Representative standard curve for A570nm-CFU relationship.

Cytokine release

Macrophages were cultured in 24-well plates (5×10^5 cells per well in 1 mL PA medium) and infected with the *P. aeruginosa* strains ATCC 27853 or PAO1 (MOI 100) for 2 h. Then the total mixture was transferred to an eppendorf tube and KC and MIP-2 levels in the supernatants were determined by ELISA according to the manufacturer's instructions.

DNA techniques

DNA isolation from mouse tails

For genotyping of *Asm*-deficient mice, app. 1-2 mm of mouse tail was cut and placed into 80 µl Tissue Lysis Buffer (TLB). The samples were incubated at 56^0C overnight and the volumes were raised to 800 ul with autoclaved ddH_2O.

Polymerase Chain Reaction (PCR) for acid sphingomyelinase or Cftr

For the identification of acid sphingomyelinase wild-type, acid sphingomyelinase heterozygotes or *Asm*-deficient mice by PCR, 1 µL of overnight tail digest was added to 1.2 µL 10 x PCR Buffer, 2.5 mM $MgCl_2$, 1 µL dNTP mix 5 units/mL Taq Polymerase and 0.1 µL each of primers ASM-PA1-2, ASM-PA2-2 and ASM-PS-2 in 0.2 ml PCR tubes. The temperature of the lid of the PCR machine was raised to 104^oC and the temperature of

the PCR block was raised to 96°C for 17 min, after which the following cycle was carried out 35 times:
Denaturation: 95°C for 1 min
Annealing: 58°C for 1 min
Elongation: 72°C for 1 min 45 sec
After the last cycle, the PCR block remained at 72°C for 5 min, after which the samples were placed at 4°C.

For the identification of wild-type, Cftr heterozygotes or $Cftr^{tm1Unc}$-$Tg^{(FABPCFTR)}$ (abbreviated *$Cftr^{KO}$*) by PCR, 2.5 µL of overnight tail digest was added to 16.25 µL dH_2O, 2.5 µL 10 x PCR Buffer, 0.5 µL dNTP, 0.25 µL Taq Polymerase, 0.5 µL dNTP mix and 1 µL each of primers IMR1125, IMR1126 and IMR1127 in 0.2 ml PCR tubes. The temperature of the lid of the PCR machine was raised to 104°C and the temperature of the PCR block was raised to 96°C for 17 min, after which the following cycle was carried out 35 times:
Denaturation: 95°C for 1 min
Annealing: 58°C for 1 min
Elongation: 72°C for 1 min 45 sec
After the last cycle, the PCR block remained at 72°C for 5 min, after which the samples were placed at 4°C.

For the identification of wild-type, Cftr heterozygotes or B6.129P2(CF/3)-$Cftr^{TgH(neoim)Hgu}$ (abbreviated *$Cftr^{MHH}$*), two PCR reactions are performed. First PCR is designed to detect 3473 fragment (mutant fragment) which includes 2.5 µL of overnight tail digest was added to 18.25 µL dH_2O, 2.5 µL 10 x PCR Buffer, 0.5 µL dNTP, 0.25 µL Taq Polymerase, 0.5 µL dNTP mix and 0.5 µL each of primers 3473f and 3473r in 0.2 ml PCR tubes. The second PCR is designed to detect 5012 fragment (wild-type fragment) which includes 2.4 µL of overnight tail digest was added to 2.9 µL dH_2O, 6 µL 2 x PCR Buffer mix D, 0.3 µL Taq Polymerase, 0.25 µL dNTP mix and 0.5 µL each of primers 5012f and 5012r in 0.2 ml PCR tubes. The temperature of the lid of the PCR machine was raised to 104°C and the temperature of the PCR block was raised to 96°C for 17 min, after which the following cycle was carried out 35 times:
Denaturation: 95°C for 1 min
Annealing: 58°C for 1 min
Elongation: 72°C for 1 min 45 sec

After the last cycle, the PCR block remained at 72°C for 5 min, after which the samples were placed at 4°C.

For the identification of mycoplasma by PCR, 1 ul of cell digest (see 3.7.1.2) was added to 2.5 ul 10 x PCR Buffer, 4.1 mM $MgCl_2$, 0.5 ul dNTP mix 1.25 units/ml Taq Polymerase and 0.25 each of primers P1 and P4 in 0.2 ml PCR tubes. The temperature of the lid of the PCR machine was raised to 104^{0}C and the temperature of the PCR block was raised to 96^{0}C for 17 min, after which the following cycle was carried out 25 times:
Denaturation: 95^{0}C for 1 min
Annealing: 60^{0}C for 1 min
Elongation: 72^{0}C for 1 min 30 sec
After the last cycle, the PCR block remained at 72^{0}C for 7 min, after which the samples were placed at 4^{0}C.

Agrose gel electrophoresis

To analyse the products of the PCR, a 1% agarose gel was poured in TBE buffer (see Materials) that contained 0.01 µg/ml ethidium bromide. The samples (15 µl) were loaded on the gel along with 0.1 µg/µl of a 100-bp-standard. The gel was run under 5 V/cm current. Visualization of the DNA fragments was performed under UV-light.

4. RESULTS

4.1 Role of acid sphingomyelinase in mediating ROS production during pulmonary *P. aeruginosa* infections of alveolar macrophages

4.1.1 *P. aeruginosa* infections activate acid sphingomyelinase and release ceramide in lung alveolar macrophages

Acid sphingomyelinase has been recently shown to play a critical role in host-pathogen interactions (Grassmé et al., 2003; McCollister et al., 2007). To investigate whether acid sphingomyelinase is involved in regulating ceramide production in macrophages upon *P. aeruginosa* infection, we infected alveolar macrophages with *P. aeruginosa* and determined the enzymatic activity of the acid sphingomyelinase and the formation of ceramide. The results reveal a very rapid activation of the acid sphingomyelinase upon *P. aeruginosa* infection peaking at approximately 15 min after infection (**Figure 4.1A**). Enhanced activity of the acid sphingomyelinase correlated with increased ceramide concentrations in wild type macrophages after *P. aeruginosa* infection (**Figure 4.1B**). This decrease might be mediated by consumption of ceramide by host cell enzymes, but also by the ceramidase activity from *P. aeruginosa* (Okino and Ito. 2007). Further, surface ceramide release was detected in wild type macrophages as determined by flow cytometry using monoclonal anti-ceramide antibodies. Deficiency of the acid sphingomyelinase in macrophages isolated from *Smpd1*$^{-/-}$ mice abrogated both, the surface release of ceramide (**Figure 4.1C**) indicating the importance of the acid sphingomyelinase for the induction of macrophage death by *P. aeruginosa*.

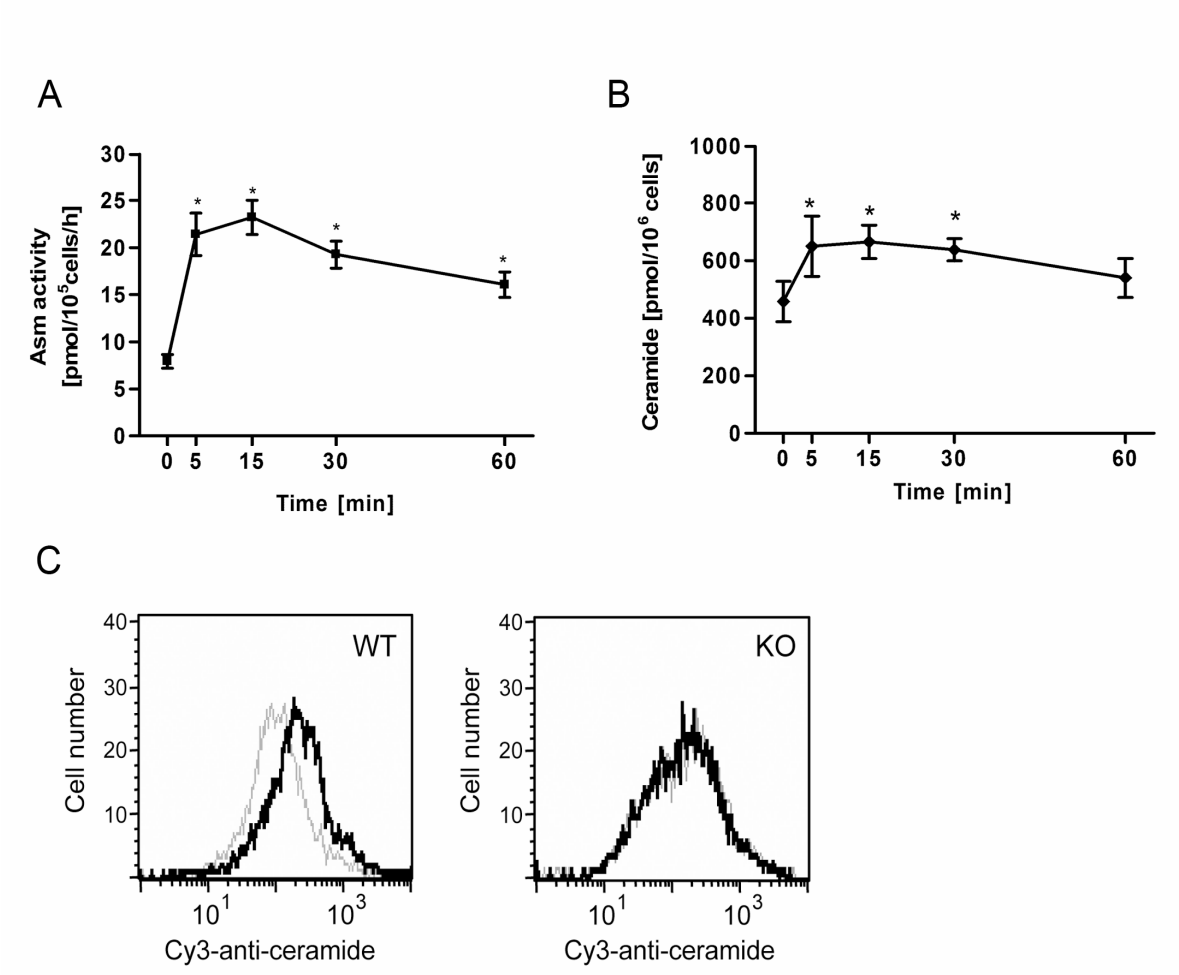

Figure 4.1 *P. aeruginosa* infections induce acid sphingomyelinase activation and ceramide generation.

(A) *P.aeruginosa* activates acid sphingomyelinase in macrophages. Freshly isolated mouse alveolar were infected (MOI = 100, 0-60 min), lysed and assayed for acid sphingomyelinase activity.
(B) DAG kinase assay for ceramide content in macrophages upon *P. aeruginosa* infections (MOI = 100, 0-60 min).
(C) Lung alveolar macrophages isolated from C57BL/6 wild type (WT) or *Smpd1*$^{-/-}$ (KO) mice lacking acid sphingomyelinase activity were left uninfected (thin line) or infected (bold line) with *P. aeruginosa* for 15 minutes. Surface ceramide release was determined by flow cytometry using Cy3-labeled anti-ceramide antibodies. A representative of three experiments is shown. Significant differences between infected and non-infected controls were determined by *t*-test and are indicated by asterisk, respectively (* $P<0.05$, *t*-test).

4.1.2 Acid sphingomyelinase is necessary for *P. aeruginosa*-induced ROS production

Previous studies showed a critical role of the acid sphingomyelinase in ROS production in macrophages, hepatocytes and endothelial cells (Zhang et.al, 2007; Hatanaka et.al, 1998; Reinehr et.al, 2005). Since ROS are critical factors for host-pathogen interactions, we tested whether acid sphingomyelinase mediates *P. aeruginosa*-triggered ROS production.

To determine the ROS burst in macrophages, cells were pre-incubated with H_2DCF-DA, a ROS probe, and then infected with *P. aeruginosa* ATCC 27853 for 30 min. As shown in **Figure 4.2A**, *P. aeruginosa* induced ROS burst in wild type cells, while no ROS-release was observed in *Smpd1*$^{-/-}$ cells after 30 min infection.

To determine intracellular ROS accumulation in macrophages, cells were loaded with the cell membrane permeable ROS probe, H_2DCF-DA. Extracellular H_2DCF-DA was washed off by PBS after the loading period. Cells were further incubated for 10 min at 37^{o}C to allow cleavage of H_2DCF-DA to cell membrane impermeable H_2DCF by intracellular esterase. Then cells were infected and DCF fluorescence was determined by flow cytometry. As shown in **Figure 4.2B**, *P. aeruginosa* time-dependently increased intracellular ROS in wild type (WT) macrophages, whereas no increase was observed in *Smpd1*$^{-/-}$ (KO) cells. It has been well documented that NADPH oxidase–derived superoxide production is a primary source of ROS generation in macrophages and neutrophils upon bacterial infection (Djaldetti et al, 2002; Karupiah et al, 2000). Consistently, DPI (50 μM, Sigma), a NADPH oxidase inhibitor, significantly attenuated *P. aeruginosa*–induced ROS production (**Figure 4.2B**). Taken together, these studies demonstrate that acid sphingomyelinase mediates *P. aeruginosa*–induced ROS production via activation of NADPH oxidase.

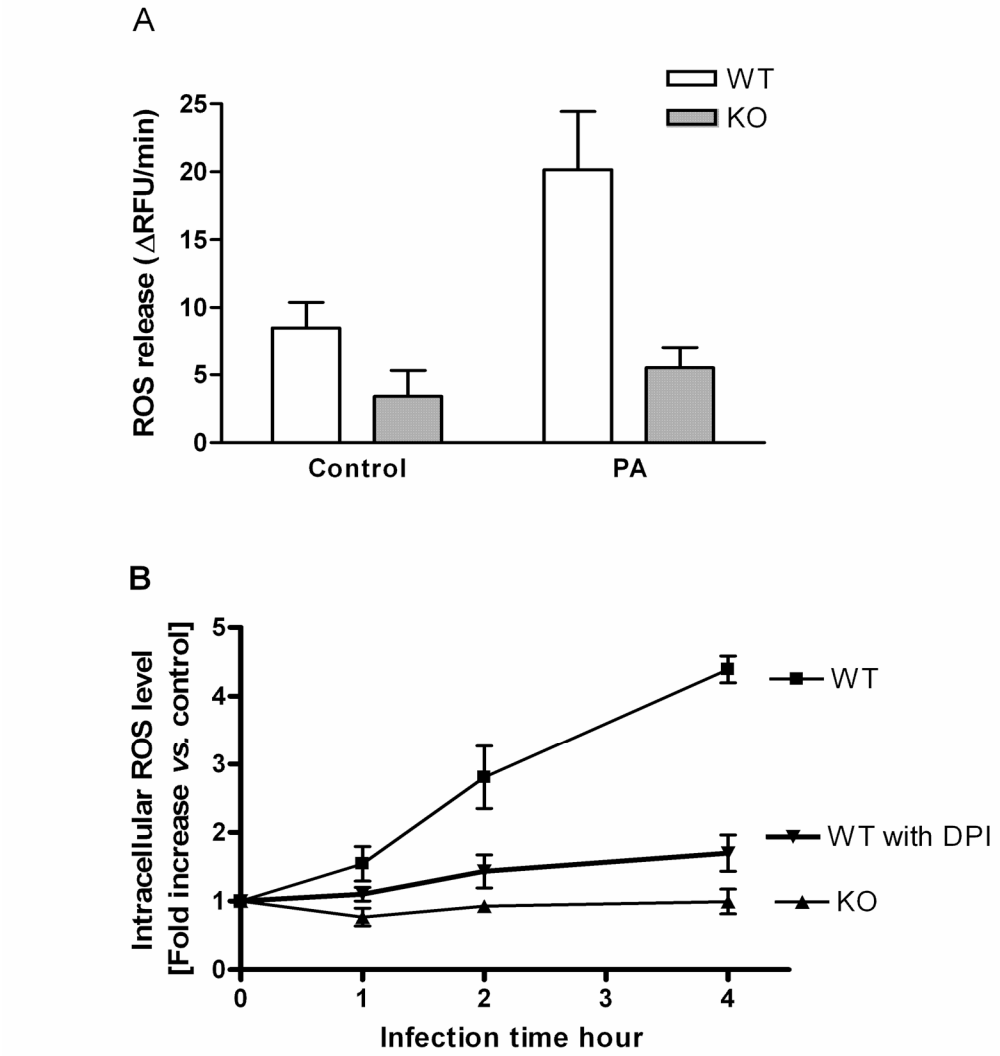

Figure 4.2 *P. aeruginosa* infections induce NADPH oxidase-derived ROS generation.

(A) To determine ROS burst, wild type (WT) or *Smpd1*$^{-/-}$ (KO) macrophages were incubated with a fluorescence probe, H_2DCFDA. Cells were infected for 30 min and fluorescence was determined by a fluorescence micro-plate reader. Relative fluorescence unit (RFU) over time (ΔRFU/min) was used to represent ROS release.

(B) Intracellular ROS accumulation is dependent on acid sphingomyelinase and NADPH oxidase activity. Wild type or *Smpd1*$^{-/-}$ macrophages were loaded with H_2DCFDA, in the absence or presence of DPI (50 μM), a NADPH oxidase inhibitor. Cells were infected for the indicated time and analyzed by FACS. Relative ROS levels were used to indicate intracellular ROS accumulation. Data are mean ± SD of four independent experiments.

4.1.3 Acid sphingomyelinase mediates *P. aeruginosa*-induced formation of ceramide-enriched membrane platforms

Activation of acid sphingomyelinase correlated with a release of ceramide in lung macrophages upon *P. aeruginosa* infection, which may induce formation of ceramide-enriched membrane platforms. NADPH oxidase consists of two membrane-bound subunits, $gp91^{phox}$ and $p22^{phox}$, which form a flavocytochrome b_{558} complex, and cytosolic subunits $p47^{phox}$, $p40^{phox}$, $p67^{phox}$ and the small GTPase Rac, which translocate to the membrane to assemble the active complex following cell activation (Vilhardt et al., 2004). Thus, the ceramide-enriched membrane platforms may serve for aggregating subunits of NADPH oxidase and activation of this enzyme complex.

This led us to examine whether acid sphingomyelinase is required for *P. aeruginosa*-induced formation of ceramide-enriched membrane platforms. Confocal fluorescence microscopy studies reveal that *P. aeruginosa* infection (MOI = 100, 15 min) induced formation of ceramide-enriched platforms in wild type cells (**Figure 4.3A**). Ceramide-enriched platforms were observed as early as 1 min after infection peaking at about 5 min (ceramide clustering in around 80% of all cells). In marked contrast, ceramide-enriched membrane platforms were absent in acid sphingomyelinase-deficient cells after infection (**Figure 4.3A**). Quantitative analysis of cells positive for ceramide-enriched membrane platforms demonstrates that acid sphingomyelinase is essential for *P. aeruginosa*-induced formation of ceramide-enriched membrane platforms (**Figure 4.3B**).

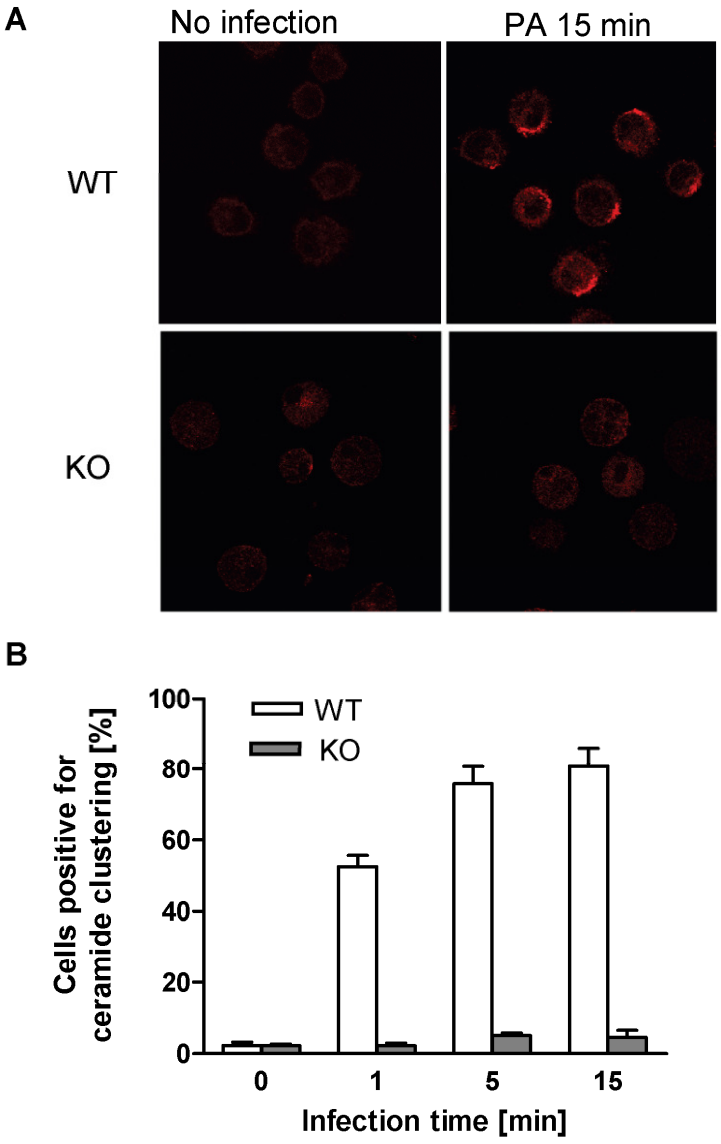

Figure 4.3 *P. aeruginosa* infections induce formation of ceramide-enriched membrane platforms.

(A) *P. aeruginosa* ATCC 27853 (PA) infection results in rapid clustering of ceramide in the membrane to form ceramide-enriched platforms. Macrophages were infected, fixed and stained with Cy3-labeled anti-ceramide. Representative confocal fluorescence microscopy images of WT or acid sphingomyelinase-deficient *Smpd1*$^{-/-}$ (KO) cells either uninfected (No infection) or infected for 15 minutes (PA 15 min) are shown.
(B) The quantitative analysis of the data from four independent experiments, which each included analysis of 200 cells/time point, shows the formation of ceramide-enriched membrane platforms in a large proportion of the cells. Displayed are the percentages of cells with a ceramide-enriched membrane platform at indicated time points. Ceramide-enriched membrane platforms were absent in *Smpd1*$^{-/-}$ cells.

4.1.4 *P. aeruginosa*-induced activation of NADPH oxidase via ceramide-enriched membrane platforms

To explore the mechanism how acid sphingomyelinase activation leads to NADPH oxidase-derived ROS production, we examined whether ceramide-enriched membrane platforms are involved in aggregation of gp91^{phox}, a major membrane subunit of NADPH oxidase. Co-staining of ceramide and gp91^{phox} demonstrates that gp91^{phox} aggregates in and co-localizes with ceramide-enriched platforms (**Figure 4.4**), events that were absent in *Smpd1*$^{-/-}$ cells revealing a critical role of the acid sphingomyelinase for the formation of active NADPH-oxidase. These data indicate that, in *P. aeruginosa*–induced acid sphingomyelinase-mediated redox signaling, ceramide-enriched membrane platforms serve to aggregate NADPH oxidase leading to activation of this enzyme and subsequent ROS production.

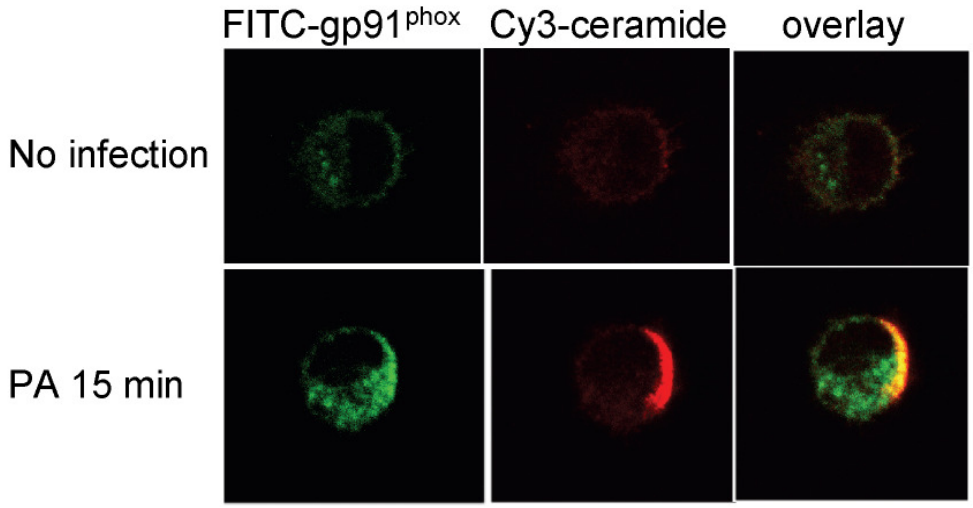

Figure 4.4 NADPH oxidase clusters in ceramide-enriched membrane platforms upon infection.

Cells were infected with *P. aeruginosa* ATCC 27853 (PA) as in **Figure 4.3** and confocal microscopy studies were performed using FITC-labeled anti-gp91^{phox} (against a major membrane subunit of NADPH oxidase) and Cy3-labeled anti-ceramide antibodies in wild type cells. The images shown are representative of three independent experiments.

4.1.5 Redox regulation of acid sphingomyelinase activation and membrane platform formation

The studies presented above indicate that acid sphingomyelinase controls ROS-generation upon *P. aeruginosa* infection. However, recent studies have suggested that acid sphingomyelinase is also subject to redox regulation (Zhang et.al, 2007; Dumitru and Gulbins, 2006; Qiu et.al, 2003; Scheel-Toellner et.al, 2004). Therefore, we first examined whether there is also a feedback regulation of ROS on acid sphingomyelinase activation upon *P. aeruginosa*-infection. As shown in **Figure 4.5A**, we detected that *P. aeruginosa*-induced acid sphingomyelinase activation was inhibited in the cells by treatment either with the NADPH oxidase inhibitor DPI (50 µM), or the H_2O_2 degrading enzyme catalase (10 unit/ml). Vice versa, acid sphingomyelinase activity was increased by H_2O_2 (1 mM). Thus, these data suggest that acid sphingomyelinase-mediated generation of ROS amplifies *P. aeruginosa*-induced acid sphingomyelinase activation in a positive feedback manner.

Next, we determined whether ROS has a similar feedback effect on acid sphingomyelinase-mediated formation of ceramide-enriched membrane platforms. *P. aeruginosa*-induced membrane platform formation was diminished by DPI or catalase, while H_2O_2 dramatically increased ceramide-enriched platform formation in wild type, but not in *Smpd1*$^{-/-}$ cells, suggesting that acid sphingomyelinase is essential for ROS-induced formation of membrane platforms (**Figure 4.5B**).

These data raise the question whether *P. aeruginosa* activate acid sphingomyelinase first, which then triggers ROS that maintain the activity of the acid sphingomyelinase high or vice versa. DPI or catalase reduced, but not completely blocked *P. aeruginosa*-induced acid sphingomyelinase activation after 15 min infection (**Figure 4.5A**, DPI *vs.* DPI+PA and Catalase *vs.* Catalase+PA), whereas early release of ROS was completely prevented in *Smpd1*$^{-/-}$ cells **Figure 4.2A**). These data indicate that an initial ROS-independent activation of the acid sphingomyelinase results in generation of ceramide-enriched membrane platforms that serve to release ROS upon infection. ROS keep the activity of the acid sphingomyelinase high leading to enhanced formation of ceramide-enriched membrane platforms and further ROS-release in a positive feed-forward loop.

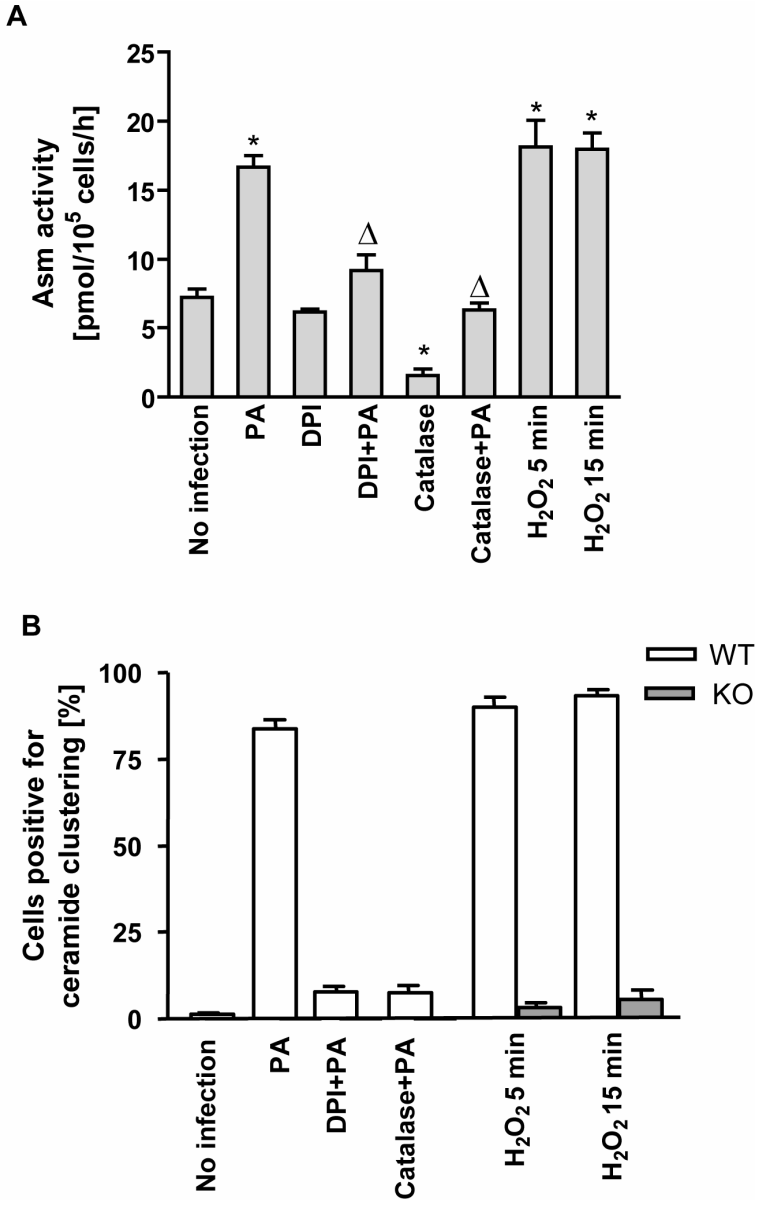

Figure 4.5 Redox regulation of acid sphingomyelinase (Asm) activation and ceramide-enriched membrane platform formation.

Macrophages were left untreated or treated with a NADPH oxidase inhibitor, DPI (50 µM) or a H_2O_2 degrading enzyme, catalase (10 unit/ml) for 30 min. Cells were infected with *P. aeruginosa* ATCC 27853 (PA) for 15 min and applied for acid sphingomyelinase activity assay or confocal microscopy. In parallel, effects of H_2O_2 (1 mM for 5 and 15 min) on acid sphingomyelinase activity and ceramide-enriched membrane platform formation were examined. (A) Acid sphingomyelinase activation upon infection was blocked by NADPH oxidase inhibition (DPI+PA) or ROS scavenging (catalase+PA), while enhanced oxidative stress by H_2O_2 increased acid sphingomyelinase activity. (B) Formation of ceramide-enriched membrane platforms was prevented by DPI and catalase. Further, acid sphingomyelinase activity is required for oxidative stress-induced formation of ceramide-enriched membrane platform since H_2O_2-induced ceramide clustering was observed in wild type, but not *Smpd1*$^{-/-}$ cells. Data for panels A and B are mean ± SD of three independent experiments. Significant differences between infected or H_2O_2 treated cells and non-infected controls were determined by *t*-test and are indicated by asterisk. Significant differences between infected cells treated with DPI or catalase and left untreated were determined by *t*-test and indicated by delta ($P<0.05$).

4.1.6 *P. aeruginosa*-induced activation of JNK is acid sphingomyelinase- and ROS-dependent

Ceramide and ROS have been reported to activate JNK (Verheij et al., 1996; Haimovitz-Friedman et al., 1997; Basu et al., 1998; Shen et al., 2004). Therefore, we examined whether acid sphingomyelinase-mediated redox signaling is involved in *P. aeruginosa*-induced JNK activation. Alveolar macrophages were infected and lysed in 1x SDS sample buffer. JNK activation upon *P. aeruginosa* infection was detected in wild type cells as early as 5 min after infection, with maximum levels reached approximately 30 min after initiation of the infection (**Figure 4.6A**), while genetic deficiency of the acid sphingomyelinase prevented JNK activation by *P. aeruginosa* infection. Likewise, wild type cells treated with the NADPH oxidase inhibitor DPI (**Figure 4.6A**) failed to activate JNK after *P. aeruginosa* infection. Further, *P. aeruginosa* infection induced phosphorylation and nuclear translocation of c-Jun in wild type cells, which was also inhibited by DPI (**Figure 4.6B**).

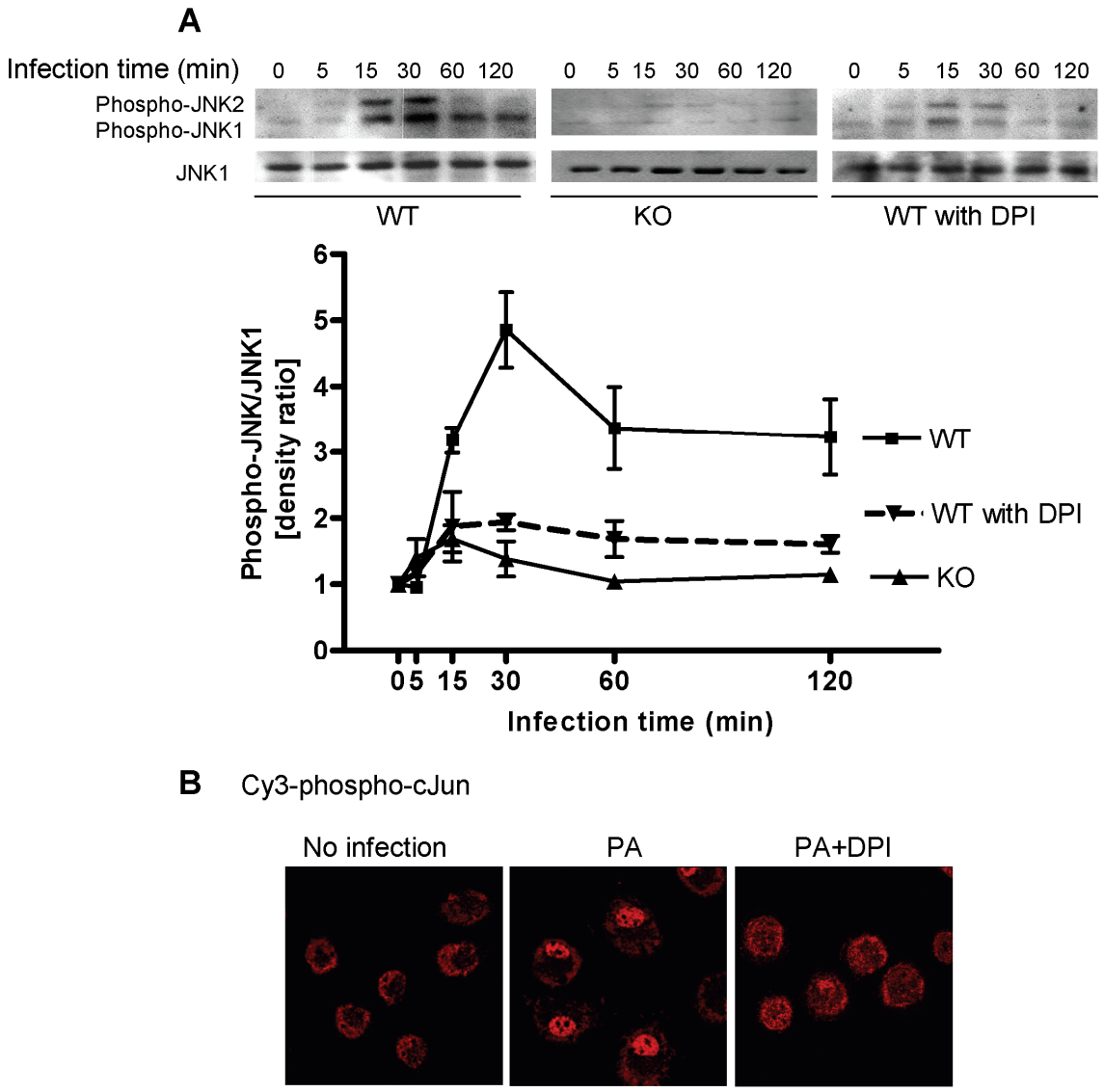

Figure 4.6 Role of acid sphingomyelinase-mediated ROS in *P. aeruginosa*-induced JNK activation.

(A) JNK activation requires acid sphingomyelinase and NADPH oxidase activation. Alveolar macrophages isolated from wild type or *Smpd1*$^{-/-}$ mice were infected with *P. aeruginosa* for indicated times and JNK activation was evaluated by Western blot analysis of phosphorylated isoforms p46 JNK1 (46 kDa, lower band) and p54 JNK2 (54 kDa, upper band). JNK activation was also evaluated in wild type cells pretreated with DPI (50 µM) for 30 minutes. JNK1 was probed as loading control. Density of the bands was scanned, quantified and relative phospho-JNK densities were normalized to the amount of JNK1. Summarized data for panels A are mean ± SD from each four independent experiments

(B) c-Jun activation depends on NADPH oxidase activation. Wild type cells were treated with DPI (50 µM) for 30 minutes or left untreated, infected, permeabilized and stained with Cy3-labeled anti-phospho-c-Jun antibodies. c-Jun activation was evaluated by nuclear detection of phosphorylated c-Jun.

4.2 Role of Cftr in determine lysosomal pH in alveolar macrophages

4.2.1 Cftr deficiency results in lysosomal alkanlization in lung alveolar macrophages

To determine whether *Cftr* deficiency affects lysosomal pH, we stained freshly isolated alveolar macrophages with LysoSensor Green DND-189, which accumulates in acidic organelles and exhibits green fluorescence. The results demonstrated that *Cftr*-deficient macrophages obtained from $Cftr^{MHH}$ mice exhibit much lower fluorescence intensity than do wild-type cells. This finding indicates that *Cftr* deficiency impairs the acidification of these vesicles (**Figure 4.7A**). Bafilomycin is known to specifically inhibit vacuolar type H^+-ATPase and, therefore, to elevate lysosomal pH (Banta et al, 1988). Pretreatment of cells with bafilomycin decreased LysoSensor fluorescence intensity in both wild-type and $Cftr^{MHH}$ cells (**Figure 4.7A**). To obtain a standard curve for LysoSensor Green DND-189 fluorescence, we permeabilized the cells with nigericin and incubated the cells that were previously stained with LysoSensor Green DND-189 in a calibration buffer with pH values ranging from 4.5 to 6.5. We found that the relative fluorescence of the LysoSensor Green DND-189 staining was linear over the investigated range of pH (**Figure 4.7B**). A linear, pH-dependent decrease of intracellular LysoSensor Green DND-189 fluorescence was observed in both wild-type and $Cftr^{MHH}$ cells. FACS analysis confirmed that bafilomycin decreased LysoSensor Green DND-189 fluorescence in wild-type macrophages (**Figure 4.7C**).

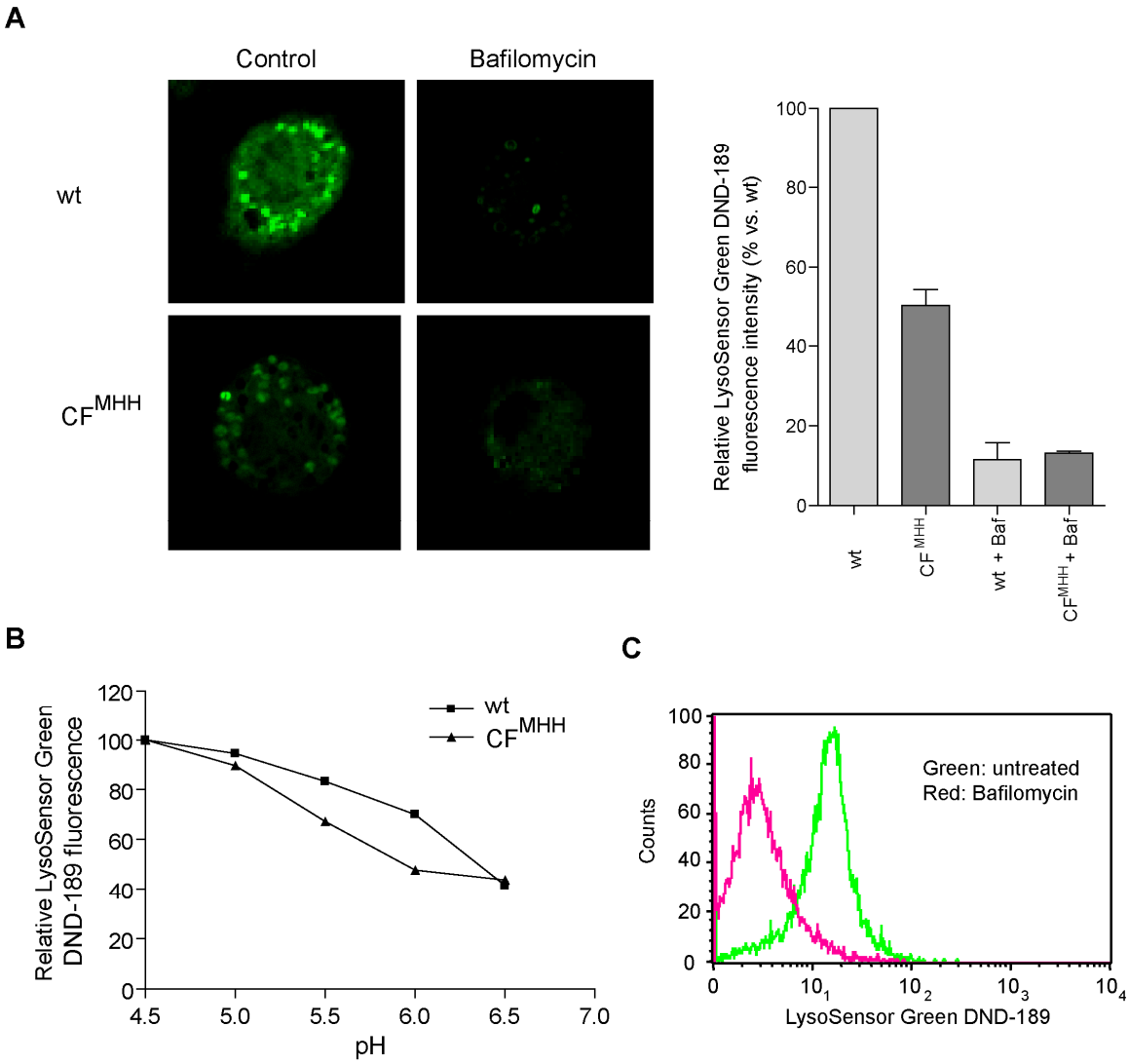

Figure 4.7 Cftr deficiency increases the pH of lysosomes

(**A**) Wild-type (wt) or *Cftr*-deficient (CF^{MHH}) macrophages were treated with bafilomycin (100 nM) for 30 min or left untreated. They were then stained with LysoSensor Green DND-189 and analyzed by fluorescence microscopy. Representative fluorescence images or the mean ± SD from four independent experiments are shown.
(**B**) Macrophages were loaded with LysoSensor Green DND-189 and incubated with or without a calibration buffer adjusted to pH values ranging from 4.5 to 6.5. Relative LysoSensor Green DND-189 fluorescence of samples with calibration buffer was calculated as the percentage of samples with a pH of 4.5. The results were repeated 3-times with similar results.
(**C**) The panel displays a representative histogram produced by flow cytometric analysis of LysoSensor Green DND-189 fluorescence in wild-type macrophages with or without pretreatment with bafilomycin. The data are representative of those from three independent experiments.

4.2.2 Cftr regulates lysosomal pH of a sub-population of vesicles that stain differentially with LysoSensor Green DND-189 and TMR-dextran

Next, we compared LysoSensor Green DND-189 staining of macrophages with TMR-dextran labeling of wild-type and *Cftr*^{MHH} macrophages. Cells were incubated cells with 1 mg/mL TMR-dextran and then stained with LysoSensor Green DND-189 (1 μM). The results show that LysoSensor Green DND-189 and TMR-dextran stain distinct vesicles (**Figure 4.8A**). Further, Cftr deficiency decreased LysosSensor DND-189 staining but had no effect on TMR-dextran staining (**Figure 4.8A**). The higher concentrations (1 mg/mL) of the weak base TMR-dextran very likely alkalinized the vesicles and thus prevented staining with LysoSensor Green DND-189, therefore, we also stained cells at lower concentrations of TMR-dextran (10, 20, 50, 200 μg/mL). As shown in **Figure 4.8B**, all vesicles that stained with TMR-dextran also stained with LysoSensor Green DND 189, but not all LysoSensor Green DN189-positive vesicles were also positive for TMR-dextran. Thus, these results indicate very clearly that Lysosensor Green DND-189 stains two populations of intracellular vesicles, one that is also stained by TMR-dextran and one that is not stained with TMR-dextran and probably consists of secretory lysosomes that are not stained with dyes that require internalization, such as TMR-dextran. *Cftr* deficiency substantially decreased the fluorescence intensity of LysoSensor Green DND-189 in these vesicles.

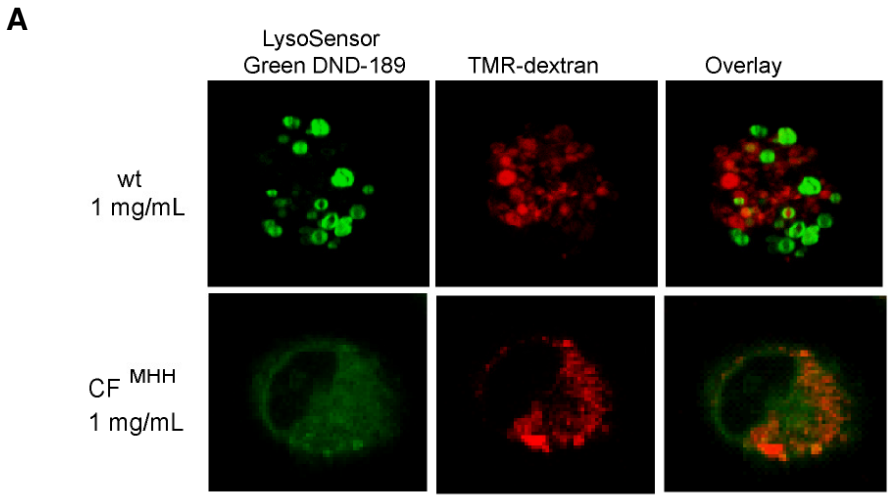

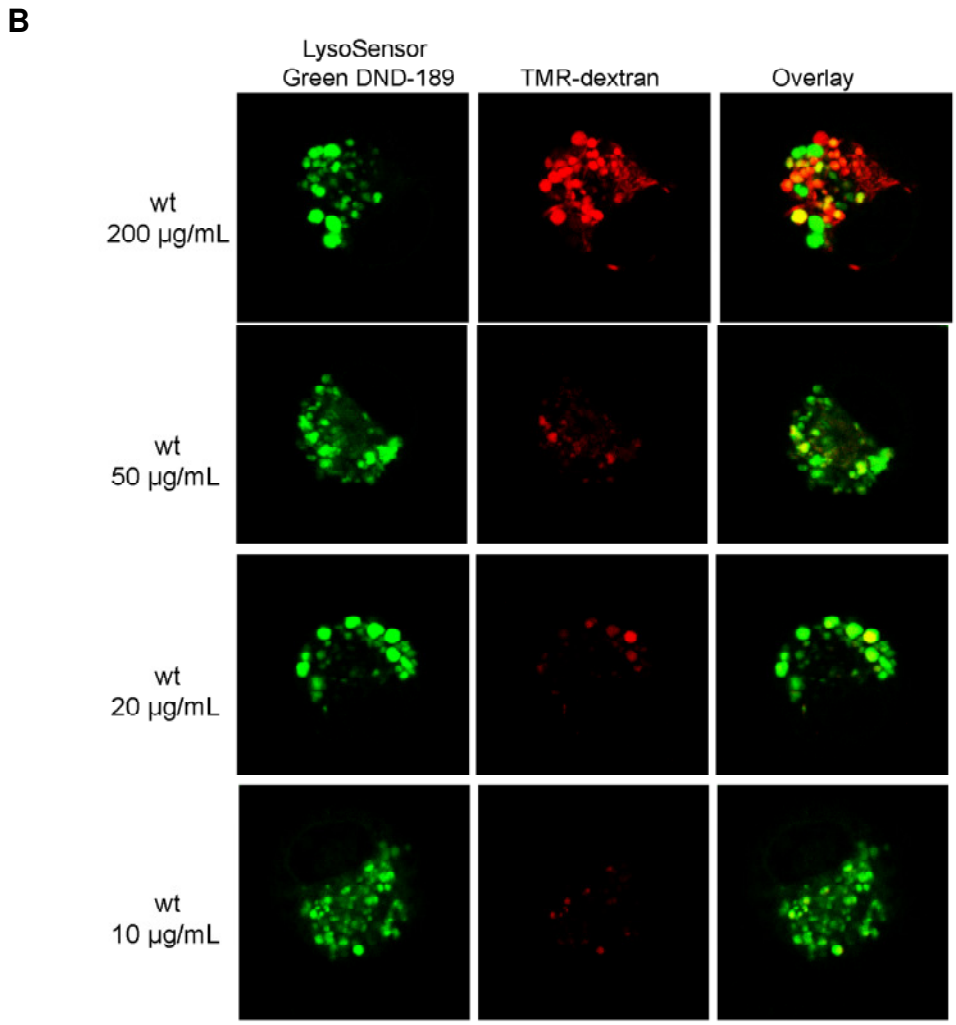

Figure 4.8 Lysosensor Green DND-189 targets a specific vesicle population that are not stained with TMR-dextran.

(**A**) Wild-type (wt) or *Cftr*-deficient (CF^{MHH}) macrophages were loaded with TMR-dextran (1 mg/mL) and then stained with LysoSensor Green DND-189 and analyzed by fluorescence microscopy. Representative fluorescence images from four independent experiments are shown.
(**B**) To determine which vesicles are stained with LysoSensor Green DND-189 and which with tetramethylrhodamine (TMR)-dextran, we loaded wild-type macrophages with lower concentration of concentrations of TMR-dextran and then stained them with LysoSensor Green DND-189. The results show that LysoSensor Green DND-189 also stains a vesicle population, which is not stained with TMR-dextran. Representative confocal fluorescence images from three independent experiments are shown.

4.2.3 Cftr deficiency does not affect total uptake or retention of Lysosensor probes

To exclude the possibility that *Cftr*-deficient cells have defects in the uptake or retention of LysoSensor probes, we stained 5×10^4 cells with LysoSensor Green DND-189, disrupted the cells in 200 µL pH calibration buffer (pH = 4 or 6.5) containing 1% Triton X-100, and then measured the total fluorescence intensity of the lysate with a fluorescence microplate reader (BMG Systems, Offenburg, Germany). No difference was found in the total fluorescence intensity of LysoSensor Green DND-189 between wild-type and *Cftr*-deficient cells either at an acidic pH of 4 or at a higher pH of 6.5 (**Figure 4.9A**).

We also stained the cells with LysoSensor Green DND-153, which exhibits bright fluorescence only at a neutral pH. The results demonstrated that at least some vesicles of *Cftr*-deficient macrophages exhibit a higher fluorescence intensity of LysoSensor Green DND-153 than do the vesicles of wild-type cells (**Figure 4.9B**). These data indicate that *Cftr* deficiency results in pH changes in some vesicles rather than in an alteration in the uptake or retention of LysoSensor probes.

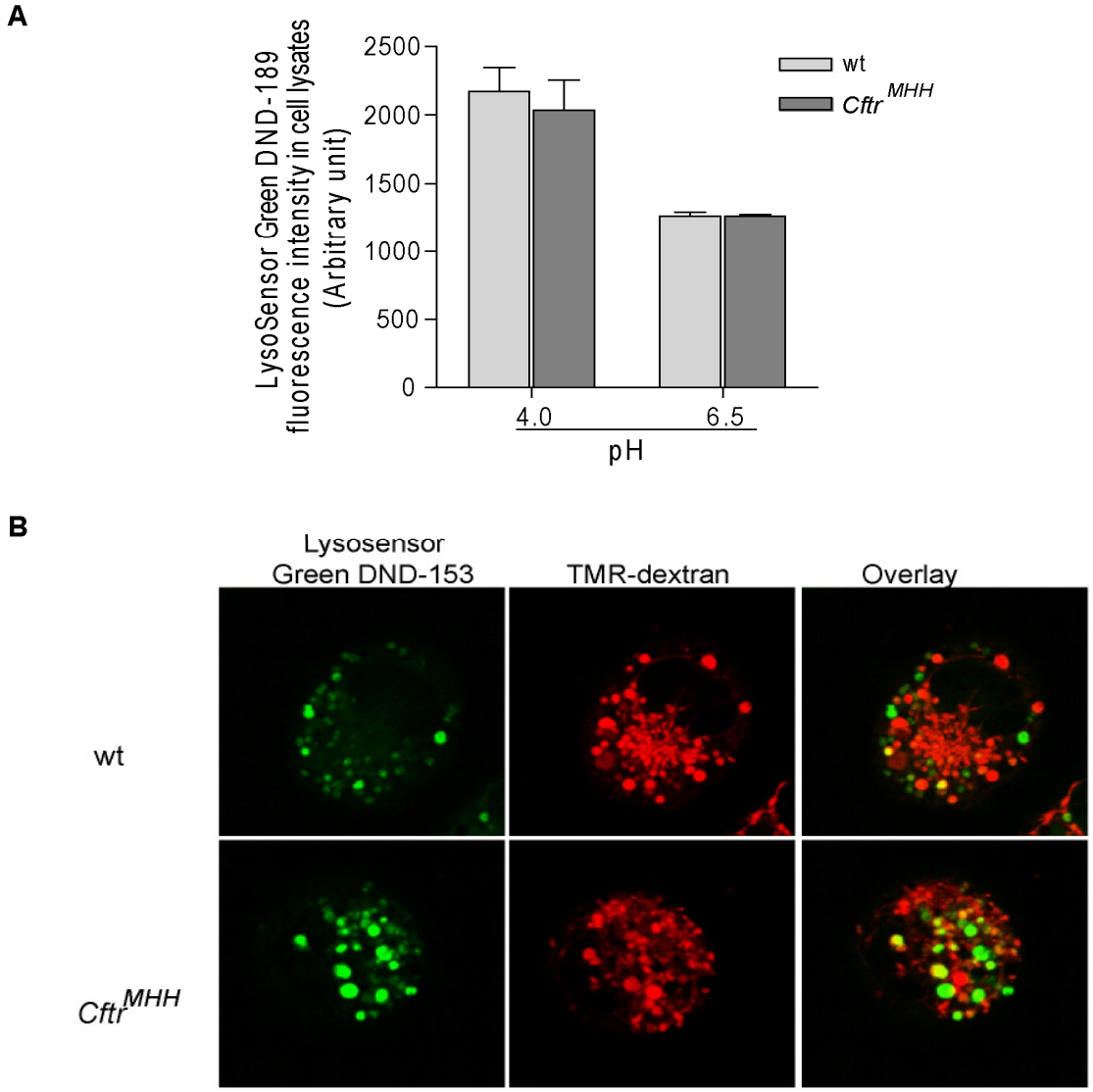

Figure 4.9 Effect of Cftr deficiency on uptake and retention of LysoSensor probes and lysosome biogenesis.

(**A**) Wild-type and *Cftr*-deficient (*Cftr*^{MHH}) macrophages were loaded with LysoSensor Green DND-189 and lysed in pH calibration buffer (pH = 4.0 or 6.5) containing 1% Triton X-100. Total LysoSensor Green DND-189 fluorescence was then determined with a fluorescence microplate reader. Results are shown as the mean ± SD of 4 independent experiments.
(**B**) Macrophages were stained with TMR-dextran and LysoSensor Green DND-153, which is fluorescent at neutral pH. Representative confocal fluorescence images from three independent experiments are shown.

4.2.4 Cftr localizes within LAMP-1-positive vesicles

To determine whether Cftr resides in lysosomal membranes, we double-stained cells for Cftr and lysosomal-associated membrane protein 1 (LAMP1). The results demonstrated that Cftr co-localizes with LAMP1 in some but not all vesicles of freshly isolated lung macrophages; this finding suggests that lysosomal membrane–associated Cftr directly contributes to the control of pH in lysosomes (**Figure 4.10**). No difference in LAMP1 staining was found between wild-type and *Cftr*-deficient macrophages, a finding suggesting that lysosome biogenesis is not changed by *Cftr* deficiency (**Figure 4.10**). The fact that *Cftr*-deficient cells do not stain with the anti-*Cftr* antibodies indicates the specificity of the staining.

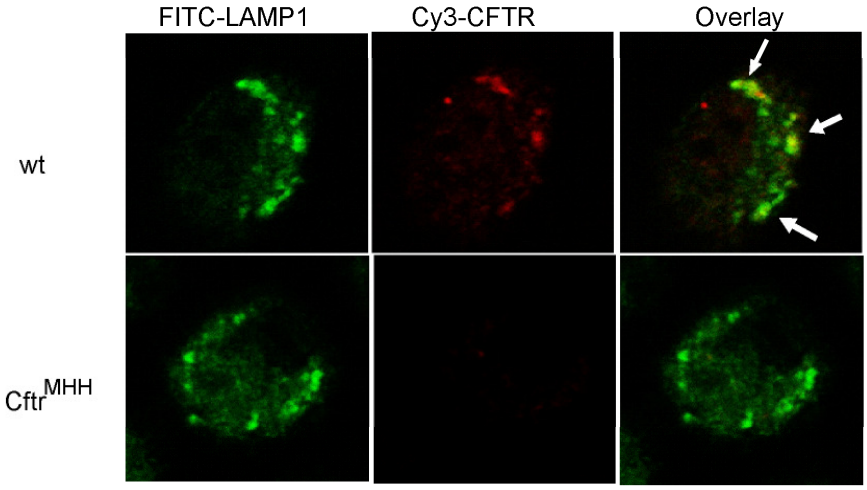

Figure 4.10 Effect of Cftr deficiency on lysosome biogenesis.

Macrophages were fixed, permeabilized, and stained with FITC-labeled anti-LAMP1, Cy3-labeled anti-Cftr, or both. Representative fluorescence images from three independent experiments are shown.

4.3 Role of Cftr in ceramide-mediated ROS production during pulmonary *P. aeruginosa* infections of alveolar macrophages

4.3.1 Cftr deficiency results in ceramide accumulation in lung alveolar macrophages

We have previously shown that *Cftr*-deficient epithelial cells accumulate ceramide (Teichgräber et al., 2008). We suggested that the impaired acidification of vesicles, cellular compartments, or both may cause an imbalance in the activities of acid sphingomyelinase and acid ceramidase, and that this imbalance may result in the accumulation of ceramide (Teichgräber et al., 2008). However, it is unknown whether ceramide also accumulates in *Cftr*-deficient macrophages. To confirm ceramide accumulation in *Cftr*-deficient macrophages, we performed DAG kinase assays that determine total cellular ceramide concentrations. We detected a substantial increase in ceramide concentrations in $Cftr^{MHH}$ and $Cftr^{KO}$ macrophages (**Figure 4.11**).

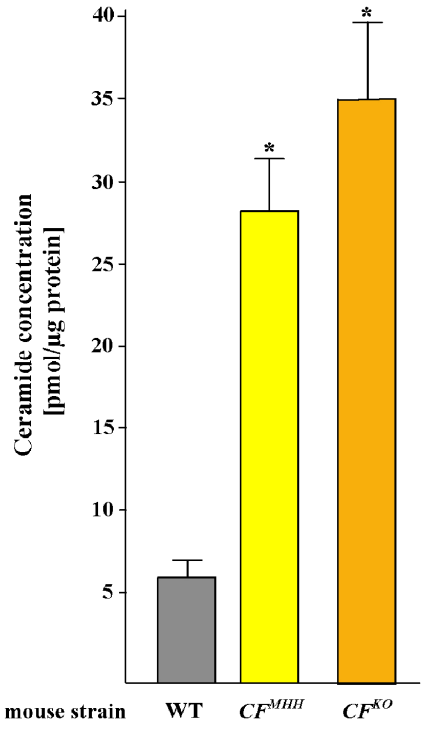

Figure 4.11 Cftr deficiency results in ceramide accumulation.

Diacylglycerol (DAG) kinase assays of total cellular ceramide contents demonstrate increased total levels of ceramide in *Cftr*-deficient (CF^{MHH} and CF^{KO}) macrophages compared to wild-type macrophages. Data are presented as the mean ± SD of results from 3 independent experiments. Significant differences of samples from *Cftr*-deficient compared to wild-type samples were determined by one-way ANOVA followed by a Bonferroni post-hoc t-test and are indicated by an asterisk (*) ($P < 0.05$).

4.3.2 Ceramide in wild-type and Cftr-deficient macrophages before and after infection with *P. aeruginosa*

The ceramide levels in macrophages were also determined by con-focal fluorescence microscopy. Wild-type and *Cftr*-deficient alveolar macrophages obtained from $Cftr^{MHH}$ mice were permeabilized and stained with anti-ceramide antibodies. We detected a marked accumulation of cellular ceramide in uninfected *Cftr*-deficient cells compared to wild-type cells (**Figure 4.12**). Infection with *P. aeruginosa* increased intracellular ceramide staining in wild-type cells but had only a minimal effect on ceramide concentrations in $Cftr^{MHH}$ macrophages (**Figure 4.12**). Infection with *P. aeruginosa* increased intracellular ceramide staining in wild-type cells but had only a minimal effect on ceramide concentrations in $Cftr^{MHH}$ macrophages (**Figure 4.12**).

The data in **Figure 4.2** have demonstrated that the activation of acid sphingomyelinase and the release of ceramide upon infection with *P. aeruginosa* trigger the release of ROS in macrophages. We therefore investigated whether *P. aeruginosa* infection induces co-localization of ceramide with $gp91^{phox}$, an important membrane-bound subunit of NADPH oxidase, in vesicles of wild-type cells, and whether Cftr is involved in the co-localization of $gp91^{phox}$ and ceramide. The results show that *P. aeruginosa* triggers co-localization of $gp91^{phox}$ and ceramide in wild-type macrophages. Some degree of co-localization of $gp91^{phox}$ and ceramide was observed in $Cftr^{MHH}$ macrophages before infection with *P. aeruginosa* (**Figure 4.12**). However, infection failed to induce further co-localization of $gp91^{phox}$ and ceramide.

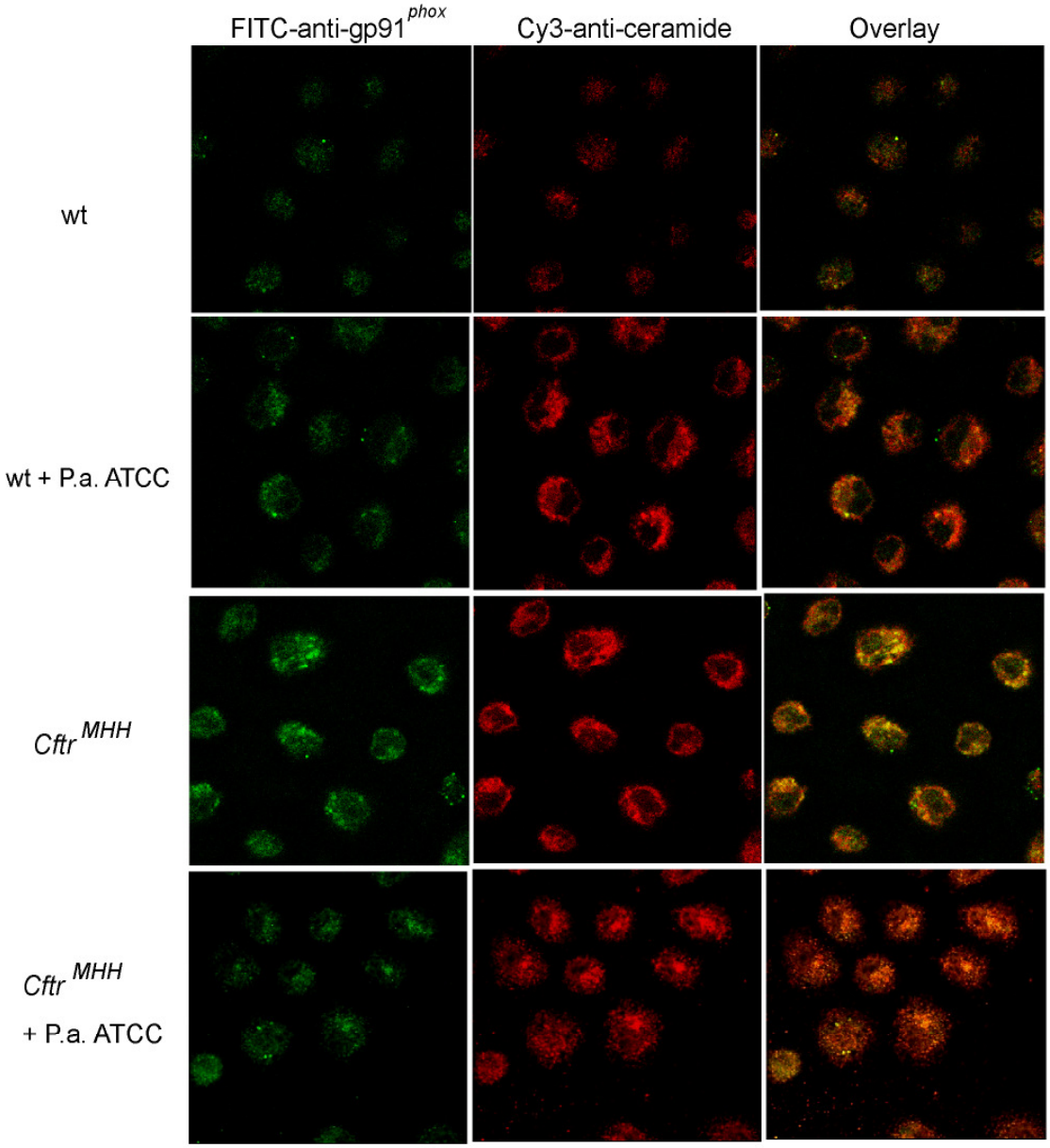

Figure 4.12 Cftr deficiency results in ceramide accumulation and co-localization with gp91phox.

Macrophages were infected with *P. aeruginosa* strain ATCC 27853. For detection of intracellular ceramide and gp91^{phox}, cells were washed, fixed, permeabilized, and stained with Cy3-labeled ceramide and FITC-labeled gp91^{phox} antibodies. Shown are representative confocal fluorescence microscopic images of wild-type and *Cftr*-deficient (*Cftr*^{MHH}) cells that were either left uninfected or infected with *P. aeruginosa* (Pa; multiplicity of infection [MOI] = 100) for 15 min (n = 3). Representative fluorescence images from three independent experiments are shown.

4.3.3 Cftr deficiency impairs *P. aeruginosa*-induced clustering of gp91phox in ceramide-enriched membrane platforms

Previous studies have shown that ceramide molecules form ceramide-enriched membrane platforms in the plasma membrane and that these ceramide molecules are crucially involved in signal transduction events that are controlled by ceramide (Grassmé et al., 2001; Jin et al., 2008). To test whether *P. aeruginosa* infections trigger the formation of ceramide-enriched membrane domains in macrophages, we stained intact cells, i.e., cells that were not permeabilized, with anti-ceramide antibodies (**Figure 4.13**). The results show that *P. aeruginosa* induces massive clustering of ceramide in the plasma membrane of wild-type cells but that only very small ceramide-enriched membrane domains are observed in $Cftr^{MHH}$ macrophages infected with *P. aeruginosa* (**Figure 4.13**). Co-staining with anti-$gp91^{phox}$ antibodies revealed that $gp91^{phox}$ is localized within ceramide-enriched membrane domains in wild-type macrophages (**Figure 4.13**). In contrast, no increase in the co-localization of $gp91^{phox}$ and ceramide was observed in $Cftr^{MHH}$ macrophages upon infection with *P. aeruginosa* (please note that cells in **Figure 4.13** are not permeabilized). However, *Cftr* deficiency alone resulted in some co-localization of ceramide and $gp91^{phox}$ in the plasma membrane already in uninfected cells.

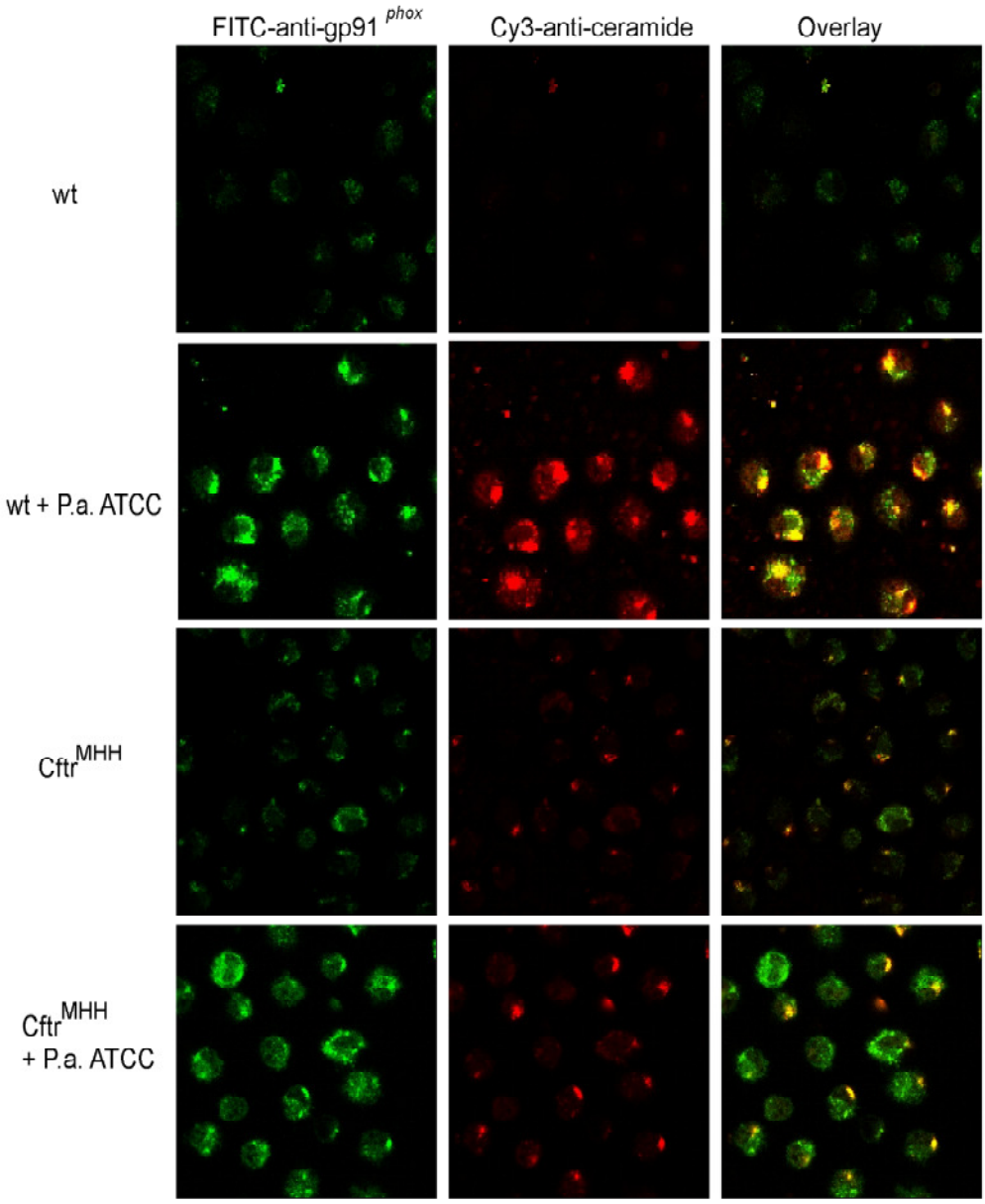

Figure 4.13 Cftr deficiency impairs *P. aeruginosa*-induced clustering of gp91phox in ceramide-enriched membrane platforms.

For detection of ceramide-enriched membrane platforms, macrophages were infected, fixed, and stained as in **Figure 4.12** except that no permeabilization was performed since ceramide clusters would not be observed in permeabilized cells. Representative fluorescence images from three independent experiments are shown.

4.3.4 *P. aeruginosa* -induced ROS release is Cftr-dependent

The impaired co-localization of $gp91^{phox}$ and ceramide in *Cftr*-deficient macrophages suggests that Cftr is also involved in the regulation of the release of ROS upon infection with *P. aeruginosa*. To examine ROS production by macrophages upon infection with *P. aeruginosa*, we loaded cells with H_2DCF, an ROS probe and infected them with *P. aeruginosa* in the absence or presence of the ROS scavengers SOD and catalase. When the cells were not infected, there was no significant difference between wild-type and *Cftr*-deficient cells in the increase of DCF fluorescence, although ROS production was slightly increased in $Cftr^{MHH}$ cells. Infection with *P. aeruginosa* ATCC 27853 or PAO1 induced a substantial increase in DCF fluorescence in wild-type macrophages including ROS production but not in $Cftr^{MHH}$ macrophages (**Figure 4.14**).

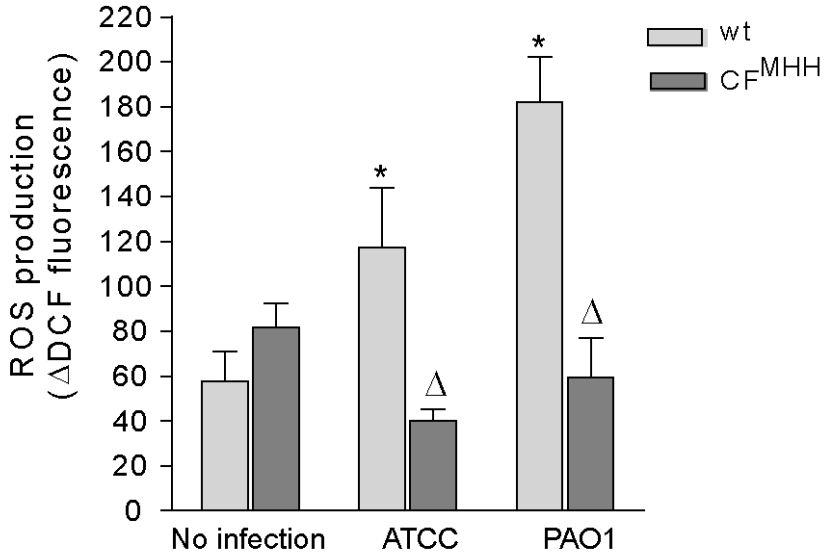

Figure 4.14 Cftr deficiency impairs the production of reactive oxygen species by macrophages

Macrophages were loaded with 2',7'-dichlorofluorescin (DCF), an ROS probe. The cells were then infected with *P. aeruginosa* ATCC 27853 or PAO1 strains (multiplicity of infection [MOI] = 100) for 1 h in the presence or absence of 100 U/ml superoxide dismutase (SOD, an ROS scavenger) and 10 U/ml catalase. The change in DCF fluorescence was determined by using flow cytometry to measure the mean fluorescence intensity "**F.**" Relative ROS production induced by *P. aeruginosa*, as indicated by the change in the fluorescence of 2',7'-dichlorofluorescin (DCF), was calculated by using the following formula: ΔDCF fluorescence = $\mathbf{F}_{[PA]}$-$\mathbf{F}_{[SOD+catalase+PA]}$ (Arbitrary Unit) where PA stands for *P. aeruginosa*. Data are presented as the mean ± SD of results from four independent experiments. Significant differences between infected samples and uninfected controls were determined by one-way ANOVA followed by Bonferroni post-hoc t-test (*, $P < 0.05$). Significant differences between infected wild-type cells and infected *Cftr*-deficient cells were determined by Student t-test (Δ, $P < 0.05$).

4.3.5 Cftr deficiency and inhibition of NADPH oxidase impair bactericidal capability of macrophages

To determine whether the impaired release of ROS by *Cftr*-deficient macrophages after infection with *P. aeruginosa* decreases the bactericidal capability of these macrophages, we incubated cells with *P. aeruginosa* at a low MOI (MOI = 1). Extracellular or attached bacteria were washed off by PBS and then intracellular survival of bacteria were determined as described in Method section. As shown in **Figure 4.15**, wild-type macrophages eliminated approximately 50% of the bacteria within 60 min when infected with *P. aeruginosa* ATCC 27853, whereas $Cftr^{MHH}$ macrophages failed to kill the bacteria. Similar results were obtained with lung macrophages from $Cftr^{KO}$ mice. The failure of *Cftr*-deficient macrophages to kill *P. aeruginosa* ATCC 27853 was mimicked by treating wild-type macrophages with the NADPH oxidase inhibitor apocynin. Similar results were found when wild-type or *Cftr*-deficient cells were infected with *P. aeruginosa* PAO1. Taken together, these findings indicate the importance of ROS for the killing of *P. aeruginosa* by macrophages.

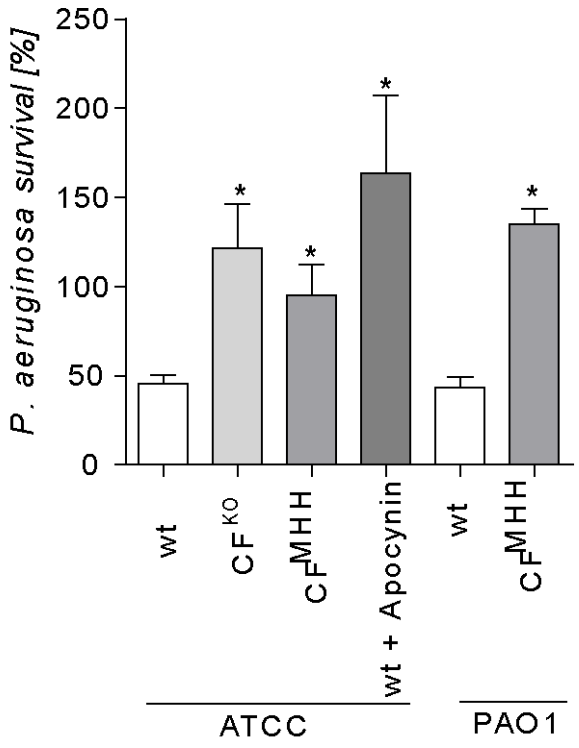

Figure 4.15 Cftr deficiency impairs the bactericidal capability of macrophages

The survival of *P. aeruginosa* ATCC 27853 or PAO1 strains in macrophages after infection for 60 min is displayed. As indicated, the macrophages were pretreated with apocynin (100 µM). Data are presented as the mean ± SD of results from three independent experiments. Significant differences between *P. aeruginosa* ATCC 27853-infected *Cftr*-deficient cells or wild-type cells treated with apocynin and wild-type controls were determined by one-way ANOVA followed by Bonferroni post-hoc t-test. Significant differences between *P. aeruginosa* PAO1-infected *Cftr*-deficient cells and wild-type controls were analyzed by Student t-test. Significant differences ($P < 0.05$) are indicated by asterisks (*).

4.3.6 *P. aeruginosa*–induced cytokine release is Cftr-independent

Lung alveolar macrophages also play a crucial role in the production of cytokines during innate immune responses. Thus, we examined whether *Cftr*-deficient macrophages exhibit defects in cytokine production upon infection with *P. aeruginosa*. However, wild-type and *Cftr*-deficient macrophages produced similar amounts of KC and MIP2 during a 2 h infection with *P. aeruginosa* ATCC 27853 or PAO1 (**Figure 4.16**A and B). These data suggest that the production of at least some cytokines (i.e., KC and MIP2) is not a consequence of *Cftr*-deficiency in macrophages.

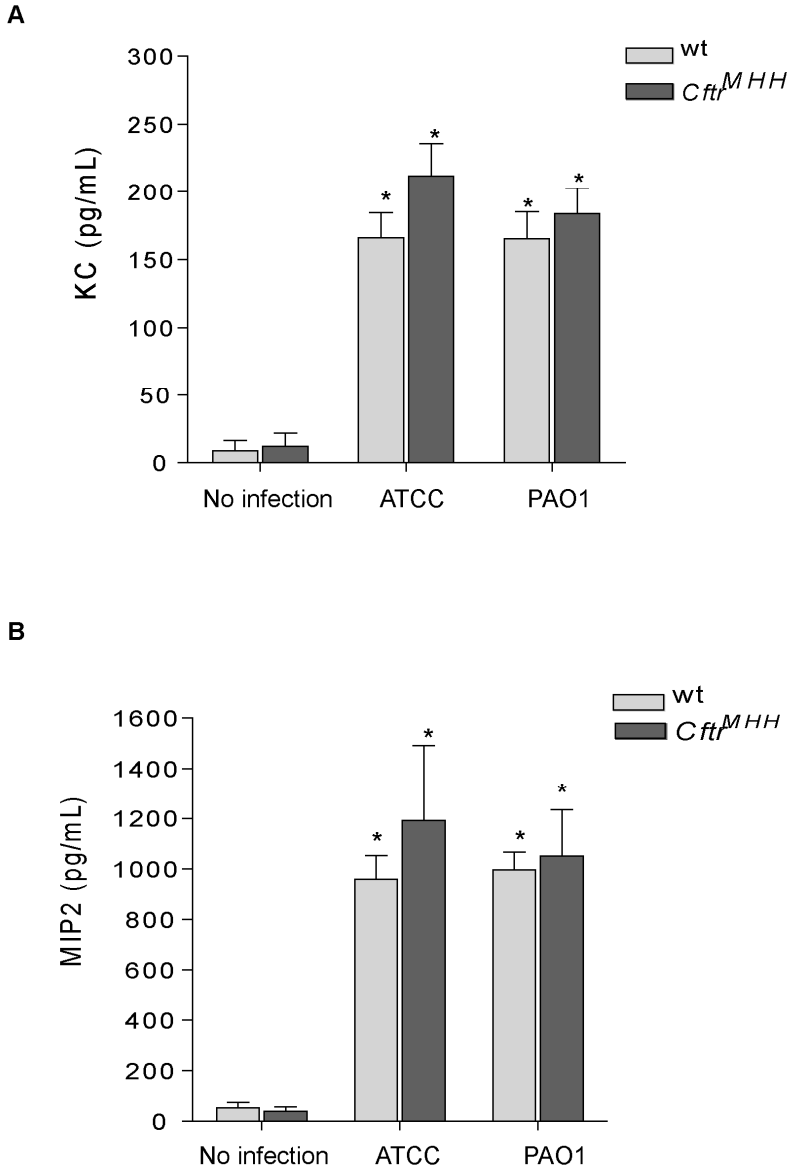

Figure 4.16 Effects of Cftr deficiency on KC and MIP2 release by alveolar macrophages upon infection with *P. aeruginosa*

Macrophages were infected with *P. aeruginosa* ATCC 27853 or PAO1 strains for 2 h. Cytokine levels of KC (**A**) and MIP2 (**B**) in the supernatants were measured with ELISA kits (R&D Systems). Significant differences between infected wild-type or *Cftr*-deficient cells and uninfected wild-type or *Cftr*-deficient controls were determined by one-way ANOVA followed by Bonferroni post-hoc t-test and are indicated by asterisks (*), ($P < 0.05$).

5. DISCUSSION

5.1 Discussion of the Methods

5.1.1 Determination of acid sphingomyelinase activity in cell lysates

The enzymatic activity of sphingomyelinase can be assayed by determining the conversion of sphingomyelin to ceramide and phosphorylcholine. However, different methods are used for assaying purified sphingomyelinase and cell lysates. For assaying purified sphingomyelinase, natural or synthetic sphingomyelin is prepared, pure or mixed with other lipids, in the form of extruded large unilamellar vesicles approximately 100 nm in diameter (Richards et al., 1986). When large unilamellar vesicles are assayed with sphingomyelinase, ceramide production in the bilayers leads to vesicle aggregation, which in turn produces an increase in turbidity or light scattering in the suspension. Thus the reaction can be followed in real time just by measuring the increase in turbidity (absorbance at 500 nm) or in light scattering (e.g. with a fluorometer with both the excitation and emission monochromators adjusted at 500nm).

Assaying sphingomyelinase activity in cell lysates requires that sphingomyelin be labeled, radioactively, fluorescently or otherwise. In the present study, the enzymatic activity was measured as the degradation of radioactive [^{14}C]-sphingomyelin to ceramide and [^{14}C]-phosphorylcholine. Because [^{14}C]-phosphorylcholine is soluble in water, it is easily separated from the substrate [^{14}C]-sphingomyelin and ceramide, which stays in organic phase following extraction. Sphingomyelin serves as substrate for three forms of sphingomyelinases that manifest acid, neutral or basic pH optima for maximal enzyme activity (Hannun, 1996). In the present study acid sphingomyelinase activity was discriminated from the neutral or basic sphingomyelinase activity by performing the assay at pH 5.0. Because of the difficulty in bringing together the enzyme and substrate molecules in the presence of cell homogenates, a suitable detergent, such as Triton X-100 was used. It should be noted that, apart from emulsifying the substrate, the detergents bind and modify the enzyme activity, thus detergent concentration and initial detergent : substrate ratio was kept constant for reproducibility of assays. Finally, it has been suggested that the acid sphingomyelinase may be located in detergent-resistant/insoluble fractions; thus, for determination of acid sphingomyelinase activity in whole-cell lysates,

no centrifugation step was performed after lysis and sonication of the cells to prevent pelleting and loss of the acid sphingomyelinase.

5.1.2 Ceramide measurement by DAG-kinase assay

In the literature, there are several methods reported for quantifying ceramide such as normal phase HPLC analysis after derivatization with a fluorescent tag (Iwamori et al., 1979; Previati et al., 1996; Yano et al., 1998; Couch et al., 1997), evaporative light-scattering detection (McNabb et al., 1999), HPTLC analysis (Motta et al., 1994), or using cells labeled with radioactive precursors (Tepper et al., 2000; Allan, 2000). Ceramide molecular species can be determined following hydrolysis and analysis of the liberated and derivatized sphingoid bases by means of HPLC (Smith and Merril, 1995; Nishimura and Nakamura, 1985) and fatty acids by means of GC/MS (Samuelsson and Samuelsson, 1970). New quantitative analysis of ceramide molecular species are based on HPLC or RP-HPLC separation of their fluorescent analogs prepared after derivatization with anthroyl cyanide (Yano et al., 1998), benzoyl chloride (Couch et al., 1997), or benzoic anhydride (Iwamori et al., 1979). Moreover, mass spectrometry methodologies have been developed for the detection of molecular species of ceramide (Watts et al., 1999; Couch et al., 1997; Allan D., 2000; Kalhorn and Zager, 1999; Mano et al., 1997; Gu et al., 1997; Liebisch et al., 1999; Karlsson et al., 1998). However, most of these methods require long periods of processing and/or analysis.

The DAG-kinase assay is a widely used method for the rapid quantification of ceramides. The primary advantages of the DAG kinase assay are the measurement of total mass levels of ceramide; the use of crude lipid extracts in the assay; and the ability of process a large number of samples in a rapid manner. DAG kinase was used as an analytical tool in measuring diglyceride levels by the demonstration of a linear relationship between the amount of diglyceride added to an *in vitro* assay and the amount of product (phosphatidic acid) formed. Ceramides share structural similarities with diglycerides, and Schneider and Kennedy reported that bacterial DAG kinase can utilize ceramide as a substrate with a K_m nearly five times greater than that for diglyceride (Schneider and Kennedy, 1973). Early attempts to use DAG kinase to quantify ceramide revealed a linear but non-quantitative relationship between substrate added and product formed. Further modification of the assay demonstrated that DAG kinase could also be used for quantitative conversion of ceramide to ceramide-1-phosphate over a range of 25 pmol to 2 nmol (van Veldhoven et al.,

1995). These refinements have required special emphasis on the protocol of lipid extraction, purity of the reagents used for the preparation of the mixed micelles and on the development of high levels of recombinant DAG kinase.

Because ceramide is highly hydrophobic, it should be extracted from cells in organic solvents. Thus, the cells are lysed in a solution containing chloroform and methanol. Acidification of lysates with hydrochloric acid helps extraction of shorter acyl chain ceramide-1-phosphates or hydroxylated ceramides. For the DAG kinase reaction, it is critical that the substrate is in a soluble form for optimal conversion to product by the enzyme. Mixed micelles containing a non-ionic detergent, such as n-octyl-ß-D-glucopyranoside, and a phosholipid, such as cardiolipin, are utilized for this purpose. Of particular importance is the level of ceramide conversion to ceramide-1-phosphate. For the DAG kinase assay to yield reliable quantitative results, the reaction must go to completion with total conversion of DAG and ceramide. Otherwise, the results become sensitive to the effects of the efficiency of the reaction (K_m and V_{max} consideration of the DAG kinase) and to possible 'competition' between DAG and ceramide as substrates. In the present study, an excess of enzyme and ATP was used which allowed linear and quantitative conversion and was sufficient for the phosphorylation of cellular ceramides as well as exogenously added ceramide.

5.1.3 Analysis of aggregated molecules and co-localized signals

The present study used fluorescent microscopical analysis to detect the co-localization of two molecules or two vesicles after staining with the respective fluorochrome-labeled antibodies or fluorescent markers. One application is to determine whether $gp91^{phox}$ clusters in ceramide-enriched membrane platforms. The major problem in detection of aggregated molecules onto the plasma membrane is the possibility of superposition of two or more membranes within the microscopical field of interest. This would lead to an amplification of the fluorescent signal and a false-positive result. To avoid this artifact, alveolar macrophages were plated with appropriate density and no clustered cells were observed in our preparation. Another critical point to detect membrane ceramide-enriched platforms is to avoid usage of detergents that usually used to permeablize cell membrane such as 0.1% Triton X-100.

When two or more stainings are performed simultaneously, the fluorescence signals might be recorded in one detection channel and might no longer be separated in the images. This is called 'cross-talk' of the fluorescence signals. Apart from preparing single-stained specimens as controls, 'sequential image analysis' of the respective samples by confocal microscopy was employed to rule out these false-positive data. The advantage of sequential analysis regarding multiple stainings lies in the ability to record a certain optical section using an instrument parameter settings (detection channel and excitation wavelength) adapted to one fluorochrome, before the system switches to different instrument parameter settings adapted for another fluorochrome. Therefore, this method is particularly useful to exclude the cross-talk between multiple fluorescent signals.

5.1.4 Bactericidal capability assay

To assay the capability of phagocytes to kill internalized *P. aeruginosa*, phagocytes are usually infected with high MOI of bacteria and then incubated with antibiotics such as gentamycin to kill extracellular bacteria. After removal of antibiotics by several washes, phagocytes are incubated further to allow intracellular killing of bacteria. This antibiotic-dependent method has been widely used based on the fact that the plasma membrane of mammalian cells are impermeable to antibiotics. However, there is concern that the antibiotics can enter into cells via endocytosis or phagocytosis and thereby affect killing of internalized bacteria. To avoid this artifact, the present study developed an antibiotic-free method. The alveolar macrophages were infected with low MOI of *P. aeruginosa* (MOI= 1). The usage of low MOI infection allows macrophages to phagocytose most of bacteria and subsequent easy removal of the extracellular bacteria.

5.2 Discussion of the Results

5.2.1 Role of acid sphingomyelinase and ceramide in redox signalling

The present study demonstrates that acid sphingomyelinase plays a critical role in *P. aeruginosa*-triggered ROS release. The results show that *P. aeruginosa* infection induces rapid activation of acid sphingomyelinase and consequent ceramide release in membranes of macrophages. *P. aeruginosa* induces respiratory ROS burst and time-dependent ROS accumulation in macrophages. These events were all absent in *Smpd1*$^{-/-}$ mice that are deficient in acid sphingomyelinase activity. Consistently, Reinehr and co-workers

demonstrated that inhibiting acid sphingomyelinase blocks the release of ROS, a finding suggesting that ROS functions downstream of acid sphingomyelinase in hepatocytes (Reinehr et.al., 2006). Similarly, inhibiting acid sphingomyelinase attenuates the ceramide and ROS production induced by histone deacetylase/perifosin, fenretinide, or sodium nitroprusside (Lovat et.al., 2004; Rahmani et.al., 2005; Sanvicens and Cotter, 2006). Taken together, these data confirmed the notion that acid sphingomyelinase activation and ceramide production are upstream signals of ROS production.

Ceramide induces the activation of ROS-generating enzymes, including NADPH oxidase, xanthine oxidase, NO synthase, and the mitochondrial respiratory chain (Corda et.al., 2001; Lecour et.al., 2006; Zhang et.al., 2001). In particular, ceramide has been shown to activate NADPH oxidase and to increase the production of ROS in a variety of mammalian cells, including human aortic smooth muscle cells and endothelial cells (Bhunia et.al., 1997; Zhang et.al., 2007). The precise mechanism that how ceramide activates NADPH oxidase is not well understood. Because NADPH oxidase activation requires aggregation of its subunits, it has been proposed that ceramide mediates the fusion of small raft domains to ceramide-enriched membrane platforms, which facilitate the aggregation of subunits of NADPH oxidase, thereby stimulating the production of ROS (Zhang et.al., 2006).

The present data suggest that a similar role of ceramide in NADPH oxidase activation exists in macrophages during *P. aeruginosa* infection. Inhibition of NADPH oxidase activity by DPI abolished *P. aeruginosa*-induced ROS production suggesting that NADPH oxidase is the major ROS-generating enzyme regulated by acid sphingomyelinase and ceramide in alveolar macrophages. The activation of acid sphingomyelinase results in release of ceramide that forms ceramide-enriched membrane platforms serving to aggregate NADPH oxidase and, thus, to produce ROS. These events were all absent in *Smpd1*$^{-/-}$ mice that are deficient in acid sphingomyelinase activity.

At present it is unknown how ceramide-enriched membrane platforms contribute to NADPH oxidase activation. It can be hypothesized that aggregation of subunits of NADPH oxidase in ceramide-enriched membrane platforms enhances interactions between subunits of NADPH oxidase, thereby stimulating the production of ROS. Ceramide in platforms may also directly enhance NADPH oxidase activity by activating small G protein Rac1/2 by activation of guanine nucleotide exchange factors (GEFs) such as Vav2 (Yi F et.al., 2007).

5.2.2 Role of ROS in acid sphingomyelinase activation

Several recent studies have demonstrated that the generation of ROS activates acid sphingomyelinase in response to various stimuli (Scheel-Toellner et.al., 2004; Charruyer et.al., 2005), which seems to conflict with the above conclusion that acid sphingomyelinase activation results in ROS production. This conundrum is discussed below and an amplifying concept is presented.

Scheel-Toellner and colleagues demonstrated that acid sphingomyelinase activation, ceramide generation, and CD95 clustering play a crucial role in the spontaneous apoptosis of neutrophils; apoptosis was substantially delayed in acid sphingomyelinase-deficient mice (Scheel-Toellner et.al., 2004). On the basis of the observation that the intracellular redox balance changes in aging neutrophils, the authors investigated the possibility that ROS may be involved in acid sphingomyelinase activation. Their study demonstrated that pretreating neutrophils with the antioxidants N-acetylcysteine and desferrioxamine substantially inhibited the events downstream of acid sphingomyelinase activation, such as ceramide generation and CD95 clustering, thus indicating that ROS release is required for acid sphingomyelinase activation (Scheel-Toellner et.al., 2004). Similarly, pretreatment with the antioxidant pyrrolidine dithiocarbamate abolished acid sphingomyelinase activation by ultraviolet (UV)-C light in U937 cells (Charruyer et.al., 2005).

Neuronal stimulation with soluble oligomers of amyloid-beta peptide results in the release of ROS and the subsequent activation of the sphingomyelinases (Malaplate-Armand et.al., 2006). The authors demonstrated that both the acid and the neutral sphingomyelinases play a crucial role in neuronal apoptosis induced by amyloid-beta oligomers, as shown by enzymatic activity assays, neutral and acid sphingomyelinase inhibitors, and antisense oligonucleotides for gene knockdown. Because treatment with antioxidant molecules and a $cPLA_2$-specific inhibitor or antisense oligonucleotide led to inhibition of sphingomyelinase activation and subsequent apoptosis, the results of their study suggest that amyloid-beta oligomers induce neuronal death by activating neutral and acid sphingomyelinases in a redox-sensitive $cPLA_2$-arachidonic acid pathway (Malaplate-Armand et.al., 2006).

Dumitru and colleagues have recently demonstrated the involvement of ROS in TRAIL-induced activation of acid sphingomyelinase and apoptosis (Dumitru et.al., 2006). Stimulation with TRAIL/DR5 led to the activation of acid sphingomyelinase and the

subsequent formation of ceramide-enriched membrane platforms, DR5 clustering, and, finally, apoptosis. Pretreatment with the antioxidants N-acetylcysteine and Tiron substantially inhibited TRAIL-induced acid sphingomyelinase activation, ceramide/DR5 clustering, and apoptosis, thus demonstrating the important role of ROS in this signaling pathway (Dumitru et.al., 2006). Finally, studies investigating the cellular effects of Cu^{2+} showed that Cu^{2+} also promotes the ROS-dependent activation of acid sphingomyelinase and leads to the death of hepatocytes (Lang et.al., 2007). The results of these studies demonstrate that the accumulation of Cu^{2+}, as in Wilson disease, activates acid sphingomyelinase in hepatocytes and triggers the release of ceramide in these cells. This process results in Cu^{2+}-induced hepatocyte death, which can be prevented by a deficiency in acid sphingomyelinase (Lang et.al., 2007).

The above-mentioned studies demonstrate that ROS are involved in the activation of acid sphingomyelinase; however, direct oxidation of the enzyme has been described only in a biochemical study by Qiu and co-workers (Qiu et al., 2003). The authors demonstrated that C-terminal cysteine (Cys^{629}) plays a crucial role in the enzymatic activity of recombinant human acid sphingomyelinase (rhASM). In particular, it appears that any change that causes a loss of the free sulfhydryl group on this amino acid also results in activation of the enzyme: i.e., copper-promoted dimerization of rhASM by C-terminal cysteine, thiol-specific chemical modification of this cysteine to form a mixed disulfide bond or a sulphur-carbon linkage, deletion of this cysteine by carboxypeptidase or recombinant DNA technology, and site-specific mutation to change the cysteine to a serine residue.

Because zinc is required for acid sphingomyelinase activity, the authors proposed a model that explains the effect of C-terminal cysteine modification on the activation of acid sphingomyelinase. In its low-activity form, free C-terminal cysteine is involved in active-site zinc coordination, either by competing with a water molecule for coordination with zinc or by forming a non-optimal 5-ligand coordination structure. Thus, C-terminal cysteine decreases zinc's ability to ionize water for the nucleophilic attack and decreases enzymatic activity. Because thiol is a better zinc ligand than water, the non-optimal structure may be energetically favorable as long as the cysteine is freely available. In the high-activity form of rhASM, however, the free cysteine is lost either by either chemical modification or by deletion and is no longer available for coordination. As a result, zinc coordinates with a water molecule to produce an optimal structure for catalysis. This model is essentially identical to the "cysteine switch" activation mechanism described previously

for the matrix metalloproteinase family (Van Wart et al., 1990). Although the "terminal cysteine" model could explain the effect of ROS on the mechanism of acid sphingomyelinase activation, the requirement of dimerization, further molecular events, or both for enzyme stimulation *in vivo* should be addressed in future studies.

In summary, these studies demonstrate that acid sphingomyelinase activity is regulated by ROS. Therefore, we proposed an amplification model for acid sphingomyelinase activation and ROS production upon *P. aeruginosa* infection. In this amplification model, initial activation of acid sphingomyelinase results in produce ROS, which further enhance activation of acid sphingomyelinase thus forms a feed-forward loop for ROS production.

5.2.3 Role of ceramide-enriched membrane platform in amplification of redox signaling

The present study demonstrates that ceramide-enriched platforms play a critical role in a feed-forward loop in amplifying NADPH oxidase-derived redox signaling. In this feed-forward loop, a primarily weak acid sphingomyelinase activation is enhanced by the production of ROS resulting in higher acid sphingomyelinase-activity and efficient formation of ceramide-enriched platforms and, thus, also NADPH oxidase activation. This feed-forward loop notion is supported by the facts that DPI (inhibiting NADPH oxidase activity) or catalase (a ROS degrading enzyme), not only inhibited *P. aeruginosa*–induced acid sphingomyelinase activation, but also prevented acid sphingomyelinase-mediated ceramide-enriched platform formation. It is of note that NADPH oxidase inhibition did not completely block acid sphingomyelinase activity. Further, acid sphingomyelinase activation preceded the release of ROS indicating that the bacteria stimulate acid sphingomyelinase via unknown mechanism resulting in ROS release, which then oxidize acid sphingomyelinase to promote further stimulation of the enzyme. As discussed above, ROS probably enhances activation of acid sphingomyelinase by dimerization of a cysteine residue to form disulfide bonds (Qiu et al., 2003). The feed-forward loop notion is further supported by the present finding that H_2O_2, a stable and cell permeable ROS, activates acid sphingomyelinase and induces formation of ceramide-enriched platform in wild type macrophages, whereas no platforms formed in *Smpd1*$^{-/-}$ cells. Taken together, acid sphingomyelinase, ceramide-enriched membrane platform, NADPH oxidase and ROS constitute a feed-forward loop resulting in a rapid and efficient amplification of NADPH oxidase activity and ROS production.

A similar model has been proposed for regulation of caspase 8 activation by acid sphingomyelinase, with a primary weak activation of caspase 8 and a feed-forward loop by acid sphingomyelinase. It has been shown that CD95 ligation, which releases ROS for the induction of apoptosis (Um et al., 1996; Gulbins et.al., 1996; Reinehr et al., 2006), primarily induces a very weak recruitment of FADD and the stimulation of caspase 8; however, this stimulation reaches only approximately 1% of the levels that are observed for maximal activation of caspase 8 (Grassmé et al., 2003). This weak activation of caspase 8 is observed in acid sphingomyelinase-deficient cells, but it is insufficient to trigger apoptosis in these cells. However, the low activity of caspase 8 is sufficient to trigger the translocation and activation of acid sphingomyelinase within seconds, with the subsequent formation of ceramide-enriched membrane platforms that cluster CD95 (Grassmé et al., 2003). Receptor clustering leads to the formation of death-inducing signaling complex (DISC) and full activation of caspase 8.

Membrane rafts and ceramide were identified to have an important function in infectious biology. Many pathogens target and employ rafts for infection of cells, including *Escherichia coli*, *Mycobacterium tuberculosis*, *Campylobacter jejuni*, *Vibrio cholerae* and *P. aeruginosa* (Grassmé et al., 2001). However, the molecular mechanisms of raft-mediated infection of mammalian cells with pathogens are largely unknown. Our data suggest that membrane rafts, at least, are involved in host-defense interaction by regulating ROS production.

5.2.4 Role of Cftr in lysosomal alkalinization

The present study demonstrates that freshly isolated lung macrophages contain at least two distinct acidic vesicle populations. Some, but not all of these vesicles exhibit a higher pH in *Cftr*-deficient macrophages than the corresponding vesicles in wild-type cells, as indicated by staining with Lysosensor Green DND-189 and DND-153.

It has been suggested that CFTR regulates pH in at least some intracellular vesicles (Barasch et.al., 1991; Poschet et.al., 2002; Di et.al., 2006; Teichgräber et.al., 2008; Deriy et.al., 2009). The acidification of intracellular vesicles requires high concentrations of protons within the vesicles; these concentrations are achieved by the activity of proton pumps, in particular the V-type adenosine triphosphatase (v-ATPase) proton pump

(Jefferies et.al., 2008). Because the v-ATPase protein pump is electrogenic, its activity requires either the accumulation of negatively charged counterions in these vesicles or the active transport of other positively charged ions out of the vesicular lumen (Mellman et.al., 1986). It has been proposed that CFTR mediates this influx of counterions into at least some intracellular vesicles (Barasch et.al., 1991; Di et.al., 2006; Deriy et.al., 2009) (**Figure 5.1**).

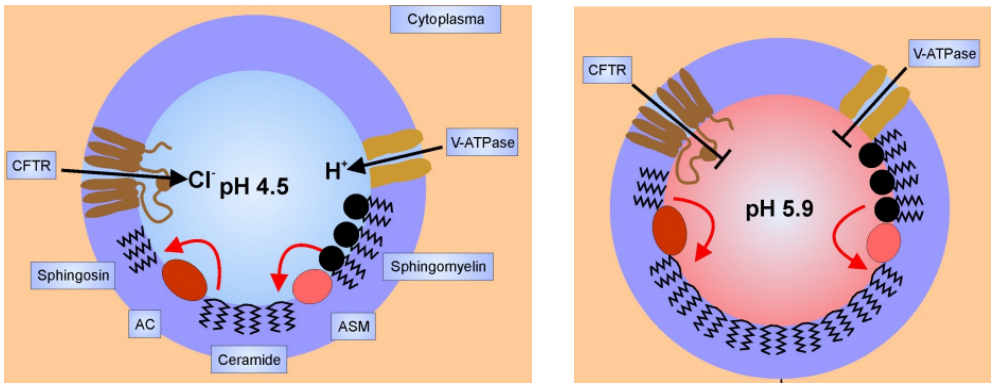

Figure 5.1 Proposed model of Cftr in controlling lysososmal pH and chronic accumulation of ceramide in Cftr-deficient lysosomes.

However, the role of Cftr in the regulation of vesicular pH is controversial. Barasch and Al-Awqati demonstrated the alkalinization of trans-Golgi and mannose-6-phosphate–positive vesicles and prelysosomes in *Cftr*-deficient cells (Barasch et al., 1991). These findings were confirmed by the results of several studies that demonstrated the alkalinization of lysosomes and phagosomes in alveolar macrophages (Barasch et.al., 1991; Di et al., 2006; Deriy et.al., 2009). In contrast, other reports have failed to detect a role of Cftr in the regulation of pH in vesicles that form after internalization (Haggie et al., 2009; Barriere et al., 2009). These studies determined the pH in TMR-dextran–positive endosomes or vesicles that contain internalized antibody-labelled or fluorescent Cftr molecules (Haggie et al., 2009; Barriere et.al., 2009). Dextran-containing endosomes are directly targeted to a subpopulation of lysosomes, and these endosomes are distinct from mannose-6-phosphate–positive vesicles and do not mix with secretory lysosomes (Stoorvogel et al., 1989). The discrepancies in findings about the role of Cftr in the regulation of vesicular pH could be caused by the fact that the reported studies used different cell systems and different techniques. Moreover, different types of vesicles express different sets of ion channels and pumps (Bradbury et al., 1999), and this fact very likely explains the differences in the effects of *CFTR* deficiency on the pH of a particular

population of vesicles. The findings of the present study confirm the notion that Cftr is involved in the regulation of the pH in a subset of intracellular vesicles, most likely secretory lysosomes.

Changes in the pH of secretory lysosomes may result in a relative overactivity of acid sphingomyelinase, which is still active at a pH of 6.0, in comparison to that of acid ceramidase, which is almost inactive at pH 6.0; this overactivity might be followed by a slow accumulation of ceramide in these vesicles of *Cftr*-deficient cells (Teichgräber et al., 2008) (**Figure 5.1**). Indeed, we observed a marked chronic accumulation of ceramide in *Cftr*-deficient alveolar macrophages. In addition, *Cftr*-deficiency prevented the acute and rapid activation of acid sphingomyelinase observed in wild-type cells after infection with *P. aeruginosa* (Yu et al., 2009), thereby preventing the acute release of ceramide upon infection. On the basis of these observations, we assume that the LysoSensor Green DND-189–positive lysosomes are secretory lysosomes containing the signaling pool of acid sphingomyelinase, that their vesicular pH is regulated by Cftr and that the increase in the pH of secretory lysosomes prevents activation of the acid sphingomyelinase. In contrast, the lysosomal form of acid sphingomyelinase, which mediates the physiological steady-state metabolism of sphingomyelin, does not seem to be affected in *Cftr*-deficient cells, since classical lysosomes in *Cftr*-deficient cells do not seem to exhibit an accumulation of sphingomyelin.

The present study further explored whether the influence of *Cftr* deficiency is linked to alterations in lysosomal biogenesis and transport. We did not detect a difference in staining with LAMP1 between wild-type and *Cftr*-deficient macrophages; this finding suggests that lysosome biogenesis is not altered in the absence of Cftr. The finding that Cftr co-localizes with LAMP1 further supports the hypothesis that Cftr resides in the lysosomal membrane and is directly involved in the acidification of lysosomes. Finally, *Cftr* deficiency exerted no effect on TMR-dextran staining. Because TMR-dextran is internalized by endocytosis and released by vesicular exocytosis, TMR-dextran staining in the cells reflects equilibrium between endocytosis and vesicular exocytosis. Thus, our findings indicate that the formation of endocytotic and secretory vesicles is not altered by *Cftr* deficiency. Taken together, our findings strongly suggest that *Cftr* is directly involved in the regulation of pH in a specific subpopulation of lysosomes but is not involved in lysosomal biogenesis or the formation of endocytic and secretory vesicles in lung alveolar macrophages.

However, it is also possible that *Cftr* deficiency affects the pH on the extracellular leaflet of the cell membrane and thereby alters the balance between acid sphingomyelinase and acid ceramidase. Moreover, it is possible that *Cftr* deficiency prevents the acute activation of acid sphingomyelinase by *P. aeruginosa* because it alters the lipid content of secretory lysosomes. Previous studies by Tabas and colleagues demonstrated that the lipid composition of membranes has a substantial impact on the activation of acid sphingomyelinase (Schissel et al., 1998). It remains to be determined whether alterations of other membrane lipids in *Cftr*-deficient cells contribute to the defect of acid sphingomyelinase activation in these cells.

5.2.5 Role of Cftr in regulation of redox signaling

Activation of the acid sphingomyelinase seems to occur in secretory lysosomes that fuse with the cell membrane (Grassmé et al., 2003; Jin et al., 2008). Ceramide then forms ceramide-enriched membrane platforms in the plasma membrane; these platforms serve the clustering and activation of NADPH oxidase and, thus, the release of ROS. The present study shows that *P. aeruginosa*–induced ROS release requires acute activation of acid sphingomyelinase and is abolished in *Cftr*-deficient macrophages. These data support the view that deficiency of Cftr results in alkalnization of secretory lysosomes and consequent prevention of acid sphingomyelinase activation and ceramide-mediated ROS production.

The role of Cftr in redox signaling seems to specific for bacterial infection (at least for *P. aeruginosa*). Di and co-workers show that Cftr deficiency does not affect phorbol 12-myristate l3-acetate (PMA)-induced ROS production in alveolar macrophages (Di et al., 2006). It is well accepted that $p47^{phox}$ phosphorylation and translocation is a crucial for agonist (such as PMA)-induced NADPH oxidase activation and ROS production in many mammalian cells. PMA is a potent stimulator for PKC, which phosphorylates $p47^{phox}$ and induces translocation of this crucial subunit of NADPH oxidase to the plasma membrane. Thus, PMA increases ROS production by direct activation of NADPH oxidase and does not require a function of Cftr.

Recent data suggest that Cftr is also involved in regulation of redox signaling by antioxidant mechanisms. IHoste and colleagues demonstrated that Cftr and ROS are involved in staurosporine-induced apoptosis of renal cells immortalized from primary cultures of proximal convoluted tubules (IHoste et.al., 2010). Staurosporine induced

increase in ROS in wild-type cells, which was impaired by a specific CFTR inhibitor (CFTR(inh)-172) and was not observed in Cftr-deficient cells. Because Cl^- and GSH share common permeation through CFTR, the role probably involves control of the intracellular ROS balance by Cftr-dependent regulation of GSH concentration (Kogan et.al., 2003).

ROS are toxic to most bacteria including *P. aeruginosa*. *In vivo*, lung bacteria clearance of *P. aeruginosa* was impaired in *Smpd1*$^{-/-}$, *p47*$^{phox-/-}$ or *Cftr*$^{-/-}$ mice compared to wild type mice (Grassmé et al., 2003; Sadikot et al., 2004; Teichgräber et al., 2008). The present study shows that the impairment in ROS release by *Cftr*-deficient macrophages decreases the bactericidal capability of these cells against *P. aeruginosa*. Thus, the present finding links the function of ceramide-enriched redox-signaling platforms with the bactericidal activity in alveolar macrophages. In contrast, *Cftr* deficiency does not affect the cytokine release response by these lung macrophages, a finding that is consistent with those of previous studies showing that Cftr is not involved in the production of cytokines (KC and MIP2) by LPS-stimulated macrophages (Kostyk et al., 2006). This situation is in marked contrast to that in *Cftr*-deficient epithelial cells, which show a marked increase in the constitutive release of pro-inflammatory cytokines such as IL-1 and IL-8 (Teichgräber et al., 2008; Tabary et al., 1998; Stecenko et al., 2001).

At present, the role of macrophages in cystic fibrosis is poorly defined. Although several studies have demonstrated that *Cftr*-deficient macrophages exhibit a defect in the intracellular killing of *P. aeruginosa* (Di et al., 2006; Deriy et al., 2009), the role of macrophages in acute pulmonary infections with *P. aeruginosa* in vivo is still open (Koh et al., 2009). A recent study demonstrated that in particular neutrophils are essential in eliminating *P. aeruginosa* from infected airways (Koh et al., 2009). Thus, macrophages might be important in regulating pathways which enhance inflammation including amplification of neutrophil recruitment. It is also possible that the inability of *Cftr*-deficient macrophages to kill sufficient numbers of *P. aeruginosa* bacteria contributes to the initial sensitivity of cystic fibrosis patients (and mice) to infections with *P. aeruginosa*, a situation that does not apply to wild-type mice. This defect in *Cftr*-deficient macrophages may result in a slow removal of the bacteria from alveoli, a longer persistence of the bacteria in the lung and finally the growth of the bacteria in the lung. It could be speculated that the survival of *P. aeruginosa* in *Cftr*-deficient macrophages may protect the pathogens from the neutrophil attack in cystic fibrosis. However, determining whether this hypothesis is true will require future studies that are beyond the focus of the present study; such

studies will probably use floxed *Cftr*-deficient mice with a specific deficiency of *Cftr* in macrophages to exactly define the function of alveolar macrophages in cystic fibrosis.

5.2.6 Significances and perspectives

The major significance of the research work in this dissertation was to clarify the role of ceramide-mediated redox signaling in the regulation of macrophage function in the host defense response in cystic fibrosis. The results presented in this dissertation increases our understanding of the signaling mechanisms responsible for the acute ROS response in macrophages during host-pathogen interaction and link the function of Cftr with ceramide-redox signaling. The notion that Cftr deficiency impairs ceramide-mediated redox signaling and normal macrophage function may contribute to the understanding why cystic fibrosis patients are susceptible to *P. aeruginosa* infections. This notion will also inspire studies about the role of NADPH oxidase enzyme family in mediating cellular functions of other cells in pulmonary systems. Elucidation of the pathogenesis of cystic fibrosis associated with the ceramide-redox signaling may direct the development of new therapeutic strategy for treatment of this disease.

6. SUMMARY

The present study first investigated the role of acid sphingomyelinase and ceramide-enriched membrane platforms in *P. aeruginosa*-induced redox signaling in lung alveolar macrophages. The major findings are:

- *P. aeruginosa* rapidly activates acid sphingomyelinase and induces ceramide release in the plasma membranes.
- Acid sphingomyelinase mediates *P. aeruginosa*–induced ROS production.
- Acid sphingomyelinase activation by *P. aeruginosa* infections results in formation of ceramide-enriched membrane platforms.
- Ceramide-enriched membrane platforms are crucial for aggregation and activation of NADPH oxidase.
- Acid sphingomyelinase-mediated redox signaling is strongly amplified via a positive feedback mechanism in ceramide-enriched membrane platforms.

The proposed signaling pathway is depicted as bellow:

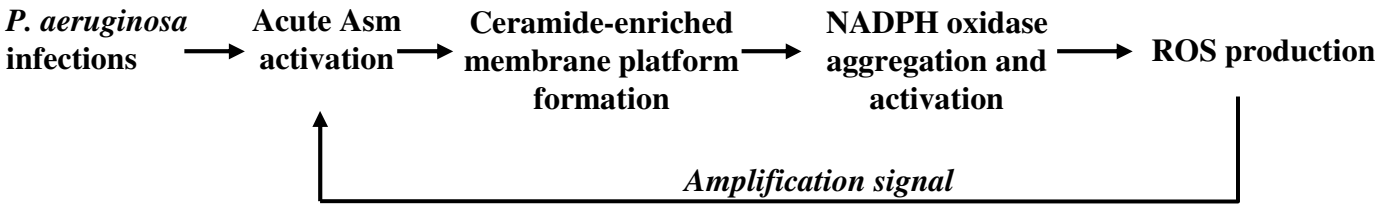

Furthermore, the present study investigated whether Cftr is involved in acidification of lysosomes and therefore involved in acid sphingomyelinase-mediated redox signaling in lung alveolar macrophages. The major findings are:

- Cftr deficiency results in alkalinization of a subset of vesicles, which include secretory lysosomes.
- Cftr deficiency results in a chronic accumulation of ceramide in macrophages, but prevents the acute release of ceramide upon infection with *P. aeruginosa*.

- Cftr deficiency results in failure to stimulate the activation of NADPH oxidase and, thus, an inability to release ROS and to kill *P. aeruginosa*.

The proposed pathway is depicted as bellow:

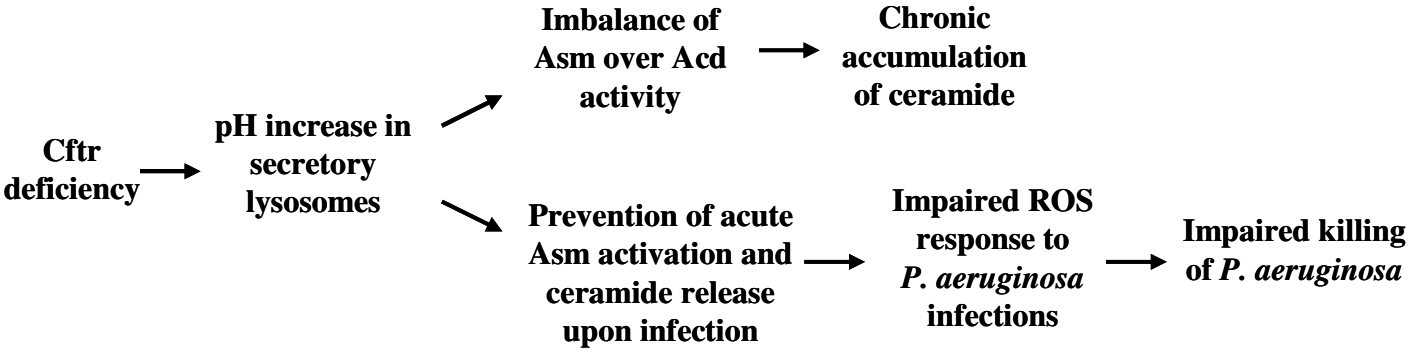

* Asm: acid sphingomyelinase; Acd: acid ceramidase

7. REFERENCES

1. Abdel Shakor AB, Kwiatkowska K, Sobota A. 2004 Cell surface ceramide generation precedes and controls FcgammaRII clustering and phosphorylation in rafts. *J Biol Chem.* 279(35):36778-87
2. Allan D. 2000 Lipid metabolic changes caused by short-chain ceramides and the connection with apoptosis. *Biochem J*. 345 Pt 3:603-10.
3. Banta LM, Robinson JS, Klionsky DJ, Em, SD. 1988. Organelle assembly in yeast: characterization of yeast mutants defective in vacuolar biogenesis and protein sorting. *J. Cell. Biol.* 107: 1369-1383.
4. Bao JX, Jin S, Zhang F, Wang ZC, Li N, Li PL. 2010 Activation of membrane NADPH oxidase associated with lysosome-targeted acid sphingomyelinase in coronary endothelial cells. *Antioxid Redox Signal.* 12(6):703-12.
5. Barasch J, Kiss B, Prince A, Saiman L, Gruenert D, al-Awqati Q. 1991 Defective acidification of intracellular organelles in cystic fibrosis. *Nature.* 352(6330):70-3.
6. Barenholz Y, Thompson TE. 1980 Sphingomyelins in bilayers and biological membranes. *Biochim Biophys Acta.* 604(2):129-58.
7. Barriere H, Bagdany M, Bossard F, Okiyoneda T, Wojewodka G, Gruenert D, Radzioch D, Lukacs GL. 2009 Revisiting the role of cystic fibrosis transmembrane conductance regulator and counterion permeability in the pH regulation of endocytic organelles. *Mol Biol Cell.* 20(13):3125-41.
8. Basu S, and Kolesnick R. 1998. Stress signals for apoptosis: ceramide and c-Jun kinase. *Oncogene* 17:3277-3285.
9. Becker KA, Riethmüller J, Lüth A, Döring G, Kleuser B, and Gulbins E. 2009. Acid sphingomyelinase inhibitors normalize pulmonary ceramide and inflammation in cystic fibrosis. *Am. J. Resp. Cell Mol. Biol.* doi:10.1165/rcmb.2009-0174OC.
10. Bezombes C, de Thonel A, Apostolou A, Louat T, Jaffrezou JP, Laurent G, Quillet-Mary A. 2002. Overexpression of protein kinase c-zeta confers protection against antileukemic drugs by inhibiting the redox-dependent sphingomyelinase activation. *Mol Pharmacol* 62:1446-1455.
11. Bhunia AK, Han H, Snowden A, Chatterjee S. 1997 Redox-regulated signaling by lactosylceramide in the proliferation of human aortic smooth muscle cells. *J Biol Chem* 272:15642-15649.
12. Bonfield TL, Konstan MW, Burfeind P, Panuska JR, Hilliard JB, Berger M. 1995. Normal bronchial epithelial cells constitutively produce the anti-inflammatory cytokine interleukin-10, which is downregulated in cystic fibrosis. *Am J Respir Cell Mol Biol* 13: 257-61.
13. Borowitz D, Durie PR, Clarke LL, Werlin SL, Taylor CJ, Semler J, De Lisle RC, Lewindon P, Lichtman SM, Sinaasappel M, Baker RD, Baker SS, Verkade HJ, Lowe ME, Stallings VA, Janghorbani M, Butler R, Heubi J. 2005. Gastrointestinal outcomes and confounders in cystic fibrosis. *J. Pediatr. Gastroenterol. Nutr.* 41: 273-285.
14. Boucher RC. 2007. Airway surface dehydration in cystic fibrosis: pathogenesis and therapy. *Annu Rev Med* 58: 157-70.
15. Bradbury NA. Intracellular CFTR: localization and function. 1999. *Physiol. Rev.* 79: S175-S191.
16. Brodlie M, McKean MC, Johnson GE, Gray J, Fisher AJ, Corris PA, Lordan JL, Ward C. 2010 Ceramide is Increased in the Lower Airway Epithelium of People with Advanced Cystic Fibrosis Lung Disease. *Am J Respir Crit Care Med* doi:10.1164/rccm.200905-0799OC
17. Brown DA, and London E. 1998. Structure and origin of ordered lipid domains in biological membranes. J *Membr Biol* 164:103-114.
18. Buccoliero R, Ginzburg L, Futerman AH. 2004. Elevation of lung surfactant phosphatidylcholine in mouse models of Sandhoff and of Niemann-Pick A disease. *J Inherit Metab Dis* 27:641-648.
19. Chalfant CE, Rathman K, Pinkerman RL, Wood RE, Obeid LM, Ogretmen B, Hannun YA. 2002. De novo ceramide regulates the alternative splicing of caspase 9 and Bcl-x in A549

lung adenocarcinoma cells. Dependence on protein phosphatase-1. *J Biol Chem.* 277: 12587-12595.

20. Charruyer A, Grazide S, Bezombes C, Müller S, Laurent G, Jaffrézou JP. 2005 UV-C light induces raft-associated acid sphingomyelinase and JNK activation and translocation independently on a nuclear signal. *J Biol Chem.* 280(19):19196-204.
21. Corda S, Laplace C, Vicaut E, Duranteau J. 2001 Rapid reactive oxygen species production by mitochondria in endothelial cells exposed to tumor necrosis factor-α is mediated by ceramide. *Am J Respir Cell Mol Biol* 24:762-768.
22. Cottart CH, Bonvin E, Rey C, Wendum D, Bernaudin JF, Dumont S, Lasnier E, Debray D, Clément A, Housset C, Bonora M. 2007. Impact of nutrition on phenotype in *CFTR*-deficient mice. *Pediatr Res* 62: 528-532.
23. Couch LH, Churchwell MI, Doerge DR, Tolleson WH, Howard PC. 1997 Identification of ceramides in human cells using liquid chromatography with detection by atmospheric pressure chemical ionization-mass spectrometry. *Rapid Commun Mass Spectrom.* 11(5):504-12.
24. Cremesti A, Paris F, Grassmé H, Holler N, Tschopp J, Fuks Z, Gulbins E, Kolesnick R. 2001. Ceramide enables fas to cap and kill. *J Biol Chem* 276:23954-23961.
25. Dacheux D, Toussaint B, Richard M, Brochier G, Croize J, Attree I. 2000. Pseudomonas aeruginosa cystic fibrosis isolates induce rapid, type III secretion-dependent, but ExoU-independent, oncosis of macrophages and polymorphonuclear neutrophils. *Infect Immun* 68:2916-2924.
26. DeLeo FR. 2004. Modulation of phagocyte apoptosis by bacterial pathogens. Apoptosis 9:399-413.
27. Deriy LV, Gomez EA, Zhang G, Beacham DW, Hopson JA, Gallan AJ, Shevchenko PD, Bindokas VP, Nelson DJ. 2009 Disease-causing mutations in the cystic fibrosis transmembrane conductance regulator determine the functional responses of alveolar macrophages. *J Biol Chem.* 284(51):35926-38.
28. Di A, Brown ME, Deriy LV, Li C, Szeto FL, Chen Y, Huang P, Tong J, Naren AP, Bindokas V, Palfrey HC, Nelson DJ. 2006 CFTR regulates phagosome acidification in macrophages and alters bactericidal activity. *Nat Cell Biol.* 8(9):933-44.
29. Djaldetti M, Salman H, Bergman M, Djaldetti R, Bessler H. 2002. Phagocytosis--the mighty weapon of the silent warriors. *Microsc Res Tech* 57:421-431.
30. Dockrell DH, Whyte MK. 2006. Regulation of phagocyte lifespan in the lung during bacterial infection. *J Leukoc Biol* 79:904-908.
31. Dumitru CA, and Gulbins E. 2006. TRAIL activates acid sphingomyelinase via a redox mechanism and releases ceramide to trigger apoptosis. *Oncogene* 25:5612-5625.
32. Eggeling C, Ringemann C, Medda R, Schwarzmann G, Sandhoff K, Polyakova S, Belov VN, Hein B, von Middendorff C, Schönle A, Hell SW. 2009 Direct observation of the nanoscale dynamics of membrane lipids in a living cell. *Nature*. 457(7233):1159-62.
33. Esen M, Schreiner B, Jendrossek V, Lang F, Fassbender K, Grassmé H, Gulbins E. 2001 Mechanisms of Staphylococcus aureus induced apoptosis of human endothelial cells. *Apoptosis.* 6(6):431-9.
34. Futerman AH, Stieger B, Hubbard AL, Pagano RE. 1990 Sphingomyelin synthesis in rat liver occurs predominantly at the cis and medial cisternae of the Golgi apparatus. *J Biol Chem.* 265(15):8650-7.
35. Göggel R, Winoto-Morbach S, Vielhaber G, Imai Y, Lindner K, Brade L, Brade H, Ehlers S, Slutsky AS, Schütze S, Gulbins E, Uhlig S. 2004 PAF-mediated pulmonary edema: a new role for acid sphingomyelinase and ceramide. *Nat Med.* 10(2):155-60. Epub 2004 Jan 4.
36. Goldman MJ, Anderson GM, Stolzenberg ED, Kari UP, Zasloff M, Wilson JM. 1997. Human beta-defensin-1 is a salt-sensitive antibiotic in lung that is inactivated in cystic fibrosis. *Cell* 88: 553-60.
37. Grassmé H, Gulbins E, Brenner B, Ferlinz K, Sandhoff K, Harzer K, Lang F, Meyer TF. 1997 Acidic sphingomyelinase mediates entry of N. gonorrhoeae into nonphagocytic cells. *Cell.* 91(5):605-15.

38. Grassmé H, Kirschnek S, Riethmueller J, Riehle A, von Kürthy G, Lang F, Weller M, Gulbins E. 2000. CD95/CD95 ligand interactions on epithelial cells in host defense to Pseudomonas aeruginosa. Science 290:527-530.
39. Grassmé H, Jekle A, Riehle A, Schwarz H, Berger J, Sandhoff K, Kolesnick R, Gulbins E. 2001a. CD95 signaling via ceramide rich membrane rafts. *J. Biol. Chem.* 276: 20589-20596.
40. Grassmé H, Jendrossek V, Gulbins E. 2001b. Molecular mechanisms of bacteria induced apoptosis. *Apoptosis* 6:441-445.
41. Grassmé H, Jendrossek V, Bock J, Riehle A, Gulbins E. 2002 Ceramide-rich membrane rafts mediate CD40 clustering. *J Immunol*. 168(1):298-307.
42. Grassmé H, Jendrossek V, Riehle A, von Kürthy G, Berger J, Schwarz H, Weller M, Kolesnick R, Gulbins E. 2003. Host defense against Pseudomonas aeruginosa requires ceramide-rich membrane rafts. *Nat Med* 9:322-330.
43. Grassmé H, Jin J, Wilker B, von Kürthy G, Wick W, Weller M, Möröy T, Gulbins E. 2006. Regulation of pulmonary Pseudomonas aeruginosa infection by the transcriptional repressor Gfi1. *Cell Microbiol* 8:1096-1105.
44. Gu M, Kerwin JL, Watts JD, Aebersold R. 1997 Ceramide profiling of complex lipid mixtures by electrospray ionization mass spectrometry. *Anal Biochem.* 244(2):347-56.
45. Gulbins E, Szabo I, Baltzer K, Lang F. 1997. Ceramide-induced inhibition of T lymphocyte voltage-gated potassium channel is mediated by tyrosine kinases. *Proc. Natl. Acad. Sci. U. S. A.* 94: 7661-7666.
46. Gulbins E, and Kolesnick R. 2003. Raft ceramide in molecular medicine. *Oncogene* 22:7070-7077.
47. Haggie PM, Verkman AS. 2009 Unimpaired lysosomal acidification in respiratory epithelial cells in cystic fibrosis. *J Biol Chem.* 284(12):7681-6.
48. Haimovitz-Friedman A, Kolesnick RN, and Fuks Z. 1997. Ceramide signaling in apoptosis. *Br Med Bull* 53:539-553.
49. Hakomori S, Patterson CM, Nudelman E, Sekiguchi K. 1983 A monoclonal antibody directed to N-acetylneuraminosyl-alpha 2 leads to 6-galactosyl residue in gangliosides and glycoproteins. *J Biol Chem.* 258(19):11819-22.
50. Hannun YA. 1996 Functions of ceramide in coordinating cellular responses to stress. *Science.* 274(5294):1855-9.
51. Harder T, and Simons K. 1997. Caveolae, DIGs, and the dynamics of sphingolipid-cholesterol microdomains. *Curr Opin Cell Biol* 9:534-542.
52. Hatanaka Y, Fujii J, Fukutomi T, Watanabe T, Che W, Sanada Y, Igarashi Y, Taniguchi N. 1998. Reactive oxygen species enhances the induction of inducible nitric oxide synthase by sphingomyelinase in RAW264.7 cells. *Biochim Biophys Acta* 1393:203-210.
53. Hauck CR, Grassmé H, Bock J, Jendrossek V, Ferlinz K, Meyer TF, Gulbins E. 2000 Acid sphingomyelinase is involved in CEACAM receptor-mediated phagocytosis of Neisseria gonorrhoeae. *FEBS Lett.* 478(3):260-6.
54. Hauser AR, and Engel JN. 1999. Pseudomonas aeruginosa induces type-III-secretion-mediated apoptosis of macrophages and epithelial cells. *Infect Immun* 67:5530-5537.
55. Hernandez OM, Discher DJ, Bishopric NH, Webster KA. 2000. Rapid activation of neutral sphingomyelinase by hypoxia-reoxygenation of cardiac myocytes. *Circ Res* 86:198-204.
56. Herz J, Pardo J, Kashkar H, Schramm M, Kuzmenkina E, Bos E, Wiegmann K, Wallich R, Peters PJ, Herzig S, Schmelzer E, Krönke M, Simon MM, Utermöhlen O. 2009 Acid sphingomyelinase is a key regulator of cytotoxic granule secretion by primary T lymphocytes. *Nat Immunol.* (7):761-8.
57. Huang HW, Goldberg EM, Zidovetzki R. 1999 Ceramides modulate protein kinase C activity and perturb the structure of Phosphatidylcholine/Phosphatidylserine bilayers. *Biophys J.* 77(3):1489-97.
58. l'Hoste S, Chargui A, Belfodil R, Corcelle E, Duranton C, Rubera I, Poujeol C, Mograbi B, Tauc M, Poujeol P. 2010 CFTR mediates apoptotic volume decrease and cell death by controlling glutathione efflux and ROS production in cultured mice proximal tubules. *Am J Physiol Renal Physiol.* 298(2):F435-53.
59. Inoue H, Massion PP, Ueki IF, Grattan KM, Hara M, Dohrman AF, Chan B, Lausier JA, Golden JA, Nadel JA. 1994. Pseudomonas stimulates interleukin-8 mRNA expression

selectively in airway epithelium, in gland ducts, and in recruited neutrophils. *Am J Respir Cell Mol Biol* 11: 651-63.

60. Ishibashi Y, Nakasone T, Kiyohara M, Horibata Y, Sakaguchi K, Hijikata A, Ichinose S, Omori A, Yasui Y, Imamura A, Ishida H, Kiso M, Okino N, Ito M. 2007 A novel endoglycoceramidase hydrolyzes oligogalactosylceramides to produce galactooligosaccharides and ceramides. *J Biol Chem.* 282(15):11386-96.
61. Iwamori M, Costello C, Moser HW. 1979 Analysis and quantitation of free ceramide containing nonhydroxy and 2-hydroxy fatty acids, and phytosphingosine by high-performance liquid chromatography. *J Lipid Res.* 20(1):86-96.
62. Jeckel D, Karrenbauer A, Birk R, Schmidt RR, Wieland F. 1990 Sphingomyelin is synthesized in the cis Golgi. *FEBS Lett.* 12;261(1):155-7.
63. Jefferies KC, Cipriano DJ, Forgac M. 2008 Function, structure and regulation of the vacuolar (H+)-ATPases. *Arch Biochem Biophys.* 476(1):33-42.
64. Jendrossek V, Grassme H, Mueller I, Lang F, Gulbins E. 2001. Pseudomonas aeruginosa-induced apoptosis involves mitochondria and stress-activated protein kinases. *Infect Immun* 69: 2675-83.
65. Jendrossek V, Fillon S, Belka C, Muller I, Puttkammer B, Lang F. 2003. Apoptotic response of Chang cells to infection with Pseudomonas aeruginosa strains PAK and PAO-I: molecular ordering of the apoptosis signaling cascade and role of type IV pili. *Infect Immun* 71: 2665-73.
66. Jin S, Yi F, and Li PL. 2007. Contribution of lysosomal vesicles to the formation of lipid raft redox signaling platforms in endothelial cells. *Antioxid. Redox. Signal.* 9: 1417-1426.
67. Jin S, Yi F, Zhang F, Poklis JL, and Li PL. 2008. Lysosomal targeting and trafficking of acid sphingomyelinase to lipid raft platforms in coronary endothelial cells. *Arterioscler. Thromb. Vasc. Biol.* 28: 2056-2062.
68. Kalhorn T, Zager RA. 1999 Renal cortical ceramide patterns during ischemic and toxic injury: assessments by HPLC-mass spectrometry. *Am J Physiol.* 277(5 Pt 2):F723-33.
69. Kamata H, Honda S, Maeda S, Chang L, Hirata H, Karin M. 2005. Reactive oxygen species promote TNFalpha-induced death and sustained JNK activation by inhibiting MAP kinase phosphatases. *Cell* 120:649-661.
70. Karlsson AA, Michélsen P, Odham G. 1998 Molecular species of sphingomyelin: determination by high-performance liquid chromatography/mass spectrometry with electrospray and high-performance liquid chromatography/tandem mass spectrometry with atmospheric pressure chemical ionization. *J Mass Spectrom.* 33(12):1192-8.
71. Karupiah G, Hunt NH, King NJ, Chaudhri G. 2000. NADPH oxidase, Nramp1 and nitric oxide synthase 2 in the host antimicrobial response. *Rev Immunogenet* 2:387-415.
72. Keller P, Simons K. 1998 Cholesterol is required for surface transport of influenza virus hemagglutinin. *J Cell Biol.* 140(6):1357-67.
73. Kerem B, Rommens JM, Buchanan JA, Markiewicz D, Cox TK, Chakravarti A, Buchwald M, Tsui LC. 1989. Identification of the cystic fibrosis gene: genetic analysis. *Science* 245: 1073-80.
74. Kogan I, Ramjeesingh M, Li C, Kidd JF, Wang Y, Leslie EM, Cole SP, Bear CE. 2003. CFTR directly mediates nucleotide-regulated glutathione flux. *EMBO J* 22: 1981–1989.
75. Koh AY, Priebe GP, Ray C, Van Rooijen N, Pier GB. 2009. Inescable need for neutrophils as mediators of cellular innate immunity to acute *Pseudomonas aeruginosa* pneumonia. *Infect. Immun.* 77: 5300-5310.
76. Kolesnick RN, Goni FM, Alonso A. 2000. Compartmentalization of ceramide signaling: physical foundations and biological effects. J Cell Physiol 184: 285-300.
77. Kostyk AG, Dahl KM, Wynes MW, Whittaker LA, Weiss DJ, Loi R, Riches DW. 2006. Regulation of chemokine expression by NaCl occurs independently of cystic fibrosis transmembrane conductance regulator in macrophages. *Am. J. Pathol.* 169: 12-20.
78. Kowalski MP, Pier GB. 2004. Localization of cystic fibrosis transmembrane conductance regulator to lipid rafts of epithelial cells is required for Pseudomonas aeruginosa-induced cellular activation. *J Immunol* 172: 418-25.
79. Kumar V, Becker T, Jansen S, van Barneveld A, Boztug K, Wolfl S, Tümmler B, Stanke F. 2008. Expression levels of FAS are regulated through an evolutionary conserved element in intron 2, which modulates cystic fibrosis disease severity. *Genes Immun* 9: 689-96.

80. Lafont F, and van der Goot FG. 2005. Bacterial invasion via lipid rafts. *Cell Microbiol* 7:613-620.
81. Lang PA, Schenck M, Nicolay JP, Becker JU, Kempe DS, Lupescu A, Koka S, Eisele K, Klarl BA, Rubben H, Schmid KW, Mann K, Hildenbrand S, Hefter H, Huber SM, Wieder T, Erhardt A, Haussinger D, Gulbins E, Lang F. 2007. Liver cell death and anemia in Wilson disease involve acid sphingomyelinase and ceramide. *Nat Med* 13:164-170.
82. Lecour S, Van der Merwe E, Opie LH, Sack MN. 2006 Ceramide attenuates hypoxic cell death via reactive oxygen species signaling. *J Cardiovasc Pharmacol* 47:158-163.
83. Lee JT, Xu J, Lee JM, Ku G, Han X, Yang DI, Chen S, Hsu CY. 2004. Amyloid-beta peptide induces oligodendrocyte death by activating the neutral sphingomyelinase-ceramide pathway. *J Cell Biol* 164:123-131.
84. Lepple-Wienhues A, Belka C, Laun T, Jekle A, Walter B, Wieland U, Welz M, Heil L, Kun J, Busch G, Weller M, Bamberg M, Gulbins E, Lang F. 1999. Stimulation of CD95 (Fas) blocks T lymphocyte calcium channels through sphingomyelinase and sphingolipids. *Proc. Natl. Acad. Sci. U. S. A.* 96: 13795-13800.
85. Lichtenberg D, Goñi FM, Heerklotz H. 2005 Detergent-resistant membranes should not be identified with membrane rafts. *Trends Biochem Sci.* 30(8):430-6.
86. Liebisch G, Drobnik W, Reil M, Trümbach B, Arnecke R, Olgemöller B, Roscher A, Schmitz G. 1999 Quantitative measurement of different ceramide species from crude cellular extracts by electrospray ionization tandem mass spectrometry (ESI-MS/MS). *J Lipid Res.* 40(8):1539-46.
87. Liu B, Hannun YA. 1997. Inhibition of the neutral magnesium-dependent sphingomyelinase by glutathione. *J Biol Chem* 272:16281-16287.
88. Liu B, Andrieu-Abadie N, Levade T, Zhang P, Obeid LM, Hannun YA. 1998. Glutathione regulation of neutral sphingomyelinase in tumor necrosis factor-alpha-induced cell death. *J Biol Chem* 273:11313-11320.
89. Lovat PE, Di Sano F, Corazzari M, Fazi B, Donnorso RP, Pearson AD, Hall AG, Redfern CP, Piacentini M. 2004 Gangliosides link the acidic sphingomyelinase-mediated induction of ceramide to 12-lipoxygenase-dependent apoptosis of neuroblastoma in response to fenretinide. *J Natl Cancer Inst.* 96(17):1288-99.
90. Malaplate-Armand C, Florent-Bechard S, Youssef I, Koziel V, Sponne I, Kriem B, Leininger-Muller B, Olivier JL, Oster T, Pillot T. 2006. Soluble oligomers of amyloid-beta peptide induce neuronal apoptosis by activating a cPLA2-dependent sphingomyelinase-ceramide pathway. *Neurobiol Dis* 23:178-189.
91. Mano N, Oda Y, Yamada K, Asakawa N, Katayama K. 1997 Simultaneous quantitative determination method for sphingolipid metabolites by liquid chromatography/ionspray ionization tandem mass spectrometry. *Anal Biochem.* 244(2):291-300.
92. Martin SF, Sawai H, Villalba JM, Hannun YA. 2007. Redox regulation of neutral sphingomyelinase-1 activity in HEK293 cells through a GSH-dependent mechanism. *Arch Biochem Biophys* 459:295-300.
93. Matsui H, Verghese MW, Kesimer M, Schwab UE, Randell SH, Sheehan JK, Grubb BR, Boucher RC. 2005. Reduced three-dimensional motility in dehydrated airway mucus prevents neutrophil capture and killing bacteria on airway epithelial surfaces. *J Immunol* 175: 1090-9.
94. McCollister BD, Myers JT, Jones-Carson J, Voelker DR, Vázquez-Torres A. 2007. Constitutive acid sphingomyelinase enhances early and late macrophage killing of Salmonella enterica serovar Typhimurium. *Infect Immun* 75:5346-5352.
95. McNabb TJ, Cremesti AE, Brown PR, Fischl AS. 1999 The separation and direct detection of ceramides and sphingoid bases by normal-phase high-performance liquid chromatography and evaporative light-scattering detection. *Anal Biochem.* 276(2):242-50
96. Megha, London E. 2004 Ceramide selectively displaces cholesterol from ordered lipid domains (rafts): implications for lipid raft structure and function. *J Biol Chem.* 279(11):9997-10004.
97. Mellman I, Fuchs R, Helenius A. 1986 Acidification of the endocytic and exocytic pathways. *Annu Rev Biochem.* 55:663-700.

98. Mitra P, Maceyka M, Payne SG, Lamour N, Milstien S, Chalfant CE, Spiegel S. 2007 Ceramide kinase regulates growth and survival of A549 human lung adenocarcinoma cells. *FEBS Lett.* 581(4):735-40.
99. Motta S, Monti M, Sesana S, Mellesi L, Ghidoni R, Caputo R. 1994 Abnormality of water barrier function in psoriasis. Role of ceramide fractions. *Arch Dermatol*. 130(4):452-6.
100. Munro S. 2003 Lipid rafts: elusive or illusive? *Cell.* 115(4):377-88.
101. Nishimura K, Nakamura A. 1985 High performance liquid chromatographic analysis of long chain bases in intestinal glycolipids of adult and embryonic Japanese quails. *J Biochem.* 98(5):1247-54.
102. Nurminen TA, Holopainen JM, Zhao H, Kinnunen PK. 2002 Observation of topical catalysis by sphingomyelinase coupled to microspheres. *J Am Chem Soc.* 124(41):12129-34.
103. Oceandy D, McMorran BJ, Smith SN, Schreiber R, Kunzelmann K, Alton EW, Hume DA, Wainwright BJ. 2002. Gene complementation of airway epithelium in the cystic fibrosis mouse is necessary and sufficient to correct the pathogen clearance and inflammatory abnormalities. *Hum Mol Genet* 11: 1059-67.
104. Okino N, He X, Gatt S, Sandhoff K, Ito M, Schuchman EH. 2003 The reverse activity of human acid ceramidase. *J Biol Chem.* 278(32):29948-53.
105. Okino N, Ito M. 2007. Ceramidase enhances phospholipase C-induced hemolysis by Pseudomonas aeruginosa. *The Journal of biological chemistry* 282:6021-6030.
106. Pfeiffer A, Böttcher A, Orsó E, Kapinsky M, Nagy P, Bodnár A, Spreitzer I, Liebisch G, Drobnik W, Gempel K, Horn M, Holmer S, Hartung T, Multhoff G, Schütz G, Schindler H, Ulmer AJ, Heine H, Stelter F, Schütt C, Rothe G, Szöllôsi J, Damjanovich S, Schmitz G. 2001 Lipopolysaccharide and ceramide docking to CD14 provokes ligand-specific receptor clustering in rafts. *Eur J Immunol.* 31(11):3153-64.
107. Pier GB, Grout M, Zaidi TS, Olsen JC, Johnson LG, Yankaskas JR, Goldberg JB. 1996. Role of mutant CFTR in hypersusceptibility of cystic fibrosis patients to lung infections. *Science* 271: 64-7.
108. Poschet JF, Skidmore J, Boucher JC, Firoved AM, Van Dyke RW, Deretic V. 2002 Hyperacidification of cellubrevin endocytic compartments and defective endosomal recycling in cystic fibrosis respiratory epithelial cells. *J Biol Chem.* 277(16):13959-65.
109. Previati M, Bertolaso L, Tramarin M, Bertagnolo V, Capitani S. 1996 Low nanogram range quantitation of diglycerides and ceramide by high-performance liquid chromatography. *Anal Biochem*. 233(1):108-14.
110. Qiu H, Edmunds T, Baker-Malcolm J, Karey KP, Estes S, Schwarz C, Hughes H, Van Patten SM. 2003. Activation of human acid sphingomyelinase through modification or deletion of C-terminal cysteine. *J Biol Chem* 278:32744-32752.
111. Rahmani M, Reese E, Dai Y, Bauer C, Payne SG, Dent P, Spiegel S, Grant S. 2005 Coadministration of histone deacetylase inhibitors and perifosine synergistically induces apoptosis in human leukemia cells through Akt and ERK1/2 inactivation and the generation of ceramide and reactive oxygen species. *Cancer Res.* 65(6):2422-32.
112. Reinehr R, Becker S, Eberle A, Grether-Beck S, Häussinger D. 2005. Involvement of NADPH oxidase isoforms and Src family kinases in CD95-dependent hepatocyte apoptosis. *The Journal of biological chemistry* 280:27179-27194.
113. Reinehr R, Becker S, Braun J, Eberle A, Grether-Beck S, Haüssinger D. 2006 Endosomal acidification and activation of NADPH oxidase isoforms are upstream events in hyperosmolarity-induced hepatocyte apoptosis. *J Biol Chem* 281:23150-23166.
114. Richards RL, Habbersett RC, Scher I, Janoff AS, Schieren HP, Mayer LD, Cullis PR, Alving CR. 1986 Influence of vesicle size on complement-dependent immune damage to liposomes. *Biochim Biophys Acta.* 855(2):223-30.
115. Riordan JR, Rommens JM, Kerem B, Alon N, Rozmahel R, Grzelczak Z, Zielenski J, Lok S, Plavsic N, Chou JL, et al. 1989. Identification of the cystic fibrosis gene: cloning and characterization of complementary DNA. *Science* 245: 1066-73.
116. Rommens JM, Iannuzzi MC, Kerem B, Drumm ML, Melmer G, Dean M, Rozmahel R, Cole JL, Kennedy D, Hidaka N, et al. 1989. Identification of the cystic fibrosis gene: chromosome walking and jumping. Science 245: 1059-65.

117. Ryan AJ, McCoy DM, McGowan SE, Salome RG, Mallampalli RK. 2003. Alveolar sphingolipids generated in response to TNF-a modifies surfactant biophysical activity. J Appl Physiol 94:253-258.
118. Sadikot RT, Zeng H, Yull FE, Li B, Cheng DS, Kernodle DS, Jansen ED, Contag CH, Segal BH, Holland SM, Blackwell TS, Christman JW. 2004. p47phox deficiency impairs NF-kappa B activation and host defense in Pseudomonas pneumonia. *J Immunol* 172:1801-1808.
119. Samet D, Barenholz Y. 1999 Characterization of acidic and neutral sphingomyelinase activities in crude extracts of HL-60 cells. *Chem Phys Lipids.* 102(1-2):65-77.
120. Samuelsson K, Sameulsson B. 1970 Gas chromatographic and mass spectrometric studies of synthetic and naturally occurring ceramides. *Chem Phys Lipids.* 5(1):44-79.
121. Santana P, Peña LA, Haimovitz-Friedman A, Martin S, Green D, McLoughlin M, Cordon-Cardo C, Schuchman EH, Fuks Z, Kolesnick R. 1996 Acid sphingomyelinase-deficient human lymphoblasts and mice are defective in radiation-induced apoptosis. *Cell.* 86(2):189-99.
122. Sanvicens N, Cotter TG. 2006 Ceramide is the key mediator of oxidative stress-induced apoptosis in retinal photoreceptor cells. *J Neurochem*. 98(5):1432-44.
123. Scheel-Toellner D, Wang K, Assi LK, Webb PR, Craddock RM, Salmon M, Lord JM. 2004. Clustering of death receptors in lipid rafts initiates neutrophil spontaneous apoptosis. *Biochem Soc Trans* 32:679-681.
124. Scheel-Toellner D, Wang K, Craddock R, Webb PR, McGettrick HM, Assi LK, Parkes N, Clough LE, Gulbins E, Salmon M, Lord JM. 2004. Reactive oxygen species limit neutrophil life span by activating death receptor signaling. *Blood* 104:2557-2564.
125. Schissel SL, Tweedie-Hardman J, Rapp JH, Graham G, Williams KJ, Tabas I. 1996 Rabbit aorta and human atherosclerotic lesions hydrolyze the sphingomyelin of retained low-density lipoprotein. Proposed role for arterial-wall sphingomyelinase in subendothelial retention and aggregation of atherogenic lipoproteins. *J Clin Invest.* 98(6):1455-64.
126. Schissel SL, Jiang X, Tweedie-Hardman J, Jeong T, Camejo EH, Najib J, Rapp JH, Williams KJ, Tabas I. 1998. Secretory sphingomyelinase, a product of the acid sphingomyelinase gene, can hydrolyze atherogenic lipoproteins at neutral pH. Implications for atherosclerotic lesion development. *J. Biol. Chem.* 273: 2738-2746.
127. Schneider EG, Kennedy EP. 1973 Phosphorylation of ceramide by diglyceride kinase preparations from Escherichia coli. *J Biol Chem.* 248(10):3739-41.
128. Schreur KD, Liu S. 1997. Involvement of ceramide in inhibitory effect of IL-1 beta on L-type Ca2+ current in adult rat ventricular myocytes. *Am. J. Physiol.* 272: H2591-H2598.
129. Schroeder TH, Reiniger N, Meluleni G, Grout M, Coleman FT, Pier GB. 2001. Transgenic cystic fibrosis mice exhibit reduced early clearance of Pseudomonas aeruginosa from the respiratory tract. *J Immunol* 166: 7410-8.
130. Seumois G, Fillet M, Gillet L, Faccinetto C, Desmet C, François C, Dewals B, Oury C, Vanderplasschen A, Lekeux P, Bureau F. 2007. De novo C16- and C24-ceramide generation contributes to spontaneous neutrophil apoptosis. *J Leukoc Biol.* 81:1477-1486.
131. Simons K, Ikonen E. 1997 Functional rafts in cell membranes. *Nature.* 387(6633):569-72. Singer SJ, Nicolson GL. 1972 The fluid mosaic model of the structure of cell membranes. *Science.* 175(23):720-31.
132. Stecenko AA, King G, Torii K, Breyer RM, Dworski R, Blackwell TS, Christman JW, Brigham KL. 2001 Dysregulated cytokine production in human cystic fibrosis bronchial epithelial cells. *Inflammation.* 25(3):145-55.
133. Stoorvogel W, Geuze HJ, Griffith JM, Schwartz AL, Strous GJ. 1989. Relations between the intracellular pathways of the receptors for transferrin, asialoglycoprotein, and mannose-6-phosphate in human hepatoma cells. *J. Cell. Biol.* 108: 2137-2148.
134. Shen HM, Lin Y, Choksi S, Tran J, Jin T, Chang L, Karin M, Zhang J, Liu ZG. 2004. Essential roles of receptor-interacting protein and TRAF2 in oxidative stress-induced cell death. *Mol Cell Biol* 24:5914-5922.
135. Smith ER, Merrill AH Jr. 1995 Differential roles of de novo sphingolipid biosynthesis and turnover in the "burst" of free sphingosine and sphinganine, and their 1-phosphates and N-acyl-derivatives, that occurs upon changing the medium of cells in culture. *J Biol Chem.* 270(32):18749-58.

136. Stecenko AA, King G, Torii K, Breyer RM, Dworski R, Blackwell TS, Christman JW, Brigham KL. 2001. Dysregulated cytokine production in human cystic fibrosis bronchial epithelial cells. *Inflammation* 25: 145-55.
137. Tabary O, Zahm JM, Hinnrasky J, Couetil JP, Cornillet P, Guenounou M, Gaillard D, Puchelle E, Jacquot J. 1998. Selective up-regulation of chemokine IL-8 expression in cystic fibrosis bronchial gland cells in vivo and in vitro. *Am. J. Pathol.* 153: 921-930.
138. Teichgräber V, Ulrich M, Endlich N, Riethmüller J, Wilker B, De Oliveira-Munding CC, van Heeckeren AM, Barr ML, von Kürthy G, Schmid KW, Weller M, Tümmler B, Lang F, Grassme H, Döring G, Gulbins E. 2008. Ceramide accumulation mediates inflammation, cell death and infection susceptibility in cystic fibrosis. *Nat. Med.* 14: 382-391.
139. Tepper AD, Van Blitterswijk WJ. 2000 Ceramide mass analysis by normal-phase high-performance liquid chromatography. *Methods Enzymol.* 312:16-22.
140. Tirouvanziam R, de Bentzmann S, Hubeau C, Hinnrasky J, Jacquot J, Peault B, Puchelle E. 2000. Inflammation and infection in naive human cystic fibrosis airway grafts. *Am J Respir Cell Mol Biol* 23: 121-7.
141. Um HD, Orenstein JM, Wahl SM. 1996 Fas mediates apoptosis in human monocytes by a reactive oxygen intermediate dependent pathway. *J Immunol.* 56(9):3469-77.
142. Underhill DM, Ozinsky A. 2002. Phagocytosis of microbes: complexity in action. *Annu Rev Immunol* 20:825-852.
143. Van Veldhoven PP, Bishop WR, Yurivich DA, Bell RM. 1995 Ceramide quantitation: evaluation of a mixed micellar assay using E. coli diacylglycerol kinase. *Biochem Mol Biol Int.* 36(1):21-30.
144. Van Wart HE, Birkedal-Hansen H. 1990 The cysteine switch: a principle of regulation of metalloproteinase activity with potential applicability to the entire matrix metalloproteinase gene family. *Proc Natl Acad Sci U S A.* 7(14):5578-82.
145. Veiga MP, Arrondo JL, Goñi FM, Alonso A. 1999 Ceramides in phospholipid membranes: effects on bilayer stability and transition to nonlamellar phases. *Biophys J.* 76(1 Pt 1):342-50.
146. Venkatakrishnan A, Stecenko AA, King G, Blackwell TR, Brigham KL, Christman JW, Blackwell TS. 2000. Exaggerated activation of nuclear factor-kappaB and altered IkappaB-beta processing in cystic fibrosis bronchial epithelial cells. *Am J Respir Cell Mol Biol* 23: 396-403.
147. Verheij M, Bose R, Lin XH, Yao B, Jarvis WD, Grant S, Birrer MJ, Szabo E, Zon LI, Kyriakis JM, Haimovitz-Friedman A, Fuks Z, Kolesnick RN. 1996. Requirement for ceramide-initiated SAPK/JNK signalling in stress-induced apoptosis. *Nature* 380:75-79.
148. Vidal F, Mensa J, Almela M, Martínez JA, Marco F, Casals C, Gatell JM, Soriano E, Jimenez de Anta MT. 1996. Epidemiology and outcome of Pseudomonas aeruginosa bacteremia, with special emphasis on the influence of antibiotic treatment. Analysis of 189 episodes. *Arch Intern Med* 156:2121-2126.
149. Vilhardt F, van Deurs B. 2004. The phagocyte NADPH oxidase depends on cholesterol-enriched membrane microdomains for assembly. *EMBO J* 23:739-748.
150. Wang H, Giuliano AE, Cabot MC. 2002. Enhanced de novo ceramide generation through activation of serine palmitoyltransferase by the P-glycoprotein antagonist SDZ PSC 833 in breast cancer cells. *Mol Cancer Ther.* 1:719-26.
151. Watts JD, Aebersold R, Polverino AJ, Patterson SD, Gu M. 1999 Ceramide second messengers and ceramide assays. *Trends Biochem Sci*. 24(6):228.
152. Worgall S, Martushova K, Busch A, Lande L, Crystal RG. 2002. Apoptosis induced by Pseudomonas aeruginosa in antigen presenting cells is diminished by genetic modification with CD40 ligand. *Pediatr Res* 52:636-644.
153. Xu X, Bittman R, Duportail G, Heissler D, Vilcheze C, London E. 2001 Effect of the structure of natural sterols and sphingolipids on the formation of ordered sphingolipid/sterol domains (rafts). Comparison of cholesterol to plant, fungal, and disease-associated sterols and comparison of sphingomyelin, cerebrosides, and ceramide.*J Biol Chem.* 276(36):33540-6.
154. Yano M, Kishida E, Muneyuki Y, Masuzawa Y. 1998 Quantitative analysis of ceramide molecular species by high performance liquid chromatography. *J Lipid Res*. 39(10):2091-8.

155. Yi F, Chen QZ, Jin S, Li PL. 2007 Mechanism of homocysteine-induced Rac1/NADPH oxidase activation in mesangial cells: role of guanine nucleotide exchange factor Vav2. *Cell Physiol Biochem.* 0(6):909-18.
156. Yu H, Zeidan YH, Wu BX, Jenkins RW, Flotte TR, Hannun YA, Virella-Lowell I. 2009. Defective acid sphingomyelinase pathway with Pseudomonas aeruginosa infection in cystic fibrosis. *Am J Respir Cell Mol Biol* 41:367-75.
157. Zhang AY, Yi F, Zhang G, Gulbins E, Li PL. 2006. Lipid raft clustering and redox signaling platform formation in coronary arterial endothelial cells. *Hypertension* 47:74-80.
158. Zhang AY, Yi F, Jin S, Xia M, Chen QZ, Gulbins E, Li PL. 2007. Acid sphingomyelinase and its redox amplification in formation of lipid raft redox signaling platforms in endothelial cells. *Antioxid Redox Signal* 9:817-828.
159. Zhang DX, Zou AP, Li PL. 2001 Ceramide reduces endothelium-dependent vasodilation by increasing superoxide production in small bovine coronary arteries. *Circ Res* 88:824-831.
160. Zhang DX, Yi FX, Zou AP, Li PL. 2002. Role of ceramide in TNF-alpha-induced impairment of endothelium-dependent vasorelaxation in coronary arteries. *Am. J. Physiol. Heart. Circ. Physiol.* 283: H1785-H1794.
161. Zhang DX, Zou AP, Li PL. 2003 Ceramide-induced activation of NADPH oxidase and endothelial dysfunction in small coronary arteries. *Am J Physiol Heart Circ Physiol* 284:H605-612.
162. Zhang AY, Yi F, Jin S, Xia M, Chen QZ, Gulbins E, Li PL. 2007 Acid sphingomyelinase and its redox amplification in formation of lipid raft redox signaling platforms in endothelial cells. *Antioxid Redox Signal.* 9(7):817-28.
163. Zhang Y, Li X, Carpinteiro A, Gulbins E. 2008. Acid sphingomyelinase amplifies redox signaling in Pseudomonas aeruginosa–induced macrophage apoptosis. *J. Immunology* 181: 4247-54.
164. Zychlinsky A, Sansonetti P. 1997. Perspectives series: host/pathogen interactions. Apoptosis in bacterial pathogenesis. *J Clin Invest.* 100:493-495.

8. CURRICULUM VITAE

PERSONAL INFORMATION:

Name:	Xiang Li
Gender:	Female
Date of Birth:	May 30, 1979
Current office address:	Department of Molecular Biology School of Medicine University of Duisburg-Essen Hufelandstrasse 55 Essen, 45122, Germany Tel: (49)-201-723-3687 Fax: (49)-201-723-5974 Email: xiang.li@uni-due.de

EDUCATION:

Sept. 1996-July. 2001	M.D. in clinical medicine, Peking University, Beijing, China
Sept. 2003-July. 2006	M.S. in Pharmacology, Department of Pharmacology & Toxicology, Medical College of Wisconsin, USA
Sept. 2006-current	Ph.D. candidate, Department of Molecular Biology, School of Medicine, University of Duisburg-Essen, Germany (supervisor: Prof. Dr. Erich Gulbins)

PROFESSIONAL EXPERIENCE:

Nov. 2001-June. 2003	Research Associate in clinical laboratory, Nanning Hospital, Guangxi, China.

AWARDS, FELLOWSHIPS AND HONORS:

2008-current	Graduate Student Fellowship from DFG (GRK1045)

RESEARCH INTERESTS:

My interests of research are to explore the mechanisms leading to pulmonary diseases and develop novel therapies. I am particularly interested in studying the role of ceramide and Cftr in the regulation of redox signaling during pulmonary infections by using pharmacological and genetic methodologies.

9. BIBLIOGRAPHY:

PUBLICATIONS AND MANUSCRIPTS

1. Li X, Becker KA, Zhang Y. Ceramide in redox signaling and cardiovascular diseases. Cell. Physiol. Biochem. 2010; 26: 41-48.
2. Zhang Y, Li X, Grassmé H, Döring G, Gulbins E. Alterations in ceramide concentration and pH determine the release of reactive oxygen species by Cftr-deficient macrophages upon infection. J. Immunol. 2010; 184: 5104-5111.
3. Zhang Y, Li X, Becker KA, Gulbins E. Ceramide-enriched membrane domains-structure and function. Biochim Biophys Acta 2009; 1788: 178-183.
4. Zhang Y*, Li X *(co-first author), Carpinteiro A, Gulbins E. Acid sphingomyelinase amplifies redox signaling in Pseudomonas aeruginosa–induced macrophage apoptosis. J Immunol. 2008 181:4247-4254.
5. Dumitru CA, Zhang Y, Li X, Gulbins E. Ceramide: a novel player in reactive oxygen species-induced signaling. Antioxid Redox Signal. 2007; 9:1535-1540.
6. Yi XY, Li X, Zhang F, Yi F, Matson DR, Jiang MT, Li PL.Characteristics and actions of NAD(P)H oxidase on the sarcoplasmic reticulum of coronary artery smooth muscle. Am J Physiol Heart Circ Physiol. 2006 290: H1136-44.

MANUSCRIPTS IN REVISION OR IN PREPARATION

7. Zhang Y, Li X, Carpinteiro A, Soddman M, Gulbins E. A novel role of kinase suppressor of ras-1 in pulmonary Pseudomonas aeruginosa infections. Nat. Med. (in revision).
8. Li X, Perrotta C, Clementi E, Gulbins E, Zhang Y. Oxidative stress triggers Calcium-dependent lysosome trafficking and activation of acid sphingomyelinase. J. Biol. Chem. (in revision).
9. Li X, Gulbins E, Zhang Y. Role of kinase suppressor of ras-1 in lipopolysaccharide-induced acute lung injury. Cell. Physiol. Biochem. (in preparation).

BOOK CHAPTERS

10. Li X, Zhang Y, Gulbins E. Lipid rafts and Pseudomonas aeruginosa infections. 2009; Handbook of Hydrocarbon and Lipid Microbiology Vol 3_00062.

10. ACHNOWLEDGENMENTS

The present study was performed at the Department of Molecular Biology, University of Duisburg-Essen. I am, therefore, thankful to all my co-workers and supervisors for their help and moral support.

First of all, I thank to **Prof. Dr. Erich Gulbins**, Director of the Dept. of Molecular Biology, for giving me the opportunity of having a Ph.D. position in his group, as well as for the excellent scientific guidance and professional support he gave me throughout my work.

I am particularly thankful to **Dr. Yang Zhang**, Dept. of Molecular Biology, for having so much patience in teaching me during the first years of my Ph.D. and for his permanent guidance and support.

I thank all my other colleagues and former colleagues: **Alexander Carpintero, Andrea Riehle, Barbara Wilker, Heike Grassme, Katrin Becker-Flegler, Martin Knüwer, Matthias Soddemann, Silvia Davies, Simone Keitsch** and **Yasmine Busch** for being much more than just co-workers.

Special thanks to **Siegfried Moyrer**, our 'computer specialist', for his constant technical and graphical assistance.

I would like to express my gratitude to Mrs. **Zimmerman**, who was like a second mother to me through her endless personal support and assistance with managing my life in Germany.

I acknowledge **Prof. Dr. Michael Roggendorf** and **Prof. Dr. Mengji Lu**, Dept. of Virology, University of Duisberg-Essen, for their continuous support and stimulatory discussion.

Finally, I would like to thank generous financial support from **DFG** for my Ph.D. research (GRK1045 fellowship since August, 2008).

Erklärung:
Hiermit erkläre ich, gem. § 6 Abs. 2, Nr. 7 der Promotionsordnung der Math.-Nat.- Fakultäten zur Erlangung der Dr. rer. nat., dass ich das Arbeitsgebiet, dem das Thema „Regulation of redox signaling by ceramide during pulmonary Pseudomonas aeruginosa infections“ zuzuordnen ist, in Forschung und Lehre vertrete und den Antrag von Frau Xiang Li befürworte.

Essen, den _____

_____
Unterschrift d. wissenschaftl. Betreuers/Mitglieds
der Universität Duisburg-Essen

Erklärung:
Hiermit erkläre ich, gem. § 6 Abs. 2, Nr. 6 der Promotionsordnung der Math.-Nat.- Fakultäten zur Erlangung des Dr. rer. nat., dass ich die vorliegende Dissertation selbständig verfasst und mich keiner anderen als der angegebenen Hilfsmittel bedient habe.

Essen, den _____

Xiang Li

Erklärung:

Hiermit erkläre ich, dass ich gemäß der Promotionsordnung der Fakultäten für Biologie und Geografie, Chemie und Mathematik, § 6 Abs. (2) e) keine andere Promotion bzw. Promotionsversuche in der Vergangenheit durchgeführt habe und dass diese Arbeit von keiner anderen Fakultät oder Fachbereich abgelehnt worden ist.

Essen, den ……..

Xiang Li